

Snowmass 2021 White Paper Axion Dark Matter

J. Jaeckel¹, G. Rybka², L. Winslow³, and the Wave-like Dark Matter Community⁴

¹Institut fuer theoretische Physik, Universitaet Heidelberg, Heidelberg, Germany

²University of Washington, Seattle, WA, USA

³Laboratory of Nuclear Science, Massachusetts Institute of Technology, Cambridge, MA, USA

⁴Updated Author List Under Construction

Abstract

Axions are well-motivated dark matter candidates with simple cosmological production mechanisms. They were originally introduced to solve the strong CP problem, but also arise in a wide range of extensions to the Standard Model. This Snowmass white paper summarizes axion phenomenology and outlines next-generation laboratory experiments proposed to detect axion dark matter. There are vibrant synergies with astrophysical searches and advances in instrumentation including quantum-enabled readout, high-Q resonators and cavities and large high-field magnets. This white paper outlines a clear roadmap to discovery, and shows that the US is well-positioned to be at the forefront of the search for axion dark matter in the coming decade.

Contents

1	Executive summary	5
2	Introduction	8
3	Axion Motivation	9
3.1	QCD Axion	9
3.2	ALPs	11
4	Axion Cosmology	12
4.1	Axion creation mechanisms	12
4.1.1	The Pre-Inflation Scenario	14
4.1.2	The Post-Inflation Scenario	15
4.1.3	Thermal Production and Evolution	15
4.2	Late-Time Structure Formation and the Local Properties	16
5	Micro-eV and Above	18
5.1	ADMX G2	19
5.2	ADMX EFR	20
5.3	HAYSTAC	21
5.4	SQuAD	23
5.5	ALPHA	24
5.6	MADMAX	25
5.7	LAMPOST	27
5.8	BREAD	27
5.9	Global Context	29
5.9.1	ORGAN	29
5.9.2	RADES	30
5.9.3	ALPS II	30
6	Below Micro-eV	31
6.1	DMRadio-m ³	31
6.2	ABRACADABRA Demonstrator	33
6.3	Search for Halo Axions with Ferromagnetic Toroids (SHAFT)	35
6.4	DMRadio-GUT	36
6.5	SRF Cavities and Related Techniques	37
7	Alternative Couplings	39
7.1	CASPER-electric	40
7.2	CASPER-gradient	41
7.3	ARIADNE	42
7.4	Magnetometer Networks	44
7.5	Broadband Axion Dark Matter Searches via Non-Electromagnetic Couplings	46

8	Solar Axions	47
8.1	IAXO and BabyIAXO	47
9	Synergies with astrophysical searches	50
10	R&D needs for future axion experiments	54
10.1	Quantum Sensor R&D	55
10.2	Magnet R&D	56
10.3	Cavity R&D	57
11	Conclusion – Towards the Ultimate Axion Facility	59

1 Executive summary

The Dark Matter Question — The nature of dark matter remains unknown, though it makes up $\sim 25\%$ of the energy density of the universe. Its sheer quantity already makes it a clear top priority for fundamental particle physics and cosmology. Simultaneously, multiple well-motivated dark matter candidates are coming within the reach of the next generation of experiments, building on rapid technological progress. This opens the door for a breakthrough in our understanding of the universe.

Axions — Among dark matter candidates, axions stand out as especially well motivated, with a clear roadmap to decisive experimental progress and potential discovery in the next decade. Axions are light pseudoscalar particles which appear in a wide variety of extensions to the Standard Model. For instance, they may arise as Goldstone bosons of a spontaneous symmetry breaking at a high energy scale f_a , leading to a small mass m_a and weak couplings to photons, gluons, leptons, and nucleons.

The most well-motivated example of an axion is the QCD axion, which arises as a consequence of the Peccei-Quinn solution to the strong-CP problem [1–4]. Its coupling to gluons leads to a well-defined relationship between m_a and f_a , which in turn leads to a narrow band of couplings to photons. The QCD axion may be produced nonthermally in the early universe by the misalignment mechanism, which, in the simplest scenarios, motivates masses $10^{-6} \text{ eV} \lesssim m_a \lesssim 10^{-4} \text{ eV}$.

By contrast, axion-like particles (ALPs) do not couple directly to gluons, leading to a broader range of possible couplings to photons. They may be also be simply produced via misalignment in the broader mass range $10^{-20} \text{ eV} \lesssim m_a \lesssim \text{eV}$, which is bracketed by astrophysical and cosmological constraints.

Context — At the time of the previous Snowmass a decade ago, no experiment had probed the QCD axion below 0.1 eV. The ADMX G2 experiment has now achieved this goal, albeit in a narrow mass range. The previous Snowmass process also spawned the Dark Matter New Initiatives (DMNI) program, which has funded DMRadio- m^3 and ADMX-EFR to develop project execution plans to reach the QCD axion in a wider range of masses. Simultaneously, a number of other demonstrator-scale experiments are beginning to probe unexplored axion parameter space.

This Snowmass marks the beginning of a renaissance in the search for axions. We now have a series of experiments that would allow us to definitively search the axion dark matter parameter space and a roadmap to realize them. Fig. 1 shows the potential mass reach of the proposed experiments discussed in this white paper. Several different techniques are needed across this broad mass range, but almost all require quantum-enabled readout, high-Q resonators and cavities, as well as large high field magnets.

Roadmap to Discovery

As a community we propose a phased approach that allows for discovery at all stages while nurturing emerging technologies. This plan has four components:

1. **Pursue the QCD Axion by Executing the Current Projects:** The ADMX G2 effort continues to scan exciting axion dark matter parameter space and the experiments

identified by the DMNI process DMRadio- m^3 and ADMX-EFR are prepared to start executing their project plans.

2. **Pursue the QCD Axion with a Collection of Small-Scale Experiments:** The entire axion mass range cannot be explored by one or two experiments; a variety of techniques must be employed. Most of the efforts described in this white paper would benefit from a concerted effort to foster small scale projects to either cover a limited range of the QCD axion parameter space, or bring the effort to a level of technological readiness required to reach the QCD axion parameter space. The DOE DMNI process was the right scale for many of these proposed experiments to make significant inroads to the QCD axion.
3. **Support Enabling Technologies:** Many of the proposed efforts share needs in ultra-sensitive quantum measurement and quantum control, large, high-field magnets, spin ensembles, and sophisticated resonant systems. These technologies overlap strongly with other HEP efforts and synergies should be exploited.
4. **Support Theory and Astrophysics Beyond the QCD Axion:** The QCD axion is an important benchmark model, but not the only motivated one. Theoretical effort should be supported to understand the role of ALPs in dark matter cosmology, and to understand the roles axions play in astrophysical phenomena.

Outlook — In the best case scenario, the axion will have already been discovered by the time of the next Snowmass, at which point efforts would have shifted to studying its properties and determining if it makes up all, or only part of the dark matter. Alternatively, significant inroads will have been made in probing the QCD axion. A number of the projects described in this white paper will have advanced to the stage of needing mid-scale support for a final push to cover the entire range of QCD axion dark matter. The well-developed projects will have matured and merged to be able to utilize a large scale ‘Ultimate Axion Facility’ to probe models of ALP dark matter beyond the QCD axion, or where only a fraction of dark matter is made of axions.

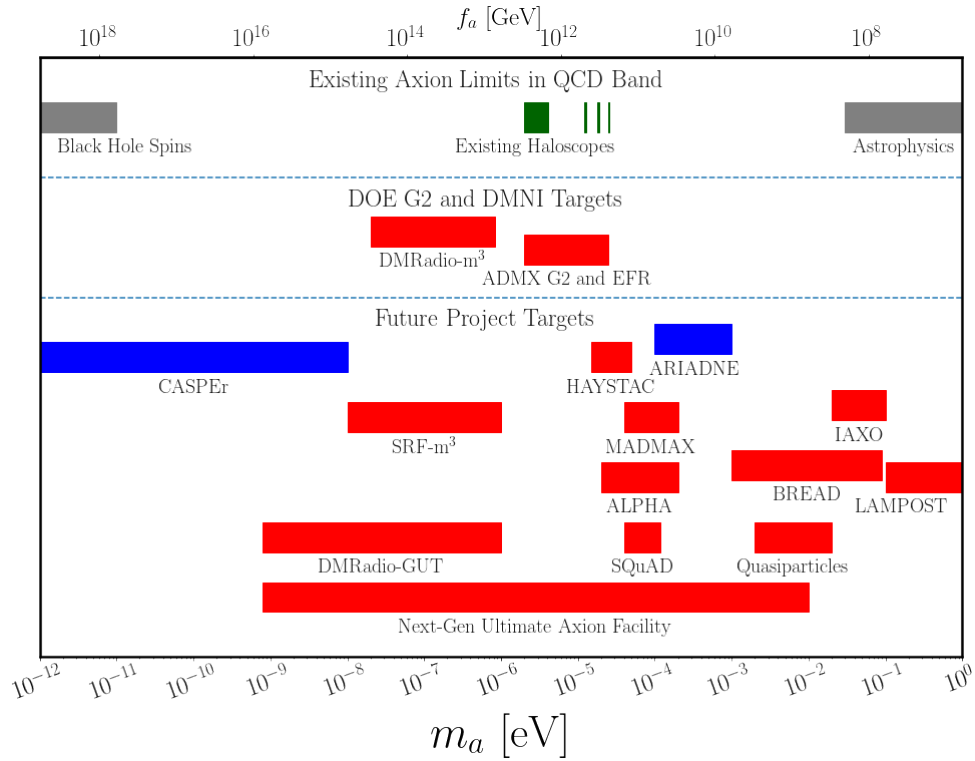


Figure 1: Potential QCD axion mass range explored by efforts described in this white paper. The green bars indicate running experiments in the QCD region, red indicate proposals that utilize the axion-photon coupling, and blue indicates proposal utilizing alternative couplings.

2 Introduction

Laboratory detection of dark matter (DM) is a cornerstone goal of fundamental physics today (see, e.g. [5] for a recent report focusing mostly on the European efforts). Astrophysical evidence for DM is abundant [6–11], but its microscopic properties remain mysterious. Many extensions of the Standard Model (SM) predict compelling DM candidates with interesting cosmological histories. One sought-after candidate is the axion, a pseudoscalar (spin zero, parity odd) field arising as a pseudo-Nambu–Goldstone boson of a broken Abelian symmetry [1, 3, 4]. This is the leading solution to the strong charge–parity (CP) problem in quantum chromodynamics (QCD) that addresses the experimental non-observation of the neutron electric dipole moment [12–15]. The axion exhibits viable DM properties [16–18] and with masses below 1 eV, its high occupation number gives rise to wave-like behaviour acting as a coherently-oscillating classical field. The interactions of the axion with SM forces and matter enable a diverse range of experiments to search for its direct evidence. Axion-like particles (ALPs) are generalised pseudoscalars whose mass and couplings that allow searches across wider parameter space.

This Snowmass white paper reviews ongoing and planned experiments aiming to directly detect axion DM in the coming decade and beyond. Particular focus is placed on experiments located and led by the US community to align with the aims of Snowmass. A wide range of models predict different couplings and masses for axions across many orders of magnitude. The present most-sensitive experiments search for the axion–photon interaction around the micro-electronvolt (μeV) mass range, motivated by the predictions of a suitable DM abundance in the simplest settings. However, multiple decades of coupling–mass parameter space remain unexplored due to longstanding obstacles of the canonical resonant cavity haloscopes. This motivates the burgeoning and vibrant program of experiments proposed to extend sensitivity above and below μeV masses. These capitalize on the interdisciplinary creativity and scientific expertise of the community to enable experimental breakthroughs for decisively testing axion DM scenarios. Realizing this program requires strengthening synergies with astrophysical probes and sustained investment in instrumentation technology crucial to opening unprecedented DM sensitivity.

With this goal in mind this white paper proceeds along the following outline. Section 3 reviews the particle physics motivation of the QCD axion and axion-like particles. Section 4 discusses the production of axions in the early universe and their late-time astrophysics. Experiments targeting axions via their couplings to photons are presented in sections 5 and 6, which emphasize axion masses above and below μeV , respectively. Section 7 discusses experiments sensitive to a wide range of other axion couplings. Section 8 considers the opportunities provided by axions produced in the sun. Synergies with astrophysical probes are presented in section 9. Important R&D directions for future experiments are discussed in section 10 before section 11 concludes with an overview of the opportunities presented by the discussed experiments and gives an outlook to a future ultimate axion facility.

3 Axion Motivation

3.1 QCD Axion

Yang-Mills theories, such as QCD, generically break the CP symmetry via a so-called $\bar{\theta}$ -term: $\mathcal{L}_\theta \sim \bar{\theta} G\tilde{G}$, where G is the gluon field strength tensor. Nevertheless, experimental measurements of a number of CP-violating observables in the strong sector, such as the electric dipole moment of the neutron, are compatible with the absence of such CP violation, setting stringent upper bounds on $\bar{\theta} \lesssim 10^{-10}$ [15]. The extreme smallness of this parameter, commonly dubbed the “strong CP problem”, constitutes a very serious fine-tuning issue that remains unresolved in the SM. Indeed, the quest to explain small parameters has been shown in the past to be an effective tool to gain a deeper understanding of Nature. The strong CP problem could therefore represent a unique guide in the search for new physics.

Not many solutions to the strong CP problem are known and probably the most compelling explanation to this puzzle is the Peccei-Quinn (PQ) mechanism [1, 2]. It minimally extends the SM with a new classically conserved global symmetry, the PQ symmetry $U(1)_{\text{PQ}}$, which is spontaneously broken at a scale $\sim f_a$ and explicitly broken at the quantum level by a mixed QCD anomaly. As an unavoidable low-energy consequence of this mechanism, a pseudo-Nambu-Goldstone boson (pNG) arises: the QCD axion a [3, 4]. This makes this scenario extremely testable. The central ingredient of the PQ mechanism is the axion coupling to QCD,

$$\mathcal{L} = \left(\frac{a}{f_a} - \bar{\theta} \right) \frac{\alpha_s}{8\pi} G^{\mu\nu a} \tilde{G}_{\mu\nu}^a, \quad (1)$$

that generates a non-perturbative axion potential, the minimum of which is CP-conserving [19]. Thus the axion dynamically relaxes the value of $\bar{\theta}_{\text{eff}} \equiv \langle a \rangle / f_a - \bar{\theta}$ to zero solving the strong CP problem.

The resulting QCD axion mass is inversely proportional to the axion decay constant f_a . It can be computed using chiral perturbation theory,

$$m_a^2 \simeq \frac{f_\pi^2 m_\pi^2}{f_a^2} \frac{m_u m_d}{(m_u + m_d)^2}, \quad (2)$$

as a function of the pion mass m_π , the decay constant f_π , and the up and down quark masses m_u and m_d . The most precise computation to date [20] yields

$$m_a = 5.691(51) \mu\text{eV} (10^{12} \text{GeV} / f_a). \quad (3)$$

The axion mass in Eq. (2) is a robust prediction of the invisible axion paradigm. Nonetheless, some extensions motivated by the PQ quality problem, predict axions parametrically lighter [21–23] or heavier [24–39].

The different strategies one can use to implement the PQ symmetry in a UV complete theory give rise to different axion models. The most paradigmatic ones are the DFSZ [40, 41], KSVZ [42, 43], and dynamical/composite axions [44], which are often

used as benchmark examples. The DFSZ model requires at least two Higgs doublets and no additional fermions, since the fermions carrying the PQ charge are those of the SM, while hadronic models, which include KSVZ and composite axions, require new fermions to implement the PQ symmetry. Another difference among these models is that both KSVZ and DFSZ axions are fundamental/elementary scalar fields whereas the dynamical axion corresponds to a bound state, a pseudoscalar meson of a new confining force.

The main properties of the QCD axion, such as its lightness and feeble derivative or anomalous interactions, stem from its pseudo Nambu-Goldstone nature. This informs us about the low energy processes that would be affected by the existence of this hypothetical particle and thus which detection strategies we should pursue. Since our detectors are particularly sensitive to the electromagnetic (EM) interactions, most of the axion experiments take advantage of the axion-photon coupling,

$$\mathcal{L}_{a\gamma\gamma} = -\frac{g_{a\gamma\gamma}}{4} a F_{\mu\nu} \tilde{F}^{\mu\nu} = g_{a\gamma\gamma} a \mathbf{E} \cdot \mathbf{B}, \quad (4)$$

where $F^{\mu\nu}$ is the EM field strength tensor and \mathbf{E} and \mathbf{B} are electric and magnetic fields. With this interaction included the Maxwell equations get modified as follows [45],

$$\nabla \cdot \mathbf{E} = \rho - g_{a\gamma\gamma} \mathbf{B} \cdot \nabla a, \quad (5)$$

$$\nabla \cdot \mathbf{B} = 0, \quad (6)$$

$$\nabla \times \mathbf{E} = -\frac{\partial \mathbf{B}}{\partial t}, \quad (7)$$

$$\nabla \times \mathbf{B} = \frac{\partial \mathbf{E}}{\partial t} + \mathbf{J} - g_{a\gamma\gamma} \left(\mathbf{E} \times \nabla a - \frac{\partial a}{\partial t} \mathbf{B} \right). \quad (8)$$

In general the axion-photon coupling has a contribution which depends on the fermionic content of the specific model and another contribution originating from the axion mixing with neutral mesons [46],

$$g_{a\gamma\gamma} = \frac{\alpha}{2\pi f_a} \left(\frac{E}{N} - 1.92(4) \right). \quad (9)$$

Here, E and N are the EM and QCD anomaly coefficients and α is the fine structure constant. The original KSVZ model predicts $E/N = 0$ while the original DFSZ model predicts $E/N = 8/3$. Due to their simplicity, the latter models are normally taken as benchmarks.

While it is common to focus on the minimal benchmark models or to assume that $E/N \sim \mathcal{O}(1)$, the axion-photon coupling $g_{a\gamma\gamma}(m_a)$ is strongly model-dependent, so that its value can be changed significantly by invoking additional assumptions about the UV structure of the theory. The anomaly coefficients E and N can vary considerably depending on the representations of the SM group under which heavy fermions of a given axion model transform [47–51]. If those fermions are magnetic monopoles the fine structure constant α entering Eq. (9) would be magnetic, enhancing the coupling to photons by $\alpha_m/\alpha_e \sim 4 \times 10^4$ [52]. Moreover, the dependence of the PQ scale f_a on the axion mass m_a can differ from the conventional relation in Eq. (2) [21, 22]. Finally, the axion photon

coupling can be enhanced/suppressed in models with multiple scalars where hierarchical charges arise due to particular axion alignments in field space such as Kim-Nilles-Peloso (KNP) mechanism, [53, 54] clockwork axions [55, 56] or multi-higgs doublet DFSZ-like models [57].

Although the axion-photon coupling is the most popular one to search for in experiments, the Lagrangian (4) is actually not specific to axions. The same kind of coupling is shared by any axion-like particle (ALP), which needs not solve the strong CP problem. To discover the QCD axion, one has to probe its coupling to gluons (1). At low energies, the latter coupling induces interactions of axions with the EDMs of nucleons. The corresponding Lagrangian is,

$$\mathcal{L}_{aN\gamma} = -\frac{i}{2}g_{aN\gamma}a\bar{\Psi}_N\sigma_{\mu\nu}\gamma_5\Psi_N F^{\mu\nu}, \quad (10)$$

where $\sigma_{\mu\nu} = \frac{1}{2}[\gamma_\mu, \gamma_\nu]$ and the nucleon N can be the neutron n or the proton p . The coupling constants $g_{aN\gamma}$ corresponding to each of the nucleons depend only on the PQ scale f_a and are given by the following expression,

$$g_{ap\gamma} = -g_{an\gamma} = -(3.7 \pm 1.5) \times 10^{-3} \left(\frac{1}{f_a}\right) \frac{1}{\text{GeV}}. \quad (11)$$

Axions are also predicted to couple to leptons at tree level in a wide range of models, such as those based on Grand Unified Theories (GUTs). Even though it is challenging to probe these interactions with current experiments, a promising avenue is to study the influence they exhibit on various astrophysical processes, where the interactions of axions with electrons can play a crucial role (see also Sec. 9). The interaction Lagrangian with leptons reads,

$$\mathcal{L}_{a\ell\ell} = \frac{C_\ell}{2f_a} \partial_\mu a \bar{\Psi}_\ell \gamma^\mu \gamma_5 \Psi_\ell, \quad (12)$$

where the coefficient C_ℓ depends on the particular lepton flavor under consideration. Note that in hadronic axion models, such as KSVZ, the couplings to leptons are suppressed, since they are generated only at the loop level through the axion-photon coupling (9), whereas DFSZ constructions predict tree-level couplings to leptons.

3.2 ALPs

The designation axion-like particle (ALP) usually refers to a more general (pseudo) Nambu-Goldstone boson of a global $U(1)$ symmetry breaking. ALPs share many similarities with the QCD axions such as their similar effective theories and their potential role as DM. However, ALPs, by definition, do not interact in the same way with the gluons as the QCD axion. Since ALPs do not acquire their masses from the non-perturbative QCD effects, the mass m_a and the decay constant f_a are independent parameters as opposed to Eq. (2) for the QCD axion. Although ALPs cannot address the strong CP problem, they are well motivated new physics beyond the Standard Model since global $U(1)$ symmetries are ubiquitous in proposed solutions to the open questions in particle physics and cosmology. The most

motivated examples include the Majoron associated with the lepton symmetry [58] that explains the neutrino masses and the familon associated with the flavor symmetry [59] that addresses the fermion hierarchical masses and mixing. In addition, ALPs are generically predicted in the low-energy effective theories from string theory [60–67]. More recently, a so-called ALPogenesis [68] scenario has been discussed where ALPs may simultaneously explain the DM abundance [69] as well as the observed cosmological baryon asymmetry [70–72] using novel axion dynamics in the early universe. ALPogenesis is of particular experimental interest because it predicts a rather precise relation between m_a and f_a that is experimentally accessible.

4 Axion Cosmology

Axion cosmology has become a broad research area and cannot be fully summarized in a few pages. This section therefore focuses on the qualities of dark matter (DM) axions and axionlike particles (ALPs) most crucial to their cosmological abundance and relevance to the research proposals covered in later sections.

As we will see the simplest models and mechanisms for dark matter QCD axions predict super- μeV axion masses whose experimental search is discussed in Sec. 5. For sub- μeV axion masses (experiments discussed in Sec. 6) non-standard assumptions for the axion models or cosmological scenarios might be required to make axions all of the DM. Examples include entropy injection, late inflation, or naturally small initial field values. These need not be *ad hoc* modifications but can arise from solving other puzzles, such as the baryon asymmetry of the Universe. More details on non-standard scenarios can be found in the corresponding paragraph in Sec. 4.1. It should be noted that ALPs with sub- μeV masses are predicted abundantly in string theory [e.g. 62, 73], and that ultralight ALPs might resolve various potential cosmological issues [e.g. 74–76].

To supplement this incomplete summary, we advise the interested reader to consult some of the excellent axion reviews [e.g. 50, 77].

4.1 Axion creation mechanisms

In the early Universe, axions can be produced both thermally and non-thermally. We focus on the non-thermal production but also comment on recent interesting developments on thermal production in Sec. 4.1.3. The bedrock of the axion’s relevance for cosmology is the realignment (or misalignment) mechanism: it generically allows QCD axions [16–18, 78, 79] and ALPs [80] to make up significant fractions of the cold DM in the Universe. Breaking of the PQ symmetry can also lead to the formation of topological defects, namely cosmic strings and domain walls [81, 82]. While they can emit axions during their evolution [83–86], topological defects may be diluted away during inflation if formed too early.

The canonical realignment mechanism. The scalar field equation for the *homogeneous* axion field $a(t) \equiv f_a \theta(t)$, where the cosmological history is described by the Hubble pa-

parameter $H(t)$, takes the form

$$\ddot{\theta} + 3H(t)\dot{\theta} + m_a^2(t)\sin(\theta) = 0, \quad (13)$$

where the one-instanton cosine potential $V[\theta] = f_a^2 m_a^2(t) [1 - \cos(\theta)]$ was assumed to describe axions and ALPs at higher temperatures. While the low-temperature QCD axion potential is known to be more complicated [46, 87], the relevant evolution of the field happens when the low-temperature result does not apply. The initial conditions are usually taken to be $\theta(0) \equiv \theta_i \in [-\pi, \pi)$ and $\dot{\theta}(0) \equiv 0$, where θ_i is referred to as the initial misalignment angle. The condition $\dot{\theta}(0) \equiv 0$ seems sensible as the solution diverges otherwise for $t \rightarrow 0$ or as a practical choice given that Hubble drag dampens the angle velocity $\dot{\theta} \simeq 0$ by the time the field becomes dynamical at $H \sim m_a$ [88, 89].

The general behavior of the solutions of Eq. (13) in standard cosmology is as follows: at early times, when $H \gg m_a$, the field is “stuck” due to Hubble friction. It is thus constant and has the same equation of state (EOS) as dark energy or an inflaton ($w = -1$). Around the time when $H \sim m_a$, the field becomes dynamical and starts to oscillate. At later times, $H \ll m_a$, the field evolution eventually becomes adiabatic and the time-averaged EOS is $\langle w \rangle = 0$ and, due to the rapid oscillation, the field effectively behaves as pressureless dust or cold DM. Under the assumption of entropy conservation, one may thus derive an estimate of the energy density today.

There exist approximate solutions to Eq. (13) using semi-analytical techniques, which can yield estimates of the axion DM abundance [e.g. 77], as well as a small number of publicly available codes for numerical solutions [e.g. 90, 91], including perturbation evolution [92, 93]. Due to the anharmonicities from the cosine potential [79, 94–98], at least some numerical analysis is required to get a precise prediction of the axion energy density, and thus constraints on the axion mass.

Despite the need for a partial numerical evolution of Eq. (13), it is still useful compare a rough estimate for the axion abundance to the DM density today, $\Omega_{\text{DM}} h^2 \approx 0.12$. For QCD axions with $f_a \lesssim 10^{17}$ GeV in a standard cosmological scenario one finds that (see e.g. Refs. [16–18, 78] for early estimates, Refs. [79, 94–98] for the inclusion of anharmonic corrections, and Ref. [99] for a recent computation)

$$\Omega_a h^2 \sim 0.12 \left(\frac{f_a}{10^{12} \text{ GeV}} \right)^{7/6} \langle \theta_i^2 \rangle, \quad (14)$$

where the average misalignment angle squared, $\langle \theta_i^2 \rangle$, depends on whether the PQ symmetry breaks before (see Sec. 4.1.1) or after inflation (see Sec. 4.1.2). In the former case we have a single $\theta_i \sim \mathcal{O}(1)$, while in the latter case $\langle \theta_i^2 \rangle \sim 4.6$ [99]. Again note that Eq. (14) is only a rough estimate and also depends on the realized scenario. That said, saturating the DM density and using the relation between m_a and f_a from Eq. (3), we find that QCD axion masses are naturally $\gtrsim \mu\text{eV}$. This suggest the aforementioned separation of experiments into super- μeV (see Sec. 5) and sub- μeV (see Sec. 6).

Axionlike particles, which need not solve the strong CP problem, often have masses that are independent of the temperature in the early universe, or feature a very different temperature dependence than the QCD axion. This has to be taken into account when

calculating their abundance. It is possible to obtain estimates for the ALP DM abundance similar to Eq. (14), which trace out natural lines in the mass vs. coupling plane (cf. [e.g. 80]). Due to the large number of possible ALP models, there is however a wide range of conceivable models and corresponding predictions for masses and couplings.

Modifications and non-standard realignment scenarios. Note that several assumptions have been made in the canonical picture, many of which have been relaxed or modified. As mentioned before, this is often done to connect axions to other physics or alter the preferred f_a region by diluting or enhancing the axion energy density. Such scenarios are an active area of research, considering e.g. particular initial conditions set by early universe dynamics, as with a large [100–103] or a small [104–107] misalignment angle, or a large initial kinetic energy as in the kinetic misalignment mechanism [69, 108]. Kinetic misalignment is intimately connected to “axiogenesis” [72]—a mechanism to explain the baryon asymmetry of the Universe; in this paradigm, the QCD axion is predicted to have a mass between $O(60 \mu\text{eV} - 60 \text{meV})$ in various axiogenesis implementations [72, 109–114], whereas for the ALP, a relation between f_a and m_a is predicted as $f_a \simeq 2 \times 10^9 \text{GeV}(\mu\text{eV}/m_a)^{1/2}$ in “ALP cogeneration” [68]. The radial mode dynamics of the PQ breaking field can also provide the axion dark matter abundance [115–117] via the so-called parametric resonance effect. On the other hand, modifications of the thermal history [118, 119] of the Universe, i.e. of $H(t)$, are conceivable, including entropy injection [e.g. 18, 120] or non-standard inflation scenarios [121–126]. Furthermore, extended axion models can introduce modifications to $V[\theta]$ and thus $m_a(t)$ or give additional terms from axion interactions. These include the relaxion mechanism [127], the “ALP miracle” [128, 129], the “fragmentation” scenario [130, 131], trapped realignment [23], or many-axions in string theory [132]. As in the “ALP miracle” case, the initial $w = -1$ behaviour of axions has inspired models for axion inflation such as “natural inflation” [133], “n-flation” [134], or “monodromy inflation” [135, 136].

4.1.1 The Pre-Inflation Scenario

In one of two primary cosmological scenarios, the PQ symmetry breaks before the end of inflation (and remains broken afterwards). This occurs when the breaking scale $\sim f_a$ is greater than the Gibbons–Hawking temperature at the end of inflation, $T_1 = H_1/2\pi$ [137] as well as the reheating temperature after inflation. Two important consequences of this scenario are that

- the observable universe is contained within one causally connected patch at the time of PQ breaking, where the misalignment angle is often assumed to be uniform randomly set, $\theta_i \sim \mathcal{U}(-\pi, \pi)$ [79], and
- there exist isocurvature fluctuations of the field of order $\delta\theta \sim H_1/2\pi f_a$.

While the homogeneous field component dominates the energy density, field fluctuations are present – either as vestiges from inflation or as imprints from interactions with other matter or radiation species. They remain Jeans-stable until matter-radiation equality.

As mentioned before, it is often assumed that topological defects are inflated away in this scenario and play no role for the axion energy density. However, depending on the values of f_a and H_I , isocurvature fluctuations can impose constraints [94, 97, 98, 138–140]. Furthermore, fine-tuning and possibly anthropic considerations need to be taken into account [141, 142]. Despite the potential limitations, this scenario can link axions and inflationary physics, which is being actively investigated [e.g. 107, 124].

Applied to a pre-inflation axion, improved CMB polarization measurements and lensing expected from experiments like AdvACT, CMB-S4, LiteBIRD, BICEP array, Simons Observatory, and SPT-3G coupled with any local measurement of f_a explored in later sections could identify at least a portion of the relic dark matter abundance as well as provide an anchor for the scale of inflation.

4.1.2 The Post-Inflation Scenario

In the complementary scenario, the PQ symmetry breaks (for the last time) after inflation has ended. The axion field, again, takes random values $\theta_i \sim \mathcal{U}(-\pi, \pi)$ in causally disconnected regions. However, the observable universe now consists of a huge number of these regions, such that the energy density of axions today can be calculated as an average over the causally disconnected regions. As a consequence, the axion DM abundance becomes independent of any one θ_i and, for QCD axions, only depends on f_a . There may also be significant local DM overdensities and thus a highly non-linear evolution, giving rise to observable consequences discussed below.

Topological defects created during PQ breaking [81] are not inflated away in this scenario. They can increase the axion DM density through their evolution and decays [83–86]. While the phenomenology of cosmic strings, domain walls, and axitons has been studied extensively over the past decades [83–86, 143–155], no definitive consensus has been reached regarding the relevance of their contribution to the axion DM density. Recently, the contribution from string decay and wall annihilation have also been considered for the case of ALPs [156, 157].

The remaining large density fluctuations create local matter-dominated regions deep within the radiation era, causing gravitational collapse of modes once the Hubble scale exceeds a large fluctuation’s Jeans scale [150, 158]. This creates mini-halos of mass up to the order of $10^{-12} M_\odot$ by redshift $z = 100$, and most are expected to contain a compact soliton core with mass relation $M_{\text{core}} \propto M_{\text{halo}}^{1/3}$ [150, 158]. The fraction of matter bound in mini-halos has been simulated to be up to 75% at the beginning of the matter-dominated era [158].

At the cost of inflationary physics insight, the post-inflation axion motivates a rich late Universe phenomenology with accompanying signatures in gravitational waves and scale-dependent features in the Large Scale Structure which will be explored by expanded galaxy surveys, improved CMB measurements, and low-frequency gravitational wave detectors.

4.1.3 Thermal Production and Evolution

Axions can also be produced thermally in the early Universe. As dark radiation, they can modify the observed effective number of neutrino species and, as hot dark matter,

influence structure formation. This leads to e.g. an upper limit on the QCD axion mass in the eV range [159]. Other constraints on QCD axions and ALPs can come from CMB spectral distortions, Lyman- α forest, space- or ground-based observatories, or structure formation [160–168].

It has recently been emphasized again that the theoretical computation of the axion production rate around the QCD crossover is problematic [169]. This will be relevant for the upcoming generation of CMB experiments, which will be able to probe QCD axions in this regime [164, 170, 171], with the first steps towards improvement already underway [172, 173].

Generally, the scale of a potential thermal axion as a component of the relic dark matter stands to be constrained by any new probe of cosmological evolution reaching into new redshift ranges, complemented by local searches like those explored below to identify the axion coupling.

4.2 Late-Time Structure Formation and the Local Properties

After entering the matter-dominated era, broader fluctuations begin to collapse gravitationally as their modes enter the Hubble horizon, forming e.g. halos and filaments, and seeding the formation of stars, galaxies, and other baryonic structures. Understanding the distribution of axions within halos and other cosmic structures, as well as their interplay with the baryons, is crucial for the efficacy of axion searches.

Several properties of the QCD axion and ALP DM distribution are important for detection: local persistent density and spectral shape, coherence qualities, and prevalence of transient structures.

See Figure 2 for an illustration of the various scales involved.

Many axion dark matter searches make use of temporal and/or spatial coherence, often on macroscopic time and length scales. Crucially, the coherence time sets the maximal usable quality factor in resonant experiments discussed in Sections 5 and 6. Similarly, the coherence length scale determines the volume where experiments can benefit from coherent enhancement, a fact that becomes particularly relevant in experiments aiming at large experiments searching for axions at higher masses [176, 177].

Roughly speaking on time/length scales smaller than the coherence time/length the field amplitude can be viewed as a simple plane wave with well-defined amplitude and phase. This only works when the energy and momentum distribution of the waves contributing to the field is sufficiently narrow and on time/length-scales small enough such that the differences in frequency and wave length can be neglected. Therefore, the coherence time is given by the energy/frequency dispersion of the field $\tau_c \sim 2\pi/\Delta E \sim 10^6(2\pi/m_a)$, and the coherence length by the momentum/wave length dispersion of the field $\lambda_c \sim 2\pi/(m\Delta v) \sim 10^3(2\pi/m_a)$, where we have used the rough estimate $\langle v^2 \rangle^{1/2} \sim 10^{-3}$ at Earth’s location in the Milkyway.

The improving sensitivity and resolution of searches allows us to test more detailed axion DM distribution models. The model space of distributions is potentially very rich due to the candidates’ unique nature as highly degenerate Bose fluids. The early standard halo model, based on a non-singular or lowered isothermal sphere, produced the first

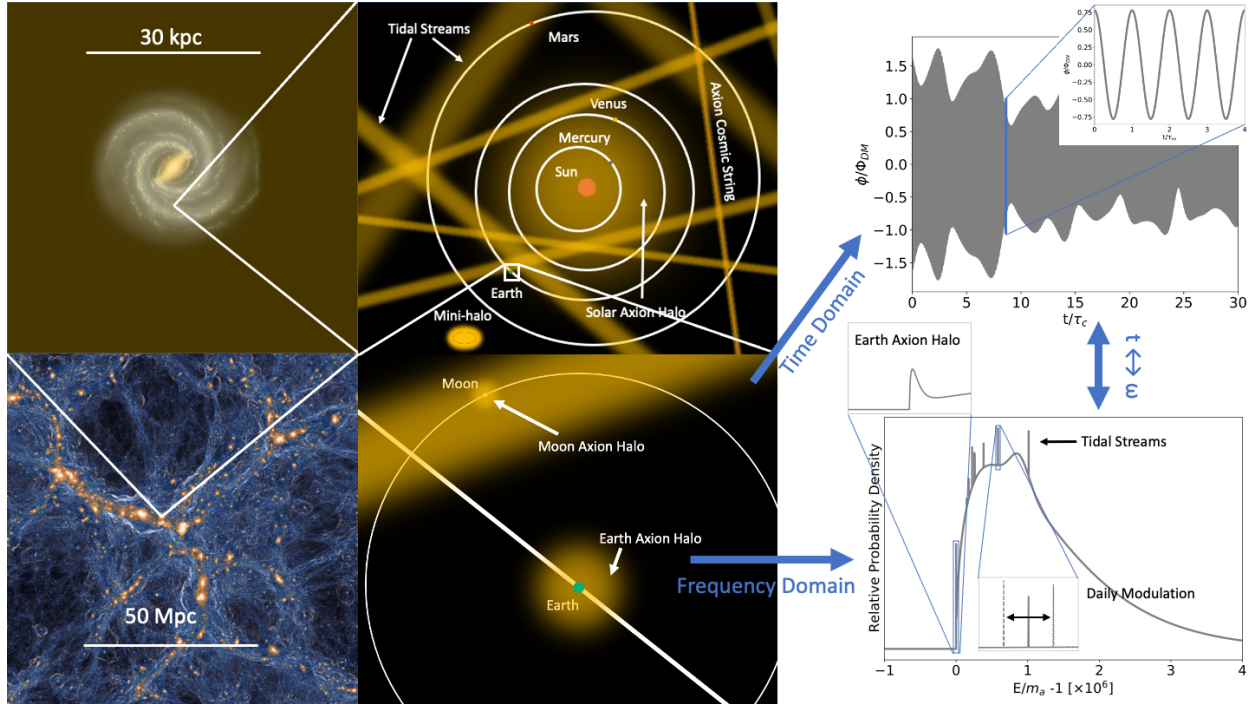


Figure 2: Illustration of Axion DM structure in the modern Universe from the scale of the cosmic web (lower left panel) to the mean axion field as may be observed by a terrestrial search (right panels). Each panel represents a view of axion DM structure at a different scale, with each of the four left panels showing the axion density in orange. The cosmic web (lower left) shows the clustering behavior of DM halos and surrounding gases. The MW (upper left) is surrounded by a halo with virial radius at least on order of magnitude larger than the Galaxy. The inner Solar System and the region immediately surrounding the Earth (middle panels) may contain axion structures beyond the diffuse component, including mini-halos and Bose stars and their tidal streams, axions bound to compact objects such as the Earth and Sun, and axion strings. The axion field as viewed by a terrestrial search (right panels) can be characterized by its coherence properties over time and the structure of its spectra. Amplitudes of sub-structures in the frequency spectra were chosen for illustrative purposes and are not necessarily indicative of a feature’s expected prominence. The cosmic web image is a snapshot of gas shocks (blue) and DM density (orange) from the Illustris TNG Collaboration’s TNG100-1 simulation [174]. The upper left panel contains an artist’s conception of the MW’s spiral structure as informed by NASA’s Spitzer Space Telescope, with image credit to NASA/JPL-Caltech/R. Hurt (SSC/Caltech) [175].

conservative estimates for the halo distribution’s line shape and response to daily and annual modulations due to the motion of Earth-based detectors [178]. Another model of Bose DM halo was also created during this period, producing line shapes containing more fine structure and sensitivity to the path of a detector [179]. Ultralight ALPs ($m \leq 10^{-20}$ eV) [180] have been simulated via a Gross–Pitaevskii (GP) wave equation in small cosmological volumes capable of holding a cluster of field dwarf galaxies of halo mass up to $10^{9-11} M_\odot$, with semi-analytical techniques extrapolating the results to larger halo and particle masses relevant to some of the searches presented below [181–184]. The typical QCD axion mass range, however, remains out of reach of having its wave nature resolved in simulations of MW-mass halos even with modern zoom-in techniques, pushing the use of pre-existing N-body simulations with pressureless DM [185]. More recent work has found that Bose DM infall may be modified from the GP model, even above the coherence scale, with preliminary N-body simulations showing novel halo distributions and the potential for fine structure [186–188].

The mini-halos and Bose stars of post-inflationary axion models are also too small to be resolved in a numerical simulation of a MW-type galaxy, and their rate of survival to the present from tidal stripping due to stars, planets and other compact objects they may encounter is unsettled [189–192]. However, the general expectation is that there exist, in our local Galactic region, some residual number of compact mini-halos and Bose stars, and ultra-cold flows of tidally stripped matter in addition to the more diffuse component. The former will be seen as transient objects to terrestrial searches. The later will be visible in the local DM distribution, but with the number, trajectory, and location of flows being uncertain and time-dependent [189–191].

5 Micro-eV and Above

As discussed in section 3, simple DM production mechanisms for the QCD axion motivate searching at masses $m_a \gtrsim \mu\text{eV}$. The most well-established technique in this mass range is the resonant cavity haloscope, first proposed by Pierre Sikivie [45], where the electromagnetic fields created by an axion in a large static magnetic field B are resonantly amplified in a microwave cavity. A cavity mode of frequency f is sensitive to axions of mass near

$$m_a = (4.1 \mu\text{eV}) \frac{f}{\text{GHz}}. \quad (15)$$

To cover a wide range of axion masses, the mode frequency must be scanned. To maintain sensitivity to the QCD axion, the scan rate scales as

$$\frac{df}{dt} \propto QV^2C^2B^4T^{-2} \quad (16)$$

where Q is the quality factor, V is the volume, C is a geometric form factor, and T is the noise temperature.

In sections 5.1 and 5.2, we discuss the current and future goals of the Axion Dark Matter eXperiment (ADMX) collaboration, which is the most advanced existing experiment

targeting $\sim\mu\text{eV}$ masses. In the following sections, we discuss upcoming and proposed experiments which target progressively higher axion masses. Here the fundamental difficulty is that in order to maintain a high form factor C , the size of a simple cavity haloscope must scale with the axion Compton wavelength $1/m_a$. As a result, the volume falls as $V \propto 1/m_a^3$, significantly decreasing the scan rate.

The HAYSTAC experiment (section 5.3) aims to compensate for this using quantum metrology techniques, which decrease the noise beyond the standard quantum limit. The SQuAD experiment (section 5.4) boosts the signal with a high-Q dielectric cavity and reduces noise using qubit-based single photon counting. The proposed ALPHA (section 5.5) and MADMAX (section 5.6) experiments instead use alternative detectors, which break the scaling relation between the volume and the axion mass. Finally, the proposed BREAD experiment (section 5.8) does not rely upon resonance at all, leading to broadband sensitivity up to the highest axion masses. There is vibrant global interest in searching for axions, and we conclude in section 5.9 by describing some efforts based outside the US.

5.1 ADMX G2

Physics goals: The ADMX collaboration is operating the “Generation-2” ADMX haloscope project in order to cover the frequency range from 0.6–2 GHz (corresponding to axion masses between 2.5–8.3 μeV) at DFSZ coupling sensitivity by 2025. The ADMX-G2 project began collecting data in late 2016 and, as of this whitepaper, has published three data-sets [193–195]. It is currently the only experiment that has reached DFSZ axion coupling sensitivity. See Fig. 6 for recent exclusion limits.

Concept: The ADMX-G2 experiment is built around a large (8.5 Tesla) high inductance (540 Henry) NbTi Superconducting Solenoid with a 60 cm inner diameter and 112 cm long placed at the bottom of a re-entrant bore cryostat that allows for an experimental package (cavity system and cold electronics) to be installed. The ADMX collaboration deployed various experimental packages of increasing sophistication. Since 1996 it operated at LLNL at pumped LHe temperatures (1.2 K) to reach KSVZ axion couplings. The magnet system was moved to the U. of Washington in 2010 and the ADMX-G2 project was designed around connecting a Janis dilution refrigerator directly onto the large (~ 140 liter) microwave cavity to reduce the physical temperature to ~ 100 mK. A second “bucking” magnet is contained in a separate LHe reservoir ~ 1 meter above the main cavity which reduces the field to ~ 10 s of Gauss in the region where the cold-electronics (circulators, switches and quantum amplifiers) provide the first stage of amplification. RF power is then routed to low-noise transistor amplifiers for a 2nd stage of amplification before the signals are routed out of the fridge where they are processed by digitizing electronics. Motion control is provided by room-temp stepper motors connected through vacuum feedthroughs to cryogenic gearboxes that move tuning rods of various size to scan frequencies. The runs are split into frequency bands to match the tunable range of the quantum amplifiers and circulators. Run 1A used a Microstrip SQUID Amplifier but subsequent runs used Josephson Parametric Amplifiers (JPAs) for amplification. The employed cavities are shown in Fig. 3. Runs 1A and 1B used two 2 inch OD copper tuning rods that ran the length of the cavity, Run 1C used two 4.4 inch OD rods and Run 1D will use a single 8.1 inch OD rod to

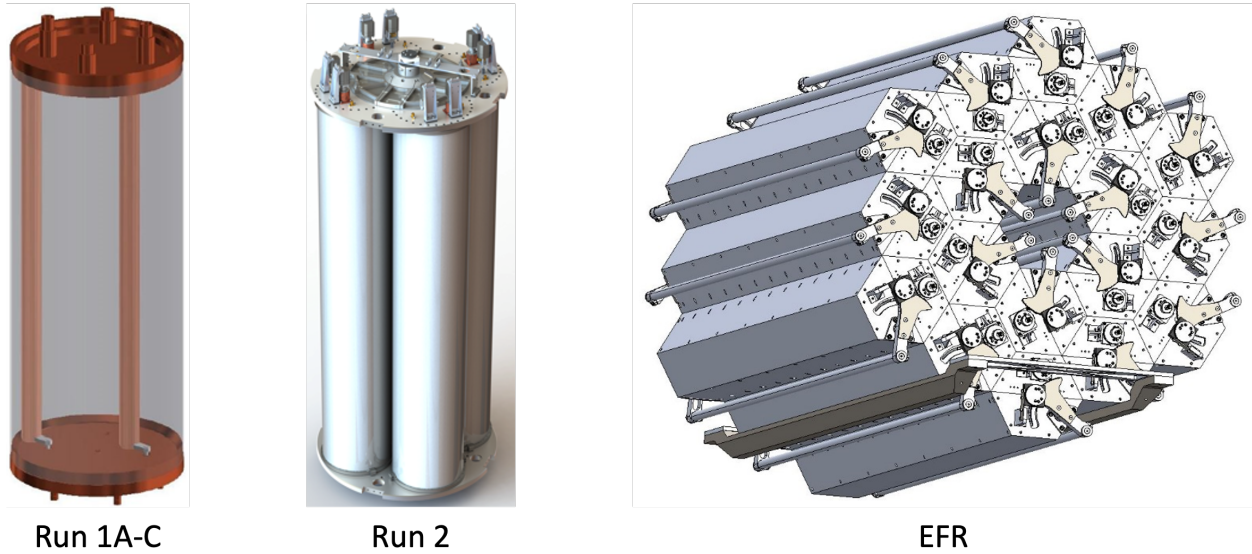


Figure 3: Cavity diagrams for Run 1A-C (Run 1D will use one tuning rod in a single cavity), Run 2A, and ADMX-EFR.

sweep to 1.4 GHz. After this Run 2A will combine 4 frequency locked cavities coherently to take advantage of the axions coherent signal to make up for the volume lost by operating a single cavity. It is anticipated that this system will complete the scan at DFSZ sensitivity by 2025.

5.2 ADMX EFR

Physics goals: The ADMX collaboration aims to cover the frequency range from 2–4 GHz with the Extended Frequency Range (EFR) experiment in the period 2024–2027. The goal is to achieve DFSZ sensitivity across this frequency range, which corresponds to an axion-mass range of 8.3–16.5 μeV (see also Figs. 6).

Concept: The cavity array inserted into the magnet is shown in Figure 8 (right). As ADMX transitions to the higher frequency parameter space, sensitivity loss due to the decreasing volume of the cavity will ensue. The ADMX collaboration will circumvent the reduction in scan rate with frequency in several ways:

1. Combine the signal from eighteen cavities to maintain the total volume (cf. Figure 3 (right));
2. Increase the magnetic-field strength through the use of high-field superconducting magnet materials such as Nb_3Sn and rare earth superconductors (REBCO);
3. Increase the quality factor by coating cavities with superconducting films or low-loss dielectrics;
4. Reduce the amplifier noise level by leveraging the properties of squeezed states or developing single photon counting techniques that evade the Standard Quantum

Table 1: Experimental parameters for ADMX-G2 and EFR runs. In Run 1 where parameters varied between runs, ranges or exceptions are given.

	Run 1A-D	Run 2A	EFR
Frequency Range	650–1390 MHz	2–4 GHz	2–4 GHz
Number of Cavities	1	4	18
Volume	106–136 ℓ	85 ℓ	80 ℓ
Q	58,000 (avg)	60,000	90,000
B Field	7.7 T (A: 6.85 T)	7.7 T	9.6 T
Avg Form Factor	0.45 (D: 0.35)	0.45	0.4
Noise Temperature	300–350 mK (A: 700 mK)	350 mK	325 mK
Operations Days	1000	300	1000

Limit.

The magnetic field will be provided by a 9.4 T magnet, currently located at UIC. The magnet bore is horizontal, simplifying access to the cavity array and enabling a new approach to the cryogenic system and to the implementation of RF electronics. Mechanical and thermal design is underway for the horizontal cryostat that minimizes dead volume in the bore and can support the cavity weight.

ADMX-EFR will use an array of eighteen cavities, shown on the right in Figure 3. The cavities use a ‘clamshell’ design that enables the tuning rods to be inserted with ease. Each cavity has a single tuning rod operated by a rotary piezo motor.

The design of the EFR signal chain is motivated by the need to achieve low system noise. Each cavity will have an independent signal chain, from the cavity to digitizer. The front-end amplification will be provided by a flux-pumped JPA for each cavity. Flux-pumped JPAs reduce the risk of contamination from the pump tone within the signal band and remove the need for a directional coupler. Signals will be digitized by phase-locked digitizers and combined after calibration accounting for phase and amplitude differences between channels.

The cryogenic electronics, not visible in Figure 8 (right), will be physically separated from the cavities and magnet. The cavities and cryogenic electronics will use independent dilution refrigerators to maintain their own ideal system temperatures. The benefits of this design are two-fold: (1) the electronics can be maintained at a lower temperature than the cavities, thereby reducing the system noise, and (2) JPAs are highly susceptible to magnetic fields, and operating them away from the magnet will protect them from magnetic flux penetration that can diminish their performance.

Table 1 shows the target performance for ADMX-EFR and various system parameters.

5.3 HAYSTAC

Predictions of the axion mass have tightened up dramatically, with the higher masses $m_a \approx 15\text{--}50 \mu\text{eV}$ (4–12 GHz) now being a particularly well motivated region [150, 196]. The Haloscope at Yale Sensitive to Axion cold dark matter (HAYSTAC)[197–199] experiment,

utilizes a quantum squeezed receiver which evades the Standard Quantum Limit (SQL) entirely, and thus enables an acceleration of the scan rate by a factor 2-3 in the exploration of the currently open axion mass range. At the same time, the HAYSTAC experiment is also intended to be an agile technology platform where the latest advancements in quantum measurements/instrumentation for axion searches can be explored over the next decade.

From its inaugural data run in 2015, HAYSTAC has been the only experiment to operate at the SQL, and since 2018, below it, the first data publication from the Squeezed-State Receiver (SSR) appearing in Nature in early 2021 [199]. It is thus one of only two experiments to employ squeezed-states in fundamental physics, the other being LIGO. In addition, optimizations in the Bayesian analysis chain [200], have accelerated the scan rate by a further factor of ≈ 3 over the standard mode of operation, and our codification of the axion haloscope analysis techniques have been adopted by several other QCD axion sensitive haloscopes [194, 201]. With these advancements in hand, the HAYSTAC experiment is transitioning to become a data production experiment that seeks to cover the ≈ 4 -6 GHz range as quickly as possible while maintaining close or better than $1.5\times$ KSVZ sensitivity.

While the current analysis efforts focused on the 4-6 GHz range, the next iterations of the HAYSTAC experiment will focus on higher mass ranges to develop the technologies and techniques for axion searches in the 10-12 GHz range. Moving forward in terms of hardware, the HAYSTAC team seeks to upgrade the current HAYSTAC magnet to a 12 Tesla Nb_3Sn magnet, demonstrate 4 dB of squeezing or better, and continue to push forward on several promising extensions of cavity designs such as a 7-rod cavity design [202] or the testing of tunable resonators utilizing photonic band gap structures to eliminate the forest of intruder TE modes with all the resonator work being led by UC Berkeley. The Josephson parametric amplifiers used in the current version of HAYSTAC, have already been proven to work effectively up to 12 GHz, but further R&D efforts will be needed to push this effective frequency range even higher. The Colorado group is simultaneously working on the Cavity Entanglement And State-swapping Experiment For Increased Readout Efficiency (CEASEFIRE) R&D project to improve the quantum axion search enhancement even further by attacking the biggest limitation in the initial demonstration of the squeezed state receiver, namely loss in transporting the squeezed microwave fields [203]. In the next three years, the goal is to deploy the CEASEFIRE concept in an axion search haloscope, demonstrating a factor of 10 or more speed up beyond the quantum limit. HAYSTAC will also continue other R&D efforts such as a quantum non-demolition Rydberg atom single-quantum detector with an eye towards higher frequency axion searches, this effort being led by Yale.

By 2023, Yale will be completing a new Physics Science and Engineering Building that includes a state-of-the-art Advanced Instrumentation Development Center which includes fabrication facilities and other vital infrastructure to support Yale's quantum science and advanced instrumentation initiatives. The building will provide new laboratory space for HAYSTAC and enable more research on quantum devices, making Yale a national center for quantum-enhanced dark matter research and providing support for upcoming HAYSTAC runs. With exciting improvements from the analysis, hardware and infrastructure, HAYSTAC lies in an excellent position to scan over a wide range well motivated unexplored axion parameter space in the ≈ 4 -12 GHz (15 - $50 \mu\text{eV}$) mass range over the

coming decade.

5.4 SQuAD

Physics Goals: The Superconducting Qubit Advantage for Dark Matter (SQuAD) experiment plans to perform resonant searches for dark matter axions with DFSZ sensitivity in a broad range from 10-30 GHz using high quality factor dielectric cavities combined with qubit-based single photon detectors which evade the quantum zero-point noise. The targeted mass range can be efficiently scanned over the course of a couple of years, possibly with multiple, simultaneously running experiments.

Concept: While contemporary axion search experiments in the GHz range overcome a poor signal-to-noise ratio by extensive averaging of the noise fluctuations, this strategy cannot work for higher frequency searches at $f = 10$ GHz and beyond. As shown in Fig. 4, the expected axion signal photon rate (black line) plummets with increasing frequency because the resonant cavity size must shrink to match the axion’s Compton wavelength. Meanwhile, the thermal or vacuum noise is incurred with each individual readout, and as the signal frequency increases, so does the readout rate and the resulting noise background rate (blue line). The current techniques are thus not scalable to higher frequencies.

The signal rate can be increased using extremely high quality factor $Q_c \approx 10^7$ dielectric cavities made by nesting a series of low loss cylindrical cavities to reflect the photon inward, keeping its electric field away from the lossy copper walls of the cavity enclosure [204]. For high $Q_c > Q_a = 10^6$, the axion signal power saturates to its maximum value as it becomes limited only by the dark matter coherence time Q_a/f . At longer time scales, the cavities can be used as incoherent photon power accumulators which store the signal energy for later readout, much as a CCD bucket would store signal electrons. The noise rate again scales with the readout rate which can now be very slow due to the extremely long cavity storage lifetimes Q_c/f . These improvements are reflected in the plot.

While higher frequency thermal photons will disappear at low temperatures, the quantum zero-point noise will be inevitable in linear amplifier readouts which measure both non-commuting quadratures of the signal photon wave. This Heisenberg uncertainty noise can be evaded by using single photon detectors which measure only the amplitude and not the phase of the photon wave [205]. Qubit-based quantum non-demolition techniques have reduced the effective dark counts by at least 4 orders of magnitude (solid red curve) relative to the quantum noise [206], thus reducing the required averaging time also by 4 orders of magnitude. The resulting rate sensitivity is shown in dashed red.

Sensitivity & Timeline: Using demonstrated experimental parameters, the SNR is favorable for $f < 30$ GHz and so experiments at these frequencies can be quickly done over the next couple of years. Due to non-negligible averaging times, efficient coverage of the mass parameter space may require multiple haloscopes to be simultaneously operated, perhaps by different experimental groups. R&D is ongoing on developing an analogous photon counting readout based on Rydberg atoms which can be operated at the higher frequencies where qubit devices become more difficult to design and fabricate. Background rates are expected to be similarly low for atom-based readout.

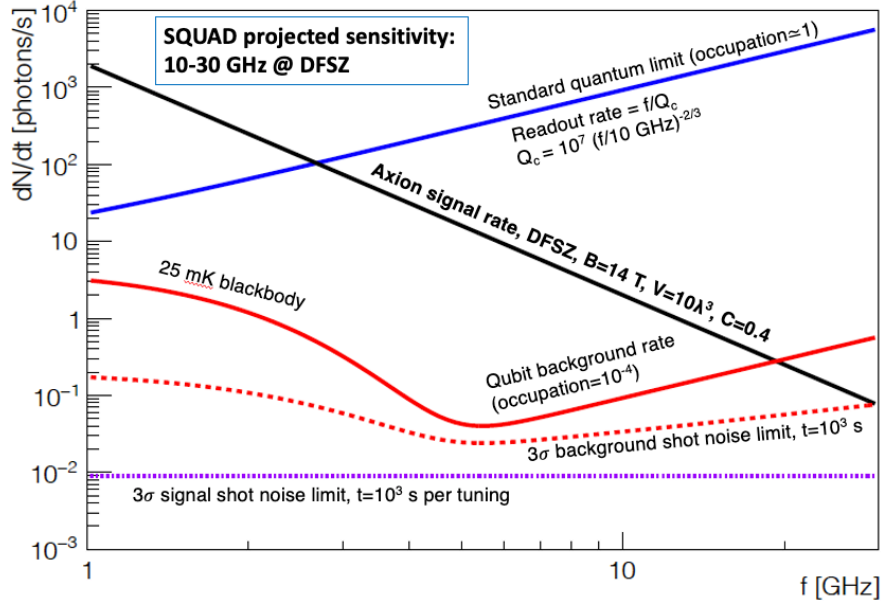


Figure 4: Predicted signal and background rates for SQuAD along with sensitivity obtained when averaging over 10^3 s integration time per cavity tuning. For demonstrated experimental parameters, DFSZ sensitivity is obtained for frequencies up to 30 GHz.

5.5 ALPHA

Physics goals: The Axion Longitudinal Plasma HALoscope (ALPHA) Consortium aims to explore high mass axions (5-50 GHz) by pioneering a plasma haloscope.

Concept: At high frequencies, the small size of simple cavities leads to a dramatic loss in signal power. In order to push above a few GHz, the tyranny of volume scaling must be ameliorated. One recent proposal of how to do so is to modify the wavelength of light inside the device, giving the photon an effective mass (plasma frequency). By matching the plasma frequency to the axion mass resonant conversion can be achieved regardless of system size [207]. This “plasma haloscope” is capable of searching for high mass axions between 5-50 GHz, depending on detector technology. For an appropriate plasma to be found, it must be tunable, low loss and capable of operating in cryogenic environments. One remarkable option is to use a wire metamaterial, [208]. As the plasma frequency is simply a function of the geometry of the wires, it can be tuned through simple geometric changes. Further, by using high quality copper or superconducting wires the medium exhibits low losses, leading to a competitive device.

Sensitivity & Timeline: The ALPHA consortium is currently performing research in service of realizing the first plasma haloscope. ALPHA is working towards a physics capable experiment by 2026, as shown in Fig. 5, which would be sensitive to well motivated axions and dark photons [209] in the range of 5-50 GHz. Significant progress has been made recently in both modelling and experimentally validating [210, 211] the properties of wire array metamaterials, which supports projections of $Q > 10,000$. The timeline for the full experiment has also been dramatically accelerated due to the commitment of a 13 T magnet, 0.5 m diameter and 1.7 m long, by the Helmholtz Forschungszentrum Berlin to ORNL.

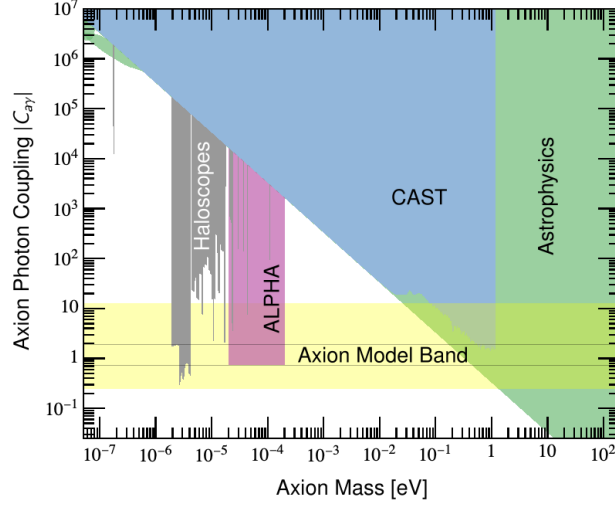


Figure 5: Axion parameter space showing the dimensionless axion-photon coupling constant C_{ay} as a function of the axion mass, m_a , with various bounds. This dimensionless coupling is defined so that it is $O(1)$ for models which solve the strong CP problem regardless of the axion mass. The axion mass gives the frequency at which the field oscillates, typically corresponding to the microwave regime (roughly 10 GHz). Haloscope experiments looking for dark matter are shown in grey, the limit from the CAST helioscope looking for solar axions is shown in blue and astrophysical limits are shown in green. The extended QCD axion model band is shown in yellow, with traditional KSVZ and DFSZ models shown as black lines. The region to be explored by ALPHA is shown in purple, covering a significant portion of well-motivated parameter space. This projection assumes a plasma haloscope with quality factor $Q=5000$ inside a 13 Tesla, 50 cm bore solenoid magnet using quantum limited detection running for three years.

This magnet will be transferred and commissioned in late 2022, and made available to ALPHA.

5.6 MADMAX

Physics Goals: The MAgnetized Disc and Mirror Axion eXperiment (MADMAX) [176, 212] is designed to probe the QCD axion in the mass range motivated by the post-inflationary symmetry breaking scenario, in particular from 40 to $400 \mu\text{eV}$ (10 to 100 GHz), complementary to the reach of ADMX-G2 [193] and ADMX-EFR [213], cf. Figure 6.

Concept: As described above, the cavity haloscope concept suffers from diminishing volume at high frequencies. The dielectric haloscope concept [212, 214, 215] generalizes the cavity to a resonator with a much reduced quality factor, however with a larger volume: Placing a dielectric disc in a dipole-magnetic field, axions can convert to electromagnetic radiation on the disc surface. By placing multiple dielectric discs in front of a metal mirror (dielectric haloscope), the emissions from the different surfaces can constructively interfere and excite resonances between the dielectrics. Both effects give rise to the so called power boost factor β^2 , defined as the ratio of power emitted by only a perfect mirror

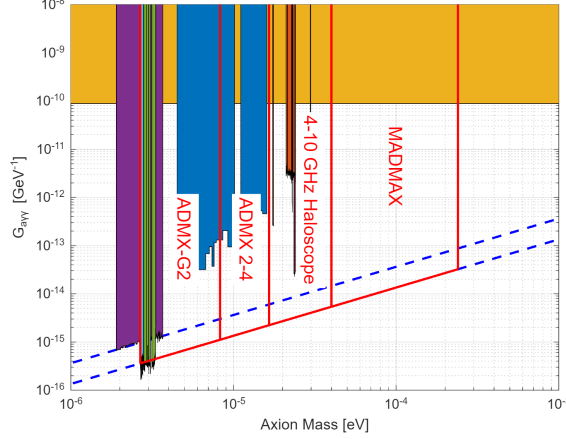


Figure 6: Expected sensitivities in the m_a - $g_{a\gamma\gamma}$ plane for ADMX-G2, ADMX2-4 and MADMAX (red contours), compared to existing limits (solid regions) and the KSVZ (DFSZ) QCD axion benchmark models denoted by upper (lower) blue dashed lines. Also shown is the potential reach of a generic future 4-10 GHz ADMX-like experiment.

in vacuum and the dielectric haloscope. Using 80 lanthanum aluminate (LaAlO_3) discs, MADMAX is expected to reach a boost factor of $\beta^2 \sim 10^5$ over a bandwidth of 20 MHz, giving an emitted power of

$$P_\gamma \approx 4 \times 10^{-22} \text{ W} \left(\frac{\beta^2}{10^5} \right) \left(\frac{B_e^2 A}{100 \text{ T}^2 \text{ m}^2} \right) \left(\frac{|C_{a\gamma}|}{1} \right)^2 \left(\frac{\rho_a}{0.45 \text{ GeV cm}^{-3}} \right), \quad (17)$$

where B_e is the external magnetic field parallel to the disc surfaces, A is the disc area and $C_{a\gamma} = -\frac{2\pi f_a}{\alpha} g_{a\gamma\gamma}$ with $|C_{a\gamma}| \sim 0.7$ for DFSZ axions.

Sensitivity & Timeline: The collaboration is planning the first ALP search using a proof-of-principle ‘closed booster system’ in the 1.6-T MORPURGO magnet at CERN at room temperature. Its sensitivity is expected to exceed existing limit from CAST at around $80 \mu\text{eV}$. The collaboration is also working on tuning the system at cryogenic temperature and in a strong magnetic field. The lessons learned will be used to construct a prototype detector shown in Figure 7. It is planned to begin its operation in 2024 at CERN and place ALP DM limits from 90 to $100 \mu\text{eV}$ with $g_{a\gamma\gamma} > 10^{-12} \text{ GeV}^{-1}$. The sensitivity of the final MADMAX will depend on outcome of the prototype booster and magnet development.

Opportunities for US Participation: The ADMX and MADMAX collaborations have identified various opportunities to exploit synergies. These include commissioning and running a ‘world’s first’ large-bore, high-field dipole magnet, reliable mechanical alignment technologies at high B -fields and low temperatures, resonator calibration, electronics and dielectric material characterization. These topics represent central R&D challenges not only to MADMAX but to the whole axion community while being largely complementary in probed mass ranges. MADMAX explicitly welcomes contributions from U.S.-based groups.

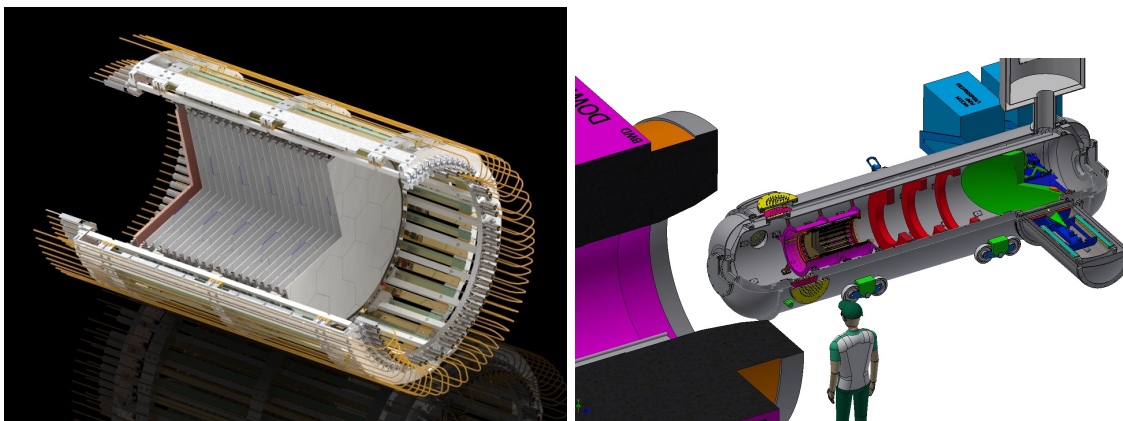


Figure 7: MADMAX Prototype design. The axion-induced radiation from the booster (left) containing 20 discs of 30 cm diameter is collected by the focusing mirror and antenna. It will be operated in the MORPURGO magnet at CERN, offering a 1.6 T dipole field (right).

5.7 LAMPOST

Physics Goals: The goal of the LAMPOST (Light a/A' Multi-layer Periodic Optical SNSPD Target) experiment [216, 217] is to search for axions in the 0.1 – 10 eV mass range, with eventual reach toward the 10 meV regime.

Concept: As described in Section 5.6, the dielectric haloscope generalizes the cavity to a resonator with structure on the scalar of the axion Compton wavelength in order to optimize axion to photon conversion over a larger volume [212, 214–216]. At optical and IR frequencies, thin film deposition techniques can be used efficiently allowing a simple manufacture of the target. To cover a larger range of masses, multiple targets can be manufactured with datataking in parallel, or a single ‘chirped stack’ can be produced with layers varying in thickness across the stack [216]. The photons emitted are focused with a lens onto a parametrically smaller area detector, allowing for excellent signal to noise ratios. A setup of dielectric 100-layer pair targets placed in a 10T magnetic field will yield sensitivity to new parameter space in the sub-eV range with currently demonstrated dark count rates with superconducting nanowire single photon detectors [217]. The ultimate goal is the development of low-noise, lower frequency single photon detection. This will extend the LAMPOST technique to the 10 meV regime and allow access to the KSVZ and DFSZ axion parameter space.

Along with lower energy detectors, under development are background rejection techniques as well as the ability of the SNSPD detector to interface with large magnetic fields; see Section 10.1.

5.8 BREAD

Physics Goals: The Broadband Reflector Experiment for Axion Detection (BREAD) [218] plans to perform broadband searches for wavelike DM across multiple decades in mass from around 0.2 THz up to astrophysical limits around optical frequencies. BREAD was recently founded as a multi-institute collaboration with substantial US leadership. Uni-

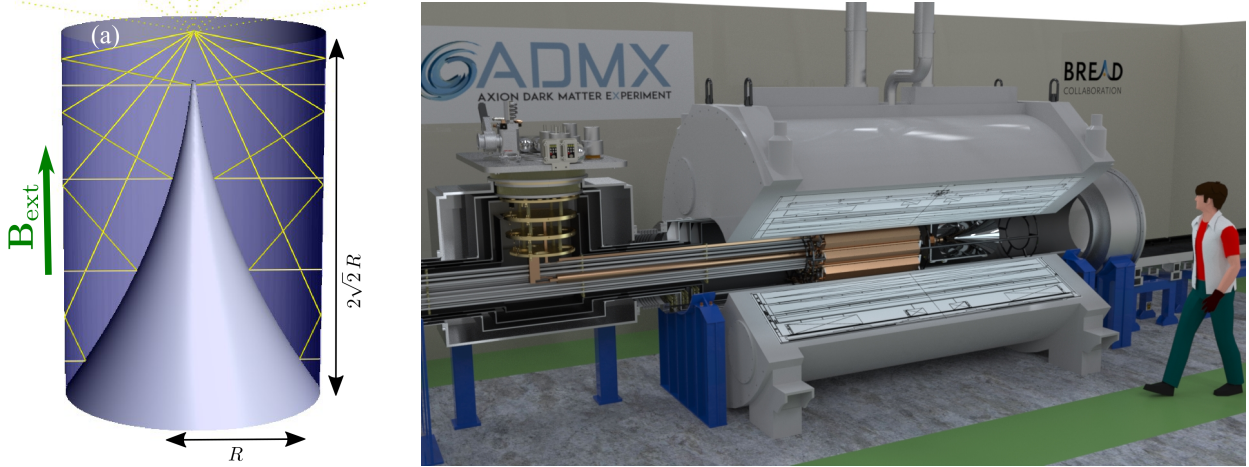


Figure 8: Left: Ray-tracing simulation of photons (yellow lines) emitted by the BREAD cylindrical barrel reflector and focused by the parabolic surface to a focus. Reproduced from Ref. [218]. Right: ADMX-EFR and the large-scale BREAD experiment will be hosted side-by-side in a former MRI magnet.

versities and national laboratories across the US are spearheading ongoing R&D efforts towards proof-of-concept pilot experiments. The experiment is planned to be located at Fermilab. Its scientific hallmark is broadband sensitivity for axion-like DM across terahertz frequencies using a unique geometry without resonant tuning to the unknown DM mass.

Concept: BREAD realizes the dish antenna concept [219] by using a cylindrical metal barrel to convert axion DM into photons, which a parabolic reflector focuses onto a low-noise photosensor. This geometry allows placement inside standard high-field solenoids and cryostats, which allows lower equipment costs. For axion-to-photon coupling $g_{a\gamma\gamma}$ and mass m_a , the emitted power is given by $P_a = \frac{1}{2}\rho_{\text{DM}}(B_{\text{ext}}^{\parallel}g_{a\gamma\gamma}/m_a)^2A_{\text{dish}}$ [219], where $\mathbf{B}_{\text{ext}}^{\parallel}$ is the external magnetic field with nonzero component parallel to the dish with area A_{dish} .

Figure 8 (left) shows the ray-tracing simulation in the BREAD geometry inside a solenoid with magnetic field B_{ext} . Photon paths are shown as yellow lines, which are emitted perpendicularly to the barrel surface with length $L = 2\sqrt{2}R$ and the parabolic surface with radius R focuses the rays to a point. Various state-of-the-art photosensor technologies for projected sensitivity studies are considered in Ref. [218]. This includes commercial cryogenic thermistors (IR LABS) alongside established solutions widely deployed for astronomy applications, namely kinetic inductance detectors (KID) and transition edge sensors (TES). Meanwhile, quantum capacitance detectors (QCDet) and superconducting nanowire single photon counters (SNSPD) exemplify emerging technologies with low-noise photon counting capabilities.

Sensitivity & Timeline: Progress towards small-scale prototype experiments targeting dark photon benchmarks (detailed in Ref. [218]) are ongoing at Fermilab. Figure 9 shows the projected sensitivity of large-scale BREAD realizations with various photosensor technologies. Specific benchmarks are assumed for the magnetic field $B = 10$ T, dish area $A_{\text{dish}} = 10\text{ m}^2$, with experimental runtimes of 10 and 1000 days. This also motivates photosensor R&D will continue to reduce noise for probing QCD axion benchmarks. These

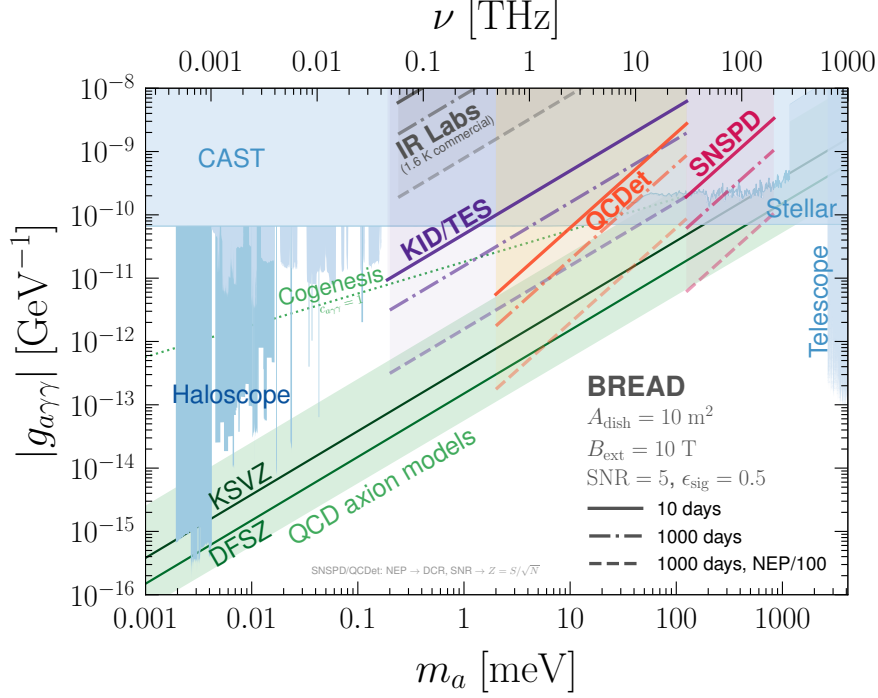


Figure 9: Projected sensitivity for BREAD by photosensor technology (thick lines) in axion coupling vs. mass plane. Different assumptions on exposure time and sensor noise equivalent power (NEP) are displayed in the legend. Reproduced from Ref. [218].

sensitivities could be achieved by hosting BREAD as a side experiment to ADMX-EFR within the same magnet, as shown in Fig. 8 (right).

5.9 Global Context

In synergy with programs in the US, wavelike dark matter programs are gaining momentum around the globe. Here we elaborate on some currently funded projects. Due to space constraints, we must omit several other projects, such as the cavity haloscopes developed at the Center for Axion and Precision Physics Research in Korea [220].

5.9.1 ORGAN

ORGAN is a high-mass axion haloscope, targeting the 15-50 GHz region (60-200 μeV). The experiment operates in a BluFors XLD system, with the capacity to reach a base level 7 mK, inside a 12.5 T environment. The pathfinding run placed the first limits on axions from a haloscope above 10 GHz, beating CAST at 26.6 GHz [221]. After this, ORGAN entered a planning and commissioning stage for long term operations (Phase 1 and 2), which commenced in 2021 [222]. Phases 1a and 1b are short, targeted scans of 15-16 GHz and 26-27 GHz ranges respectively, using equipment on hand (HEMT amplifiers and established resonator designs). Phase 2 encompasses the entire 15-50 GHz region, broken down into 5 GHz sub-phases, which will re-scan the regions in Phase 1 with enhanced

sensitivity, using single photon counters (SPCs), or quantum limited amplification. With efficient GHz SPCs, ORGAN aims to reach the DFSZ axion limits. Phase 2 is expected to commence in 2023. Phase 1a ran in 2021, successfully excluding ALP Cogenesis models between 15.3–16.2 GHz (63-67 μeV) [222]. Phase 1b is in commissioning, expected to commence in 2022, using HEMT amplification, and newly designed sapphire loaded cavity resonators with dielectric-boosted sensitivity [223, 224].

5.9.2 RADES

The RADES project is developing axion dark matter haloscopes to be used in dipole magnets. Up to the present day, RADES has collected data at CAST and SM18 magnets (CERN), and in the long run it plans to use the BabyIAXO and Canfranc magnets for new data campaigns. Most cavities of RADES are based on an arrangement commonly used in radio-frequency filters: an array of small microwave sub-cavities, whose size controls the operation frequency, connected by rectangular irises, providing high volumes. The detection principle, the theoretical framework and the haloscope details, can be found in a recent overview [177]. Besides the goal of increasing the sensitivity of detection through achieving large geometric factors and high quality factors, a key feature of the system must be the tuning of the resonant frequency. RADES designed and built a mechanical tuning system, but they are also working on another tuning method: electrical tuning by ferroelectric materials, which can provide an avenue that is less prone to mechanical failures and thus complements and expands existing techniques. Also, ferroelectrics allow the ability to independently adjust the many different cavity frequencies to maintain the correct mode structure and field pattern.

5.9.3 ALPS II

The Any Light Particle Search II (ALPS II) probes for axion-like particles with a coupling factor of $g_{a\gamma\gamma} \geq 2 \times 10^{-11} \text{GeV}^{-1}$ at all masses below 0.1 meV [225, 226]. Axion-like particles with similar coupling factors would explain astronomical observations such as TeV transparency and larger than expected stellar cooling rates [227, 228]. ALPS II is also sensitive to potential scalar cousins of the pseudo-scalar axion and to hidden sector photons.

Method: Light-shining-through-a-wall (LSW) experiments such as ALPS II are broadband experiments which send a strong laser beam through a magnetic dipole field. Some of the photons will be turned into axions which pass through a photon-blocking wall behind which they enter a second magnetic field. Inside this field, a small fraction of these axions reconvert back into photons. Compared to the other methods described in this whitepaper, this method is less sensitive to weak axion couplings, but does not require the axion to comprise dark matter.

ALPS II uses two 120 m long strings of straightened HERA dipole magnets (5.3 T) in series, a 70 W laser system similar to the advanced LIGO laser systems, and two high finesse 122 m long optical cavities to enhance the source and the signal photons on each side of the wall. This setup increases the regenerated photon rate by 12(!) orders of magnitude compared to earlier LSW experiments [229].

Current schedule: The ALPS collaboration is an international collaboration with groups from Germany, the UK, and the US which is currently commissioning the ALPS experiment at DESY in Hamburg, Germany. The first science data sets with sensitivities reaching $g_{\gamma\gamma} < 10^{-10} \text{ GeV}^{-1}$ for pseudo-scalar (axion-like) and for scalar particles as well as for hidden sector photons are expected for the fall 2022. It will take a few more years and a few improvements such as better cavity mirrors with improved surface roughness before the final sensitivity will be reached.

Future plans: Unfortunately, the sensitivity does not scale well with experimental parameters and another leap in sensitivity using the LSW method is unlikely. However, the magnet strings and optical infrastructure enables additional ground-breaking experiments such as measurements of vacuum birefringence predicted by Heisenberg and Euler in 1938(!) or high frequency gravitational waves [230, 231].

6 Below Micro-eV

It is also interesting to consider axions with mass well below μeV , corresponding to axion frequencies below GHz. As noted in section 4, ALPs can be produced with the appropriate dark matter abundance in this range through the ordinary misalignment mechanism. The QCD axion could also comprise dark matter, given a tuning of the initial misalignment angle, anthropic arguments or modified cosmologies [e.g. 18, 118–126, 141, 142, 232].

In this mass range, the cavity haloscopes introduced in section 5 cannot be used, since it is impractical to build a cavity large enough to have a sufficiently low mode frequency. Instead, most experiments use the lumped element approach, where the electromagnetic fields produced by the axion drive a current through a pickup coil. In sections 6.2 and 6.3, we discuss ABRACADABRA and SHAFT, two pioneering experiments which used this technique to achieve broadband sensitivity. In sections 6.1 and 6.4, we discuss the current and future plans of the DMRadio experiment, which aims to probe the QCD axion by amplifying the axion-induced current in a resonant LC circuit.

Finally, in section 6.5, we discuss the recently proposed heterodyne approach with SRF cavities, which decouples the axion frequency and the mode frequency by using a superconducting cavity containing an oscillating background magnetic field. The presence of this field introduces new noise sources, but also significantly increases the signal power, especially at low axion masses. This approach thus achieves comparable sensitivity to axions without requiring large, high-field magnets or quantum sensing techniques.

6.1 DMRadio- m^3

Physics goals and status: The DMRadio- m^3 experiment aims to search for the QCD axion over the mass range $20 \text{ neV} \lesssim m_a \lesssim 800 \text{ neV}$, achieving DFSZ sensitivity over the range $120 \text{ neV} \lesssim m_a \lesssim 800 \text{ neV}$ with a 5 year total scan time. This mass range begins to probe the top of the GUT-scale QCD axion masses, in addition to testing a wide swath of interesting ALP parameter space (see Fig. 10.) DMRadio- m^3 will extend the reach of the DMRadio-50L experiment that will probe the ALP parameter space between 5 kHz and 5 MHz ($20 \text{ peV} \lesssim$

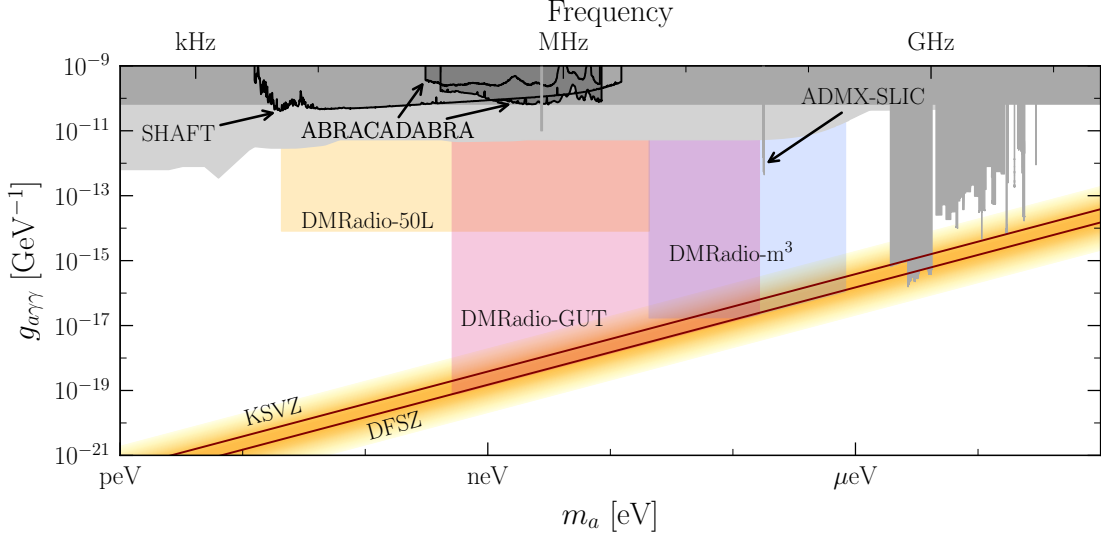


Figure 10: The projected sensitivities for DMRadio-50L, DMRadio- m^3 , and DMRadio-GUT. The DMRadio program aims to probe the QCD axion below $1 \mu\text{eV}$. This assumes scan times of 3 years for DMRadio-50L, 5 years for DMRadio- m^3 , and 5 years for DMRadio-GUT.

$m_a \lesssim 20 \text{ neV}$). The DMRadio program also opens the door for an ambitious and definitive search for the GUT-scale QCD axion called DMRadio-GUT (see Sec. 6.4).

Experimental approach: DMRadio- m^3 uses a lumped element approach consisting of a coaxial inductive pickup inside of a solenoidal magnet, with a tunable capacitor providing an LC resonant enhancement. This technique builds on the work of the ABRACADABRA-10 cm broadband axion search [233, 234], DMRadio-Pathfinder resonant dark photon experiment [235] and techniques originally proposed in [236–238].

DMRadio- m^3 will consist of a series of interchangeable coaxial inductive pickups with volume up to $\sim 1.2 \text{ m}^3$ inside of a 4 T solenoidal magnet. The experiment will scan the frequency range from 5 MHz to 200 MHz. Since the pickup sits inside a large magnetic field, it will be constructed from normal conducting OFHC copper. The resistive losses in the copper will dominate the loss in the circuit. However, this is mitigated by a relatively low anomalous surface resistance at frequencies and temperatures relevant for DMRadio- m^3 as well as a relatively large volume to surface ratio. Approaches to decrease this loss using superconducting coatings are being pursued by other experiments (see [239, 240] and Sec. 10.3) and may be considered in the future. Multiple coaxial pickups of decreasing size are required to keep the detector in the magneto-quasistatic limit as the detector probes to progressively higher frequencies and the experiment will be designed to allow efficient exchange of the pickup components.

The resonance frequency will be scanned using a tunable capacitor made from superconducting material and low-loss dielectrics like sapphire. The target Q-factor for DMRadio- m^3 is $Q \sim 10^6$ at 30 MHz and is limited by loss in the copper pickup. The signal will be read out by low noise SQUID amplifiers with a target noise level of $20\times$ the standard quantum limit or better. Eventually, the sensitivity could be further improved by incorporating next-generation beyond-SQL sensors, discussed in Sec. 10.1.

The detector will be cooled in a large dilution refrigerator to an operating temperature of 20 mK to reduce the thermal noise. Cryostats of this scale have been demonstrated before [241].

Projected sensitivity and timeline: The experimental scan rate $\partial \log \nu_r / \partial t$ at resonant frequency ν_r is proportional to the quantity $c_{\text{PU}}^4 B_0^4 V^{10/3} \bar{\mathcal{G}}(\nu_r, k_B T, n_A)$, where B_0 and V are the characteristic magnetic field and pickup volume and c_{PU} is a geometric coupling which can be related to a flux coupling in the magneto-quasistatic limit [242]. $\bar{\mathcal{G}}$ is a coefficient which relates the thermal noise temperature, $k_B T$, and the number of noise photons added by the amplifier, n_A , to the scan rate. In the low frequency range, where the noise budget is dominated by thermal noise photons $n_{\text{th}} = (\exp(h\nu/k_B T) - 1)^{-1}$, and assuming the readout circuit to be optimally coupled for fastest scan rate, this coefficient is given approximately by $\bar{\mathcal{G}} \approx (12\sqrt{3}n_{\text{th}}n_A)^{-1}$. In the frequency range relevant for DMRadio-m³, $\bar{\mathcal{G}}$ takes a more complex form given in [242] with extended discussion in [243].

The projected DMRadio-m³ sensitivity is presented in Fig. 10. DMRadio-m³ aims to achieve DFSZ sensitivity over the range from 30 MHz to 200 MHz ($120 \text{ neV} \lesssim m_a \lesssim 800 \text{ neV}$) and sensitivity to the QCD axion all the way down to 5 MHz (20 neV). DMRadio-m³ is designed for a 5 year scan time and targets data taking in 2026.

6.2 ABRACADABRA Demonstrator

Physics goals and status: ABRACADABRA-10 cm aims to search for axion dark matter through the electromagnetic coupling in the sub- μeV mass range using the lumped element detection technique.

Experimental approach: ABRACADABRA-10 cm uses a toroidal geometry based on the proposal [236]. The detector consists of a 10 cm toroidal magnetic with a maximum field of 1 T. Axion dark matter converts the DC, toroidal, magnetic field into an AC magnetic field through the center of the toroid – a region that would otherwise be free of any magnetic field. In the Run 1 configuration [244], the central region was read out in a broadband configuration by a superconducting pickup loop connected to a two-stage SQUID readout. The magnet and loop were shielded inside of a superconducting shield to protect them from environmental noise. The detector and SQUIDs were cooled to an operating temperature of 700 mK in a dilution refrigerator. Vibrational noise was mitigated using a vibration isolation system, and the detector was shielded with a simple MuMetal shielding. A calibration procedure injected a current into a dedicated loop inside the magnet to generate an axion-like magnetic field allowing a direct reconstruction of the detector gain. This procedure indicated parasitic inductance in the readout scheme which decreased the sensitivity by a factor of ~ 6.5 .

The SQUID voltage was sampled continuously at a rate of 10 MS/s for weeks-long runs. The timestream was FFT'd in real time, downsampled, and FFT'd again, building multiple spectra capable of searching the full axion mass range from 50 kHz to 5 MHz with sufficient spectral resolution. Data were collected in magnet-on and magnet-off configurations, the former being used for the axion dark matter search, and the latter to veto spurious signals from other sources. Run 1 consisted of 2.6×10^6 s of magnet-on data, plus another 2 weeks worth of magnet-off data.

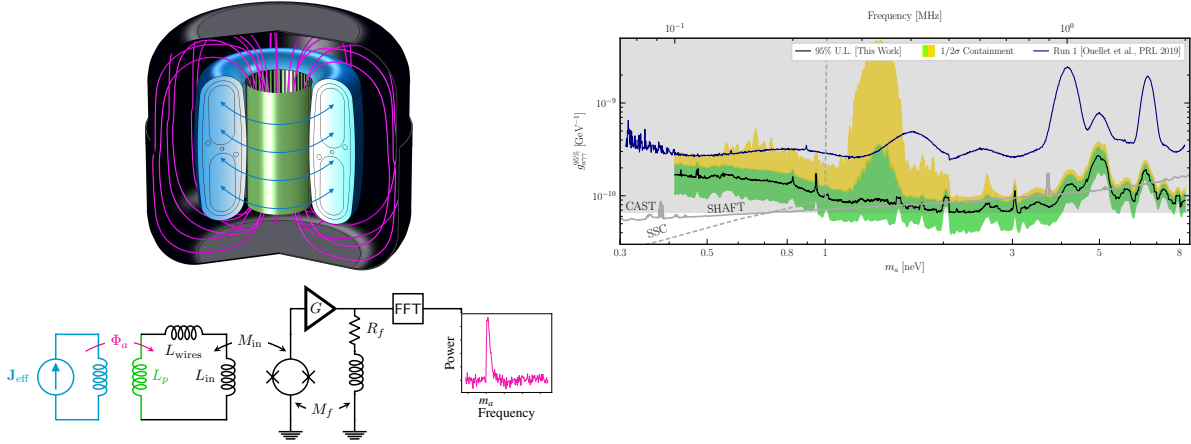


Figure 11: Left Top: Diagram of the ABRACADABRA-10 cm detector used for the Run 3 results. A ~ 10 cm-scale 1 T toroidal magnet (blue) drives the axion induced magnetic field (purple lines) which is screened by the cylindrical pickup (green). The detector is enclosed within a superconducting shield. Left Bottom: Schematic of the broadband readout. The axion effective current (blue) drives a flux through the inductive pickup (green), which is inductively coupled to a SQUID readout in flux lock mode and monitored. Right: 95% CL exclusion limits from Runs 1 and 3 of the ABRACADABRA-10 cm prototype. Figures from [245].

After the first run, the detector underwent an upgrade to increase its sensitivity to axion dark matter. The pickup loop was replaced by a pickup cylinder, which improved the coupling to the axion induced magnetic-field – i.e. driving more current for the same size axion induced magnetic field (see Fig. 11). The readout wiring was improved to reduce the parasitic inductance. The SQUIDS were moved to the coldest stage of the cryostat and cooled to an operating temperature of ~ 150 mK, while the magnet stayed at ~ 700 mK. Runs 2 and 3 were collected in this configuration, but Run 2 data were eventually discarded due to excess noise. Run 3 consisted of ~ 2 weeks of magnet-on data, and ~ 1 week’s worth of magnet-off data.

Results and Future Outlook: The ABRACADABRA-10 cm experiment collected Run 1 data in Summer 2018 and Run 3 data in Summer 2020. The ABRACADABRA-10 cm collaboration developed an analysis procedure to search the millions of mass points collected simultaneously in a broadband search – which does not have rescan capabilities. This procedure based on [246] correctly accounts for the “look-elsewhere effect.”

ABRACADABRA-10 cm placed the first laboratory based limits on axion dark matter below $1 \mu\text{eV}$ and was the first to demonstrate the lumped element approach to axion dark matter detection. The Run 1 results probed the mass range $0.31 \text{ neV} < m_a < 8.3 \text{ neV}$ ($75 \text{ kHz} - 2 \text{ MHz}$), setting 95% C.L. limits down to $g_{a\gamma\gamma} < 1.4 \times 10^{-10} \text{ GeV}^{-1}$ [244, 247]. The Run 3 results improved on this, setting 95% C.L. limits down to $g_{a\gamma\gamma} < 3.2 \times 10^{-11} \text{ GeV}^{-1}$ [245].

At low axion masses, the sensitivity was limited by vibrational noise coming from stray DC fields from the magnetic being transduced by vibrational noise from the pulse tube cooling system. In the axion search region, the sensitivity was limited by the SQUID flux

noise floor. Further upgrades to ABRACADABRA-10 cm could continue to improve sensitivity by factors of a few and perhaps extended in mass range, however, the detector is transitioning to a test bench for future R&D.

6.3 Search for Halo Axions with Ferromagnetic Toroids (SHAFT)

Physics goals and status: The SHAFT experiment is sensitive to the electromagnetic coupling $g_{a\gamma\gamma}$ of axion-like particles. The goal is to search for axion-like dark matter in the broad mass range between $\approx 10^{-12}$ eV and $\approx 10^{-8}$ eV, with coupling strength sensitivity down to 10^{-12} GeV $^{-1}$. SHAFT aims to explore the region of parameter space where ALP-photon mixing could explain the anomalous transparency of the universe to TeV gamma-rays [248–250]. The first-generation search has reported limits on the electromagnetic interaction of axion-like dark matter in the mass range that spans three decades from 12 peV to 12 neV [251]. Over part of this mass range it improved the CAST limits, at 20 peV reaching 4.0×10^{-11} GeV $^{-1}$ (95% confidence level), Fig. 12.

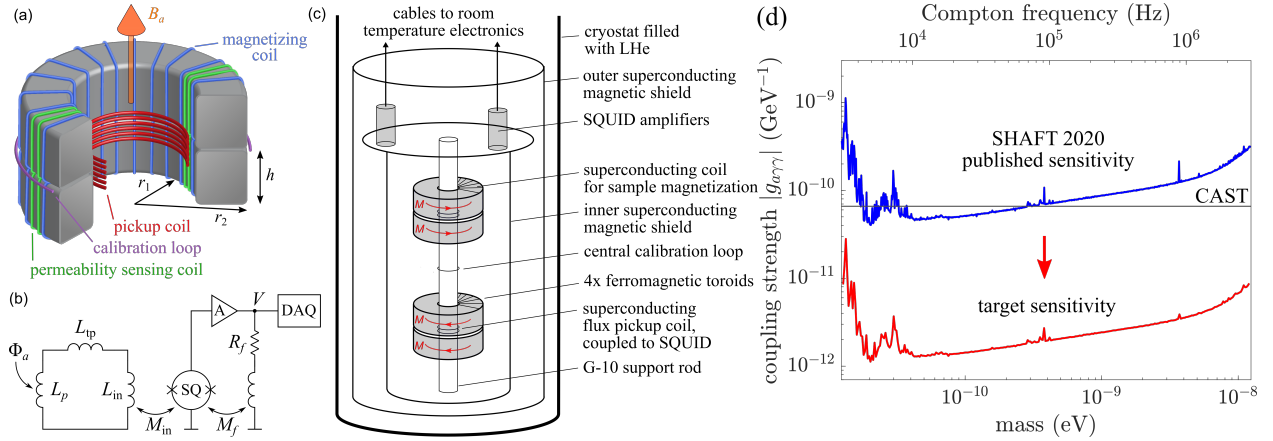


Figure 12: The SHAFT experiment and projected sensitivity [251]. (a) Schematic of a single detection channel. Two permeable toroids are independently magnetized by injecting current into a magnetizing coil wrapped around each toroid. (b) The circuit model that shows the axion-induced flux Φ_a coupling into the pickup coil (inductance L_p). The pickup coil is coupled to the SQUID magnetic flux sensor (SQ) via twisted pair leads (inductance L_{tp}) and input coil (inductance L_{in}). The SQUID is operated in the flux-locked-loop mode, with feedback resistance R_f . The feedback voltage V was digitized and recorded by the data acquisition system (DAQ). (c) The SHAFT experimental schematic. The apparatus contains four permeable toroids, shown such that the top and bottom channels are magnetized in opposite directions, to make use of phase-sensitive systematic rejection. The experiment operates at 4.2 K in a liquid helium bath cryostat. (d) Published limits set by the first-generation SHAFT search are shown in blue [251]. Target sensitivity of next-generation SHAFT search is shown in red.

Experimental approach: SHAFT takes the lumped-circuit approach, based on a modification of Maxwell’s equations in the presence of axion-like dark matter, which mixes with a static magnetic field B_0 to produce an oscillating magnetic field [236–238, 243, 245, 252].

An inductively-coupled SQUID is the detector of this oscillating magnetic field, with sensitivity of $150 \text{ aT}/\sqrt{\text{Hz}}$, which is at the level of the most sensitive magnetic field measurements demonstrated with any broadband sensor [251]. A toroidally-shaped permeable iron-nickel alloy material enhances the magnitude of the static magnetic field B_0 by a factor of 24, and thus improves sensitivity to axion-like dark matter. Systematic rejection is especially important to ensure discovery potential of broadband ultralight dark matter searches. The unique systematic rejection mechanism in SHAFT is the design that incorporates two independent detection channels, allowing discrimination between an axion-like dark matter signal and electromagnetic interference systematics. For collecting data sensitive to axion-like dark matter, the top channel toroids are magnetized counter-clockwise, and the bottom channel toroids clockwise, viewed from the top, Fig. 12(c). An axion-like dark matter signal would then appear in the two detector channels with opposite sign (180° out of phase). Electromagnetic interference, uncorrelated with toroid magnetization, would not have such a phase relationship and can be distinguished from an axion-like dark matter signal by forming symmetric and antisymmetric combinations of the two detector channels.

Projected sensitivity and timeline: The first-generation SHAFT sensitivity was limited by SQUID thermal noise at 4.2 K, apparatus vibrations, and the data taking timescale restricted to 41 h by liquid helium boil-off. As of 2022, the second-generation search is ongoing, aiming to improve sensitivity by a factor of 12 by mounting the setup in a cryogen-free dilution refrigerator, which will cool the SQUID sensors to millikelvin temperature and allow longer data-taking runs. We project that by the end of 2023 SHAFT will achieve sensitivity to $g_{a\gamma\gamma}$ at the level of $3 \times 10^{-12} \text{ GeV}^{-1}$ in the mass range $\approx 10^{-12} \text{ eV}$ to $\approx 10^{-8} \text{ eV}$. Scaling up the toroid volume by a factor of 3 will improve sensitivity to $10^{-12} \text{ GeV}^{-1}$ in 2024, Fig. 12(d).

6.4 DMRadio-GUT

Physics goals: DMRadio-GUT is a search for QCD axions at the GUT scale [253]. As shown in Fig. 10, the experiment would reach DFSZ sensitivities to masses from 0.4 neV to 120 neV, the bottom of DMRadio- m^3 's range (Sec. 6.1). At these low masses, the QCD axion-photon coupling is very small, $g_{a\gamma\gamma} \propto m_a$, necessitating technological advancements outlined here.

Experimental approach: DMRadio-GUT is based on the lumped element technique pioneered in ABRACADABRA-10 cm (see Sec. 6.2) that uses an LC circuit to couple to the axion field. For optimal sensitivity, the GUT experiment will have a resonant readout, with scan rate (in the relevant thermal noise-dominated regime)

$$\frac{d\nu_r}{dt} \sim \frac{10^6}{\text{SNR}^2} \left(g_{a\gamma\gamma}^4 \rho_{DM}^2 \nu_r \right) \left(c_{PU}^4 \frac{QB_0^4 V^{10/3}}{\eta_A k_B T} \right), \quad (18)$$

where the final term contains all of the experimental parameters [253]. Our goal is to have a scan time ~ 6 years, which we can accomplish by tuning the parameters shown in Eq. (18). Here we lay out a baseline scenario and R&D path. However, there are a variety

of combinations of these parameters which can achieve our goal sensitivity, and so if some R&D thrusts prove challenging, success improving other parameters can compensate.

The first design decision is the magnet. DMRadio-GUT will likely be a toroid, which keeps magnetic fields away from the sensitive readout electronics. The fastest way to increase the scan rate is to improve the strength of the magnetic field, B_0 , and experimental volume, V . In order to obtain DFSZ sensitivities throughout the mass range, our baseline goal is a 10 m^3 magnet with 12 T RMS field ($\sim 16\text{ T}$ peak field for a rectangular toroid with $r_{in}/r_{out} = 1/2$). This is achievable with Nb_3Sn or REBCO, as demonstrated by several recent and upcoming projects such as the High-Luminosity LHC [254, 255], and the SPARC tokamak [256].

The scan rate also scales with the fourth power of c_{PU} , a factor similar to the overlap factor in cavities, that describes how well coupled the energy from the axion current is into the pickup structure. Based on the calculations in [257], we can expect $c_{PU} \approx 0.1$.

The quality factor of the LC resonator, Q , is 20×10^6 in our baseline scenario. This number is twenty times the goal Q value for DMRadio-50 L. To reach this goal, we have started R&D on both superconducting resonators and active feedback at low frequencies. Either or both of these may be used to improve the readout circuit.

Finally, $k_B T$ and η_A represent the thermal and amplifier-added noise, respectively. By running at 10 mK, the GUT experiment will minimize thermal backgrounds. We hope to reduce η_A to -20 dB below the standard quantum limit through techniques like backaction evasion with devices such as Radiofrequency Quantum Upconverters [258, 259]. Although DMRadio-GUT is thermally limited, reductions in amplifier noise can still greatly improve the experiment's scan rate by increasing the sensitivity bandwidth, the bandwidth over which a given configuration can maintain an approximately constant SNR.

Projected sensitivity: With these baseline parameters, DMRadio-GUT can achieve DFSZ sensitivities to axions over almost two decades of axion masses in ~ 6 years of scan time, as shown in Fig. 10. Although some of the technologies needed to achieve this reach are still in development, there are several R&D paths that would be able to maintain the goal sensitivity and mass range with scan times under ten years. Building off of the successes of predecessor lumped element experiments with a multi-thrust R&D campaign, DMRadio-GUT will be able to definitively probe low-mass QCD axions down to below 1 neV.

6.5 SRF Cavities and Related Techniques

The previous subsections describe experiments with static magnetic fields, in which axion dark matter sources an effective current oscillating with frequency m_a . By contrast, in the recently proposed heterodyne approach [260–262], a microwave cavity is prepared by driving a pump mode with nonzero frequency $\omega_0 \sim 1\text{ GHz} \gg m_a$. The dark matter axion field causes frequency upconversion, driving power into a signal mode with nearly degenerate frequency $\omega_1 \simeq \omega_0 + m_a$ and distinct spatial geometry. This process is efficient provided that the pump B -field and signal E -field have a large overlap $B_0 \cdot E_1$ when integrated over the volume of the cavity. This is the case when the pump and signal modes are, e.g., low-lying TE and TM modes. A scan over axion masses can be performed over an extremely large range by only slightly perturbing the cavity geometry, which alters the

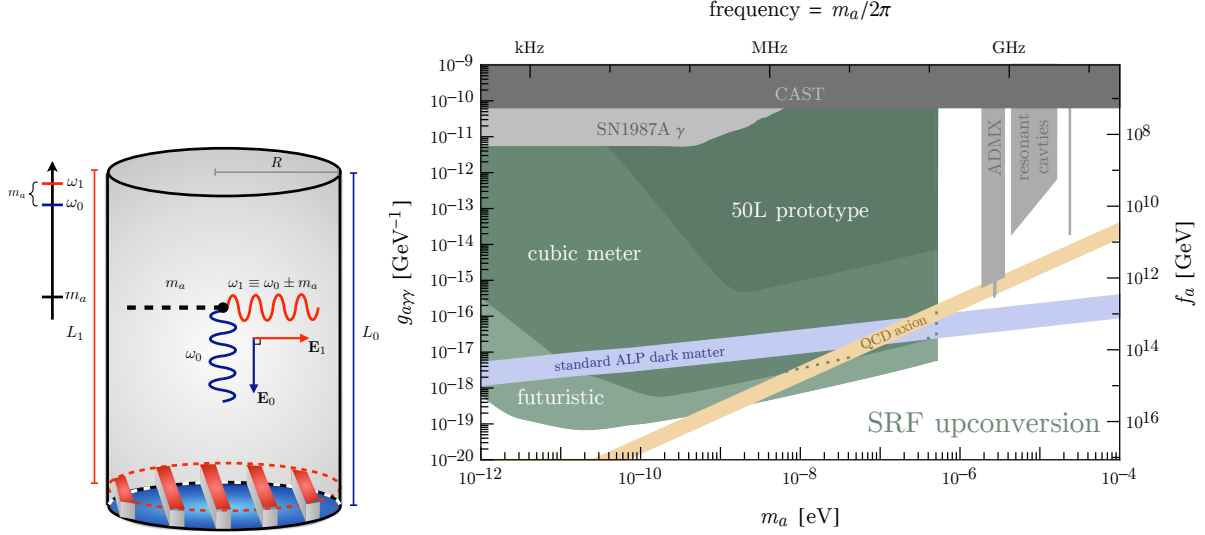


Figure 13: (Left) A schematic of the heterodyne/upconversion experimental setup of Sec. 6.5 (taken from [260]). In an SRF cavity, a pump mode photon of frequency $\omega_0 \sim \text{GHz}$ is converted by axion dark matter into a nearly degenerate photon of frequency $\omega_1 = \omega_0 + m_a$. (Right) The projected sensitivity of a superconducting upconversion setup. As three representative examples, we show the projected sensitivity of a 50L prototype, a 1 m^3 setup, as well as a futuristic experiment with a total instrumented volume of 5 m^3 . See text for additional details. Regions motivated by the QCD axion and dark matter produced by the misalignment mechanism are also shown as orange and blue bands, respectively.

splitting $\omega_1 - \omega_0$. A schematic of the setup is shown in the left panel of Fig. 13.

The upconversion process leads to a GHz frequency axion signal, even for axion frequencies/masses much smaller than $1 \text{ GHz} \sim 1 \mu\text{eV}$. Compared to other static field approaches targeting long wavelength axions, upconverting the signal to GHz frequencies is advantageous. This is because: 1) the signal power is parametrically enhanced by $\sim \text{GHz}/m_a \gg 1$ and 2) high-frequency GHz resonators can couple to very slowly oscillating axion signals, opening up sensitivity to axion masses below a kHz, a region typically inaccessible with static field resonators. This signal can be efficiently read out with well-developed experimental tools, without requiring quantum metrology techniques, cooling beyond liquid helium temperatures, or magnetic fields in excess of $\mathcal{O}(100)$ mT. Furthermore, since the axion signal is extremely narrow, $\Delta\omega/\omega \sim 10^{-6} m_a/\omega_1 \ll 10^{-6}$, it benefits from the high quality factors $Q_{\text{int}} \sim \text{few} \times 10^{11}$ [239] achieved by superconducting radiofrequency (SRF) cavities. The top curve in the right panel of Fig. 13 shows the reach of a 50L prototype using existing SRF cavities and commercially available technology, assuming a modest quality factor of $Q = 10^{10}$. The middle curve shows the potential of a dedicated experimental design of a cubic meter cavity and $Q = 10^{12}$. The bottom curve shows the reach of a more futuristic setup, still assuming $Q = 10^{12}$, but a larger volume of 5 m^3 ; this corresponds to a total instrumented volume approximately 100 times larger than today's individual SRF cavities (although note that this is only a fraction of the total instrumented

volume of SRF-based accelerators, such as PIP II, LCLS 2, and XFEL). In the prototype and cubic meter setups, we assume a peak magnetic field strength of $B_{\text{pump}} = 0.2$ T (no larger than that employed in modern SRF cavities), while for the futuristic setup we assume $B_{\text{pump}} = 0.4$ T. In the above projections, we fix the integration time to correspond to $\sim 10^7$ sec to cover an e -fold in axion mass. Instead, for a search specifically optimized for the QCD axion, we find that the cubic meter setup could probe the DFSZ parameter space for axion masses ranging 9×10^{-9} eV to 10^{-6} eV, while the futuristic setup would be sensitive to the DFSZ region for axion masses of 1×10^{-10} eV to 10^{-6} eV, both assuming a total integration time of ~ 6 years. A cubic meter setup could also cover dark matter motivated parameter space for $m_a \gtrsim 10^{-11}$ eV, as well as unexplored parameter space at ultralow (\lesssim kHz $\sim 10^{-11}$ eV) frequencies/masses.

The most important determinant of the sensitivity is the “leakage” of noise power from the pump mode to the readout, such as through imperfections of the cavity geometry and vibrations of the walls. These effects were previously studied by the MAGO [263] and DarkSRF [264] collaborations, which precisely controlled separate aspects of SRF cavities. In Fig. 13, the prototype sensitivity assumes no attenuation of mechanical vibrations, whereas the projections for the cubic meter and futuristic setups assume 100 dB and 130 dB of vibrational attenuation, respectively. This is no larger than the vibrational attenuation employed in current resonant bar experiments searching for gravitational waves. Currently, potential cavity geometries and tuning mechanisms are being studied at SLAC (funded by an LDRD grant), CERN, and the SQMS center at Fermilab. Ongoing developments at SQMS are aimed at performing in-situ measurements of leakage noise arising from, e.g., microphonics and surface imperfections, as well as the design and construction of a prototype using state of the art cavities. Such developments in SRF technology will also benefit related experiments searching for dark photons, millicharged particles, and gravitational waves, as discussed in Ref. [265].

A close relative of this approach was first proposed by Refs. [266, 267]. In that setup, the signal mode is excited as well, and the axion causes its frequency to periodically shift, so that its effect can be detected by precision frequency metrology. A prototype built at the University of Western Australia has already demonstrated the principle of operation [268, 269]. Future work will improve the sensitivity by better stabilizing the oscillators, which will also be relevant for the frequency conversion approach.

7 Alternative Couplings

Due to the exquisite control achievable for electromagnetic fields, many axion searches are focused on the interaction with two photons. However, as already mentioned above, establishing the nature of a QCD axion requires confirmation of the coupling to gluons. Moreover, the need to explore a mass range spanning many orders of magnitude also encourages the exploration of new methods based on other couplings of the axion. This section highlights the developments in this direction.

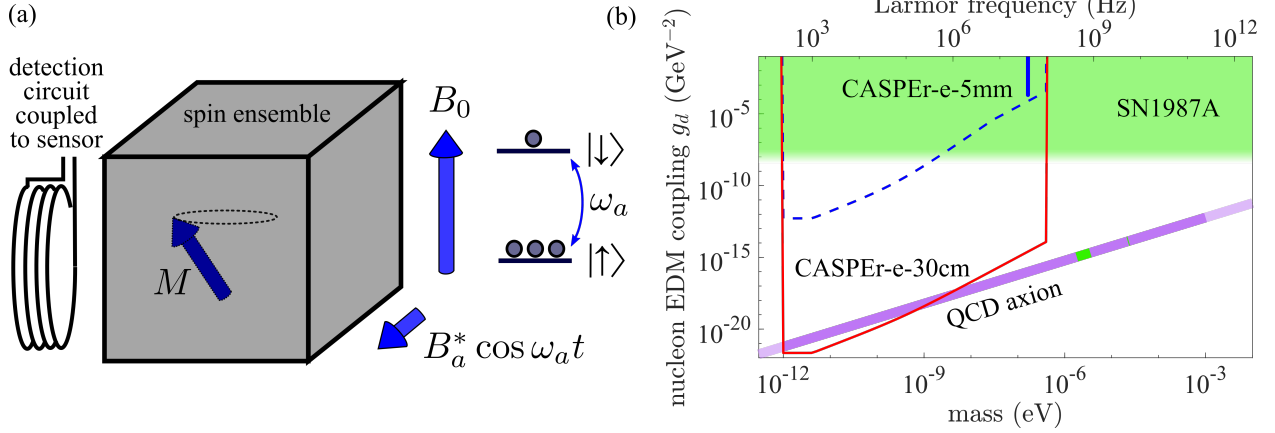


Figure 14: The CASPER experimental schematic and CASPER-e projected sensitivity. (a) The CASPER experimental schematic, showing the nuclear spin ensemble whose spin states are split by the applied bias field B_0 . When this splitting is resonant with the axion-like dark matter Compton frequency ω_a , the ensemble magnetization M is tilted and undergoes precession that is detected by an inductively-coupled sensor. (b) CASPER-e projected sensitivity, showing the published limits (blue) and the sensitivity of the search with a 5 mm sample (blue dashed line) [271]. The red line shows the quantum spin projection noise-limited sensitivity of a CASPER-e search with a 30 cm sample. The green region is excluded by constraints on excess cooling of SN1987A [250, 272, 273]. The QCD axion is in the purple band, whose width shows theoretical uncertainty [272].

7.1 CASPER-electric

Physics goals and status: The Cosmic Axion Spin Precession Experiments (CASPER) use the nuclear magnetic resonance approach to search for axion-like dark matter. The CASPER-electric experiment at Boston University searches for the defining model-independent interaction of the QCD axion, which solves the strong-CP problem [270]. Any claim of QCD axion detection will need to verify the existence of this EDM coupling g_d , which is equivalent to the coupling constants given in section 3.1: $g_d = |g_{apy}| = |g_{any}|$, see eq. (11). CASPER-e is also sensitive to the nucleon spin gradient coupling g_{aNN} , which is equivalent to the coupling constant given in eq. (12). The goal of CASPER-e is to search for axion-like dark matter in the mass range between 10^{-12} eV and 10^{-6} eV, with sufficient sensitivity to detect the QCD axion with mass between 10^{-12} eV and 5×10^{-9} eV. This corresponds to the theoretically-favored range of axion decay constants f_a near the grand unified and Planck scales. The first-generation search in the mass range 162 neV to 166 neV has reported limits on the EDM and gradient interactions of axion-like dark matter [271]. Measurements with a 5 mm sample place the upper bounds $|g_d| < 9.5 \times 10^{-4} \text{ GeV}^{-2}$ and $|g_{aNN}| < 2.8 \times 10^{-1} \text{ GeV}^{-1}$ (95% confidence level) in this mass range. The constraint on g_d corresponds to an upper bound of $1.0 \times 10^{-21} \text{ e} \cdot \text{cm}$ on the amplitude of oscillations of the neutron electric dipole moment, and 4.3×10^{-6} on the amplitude of oscillations of CP-violating θ parameter of quantum chromodynamics.

Experimental approach: CASPER-electric uses precision solid-state magnetic resonance to

search for an oscillating spin torque induced by interaction of axion-like dark matter with nuclear spins, Fig. 14(a). Such an interaction can be represented by a pseudo-magnetic field $B_a^* \cos(\omega_a t)$, which oscillates at the axion Compton frequency $\omega_a = m_a c^2 / \hbar$, with the amplitude B_a^* proportional to the axion-spin coupling strength: $B_a^* \propto g_d$ or $B_a^* \propto g_{aNN}$ [270, 272]. A solid sample is chosen to maximize the magnitude of this interaction. CASPER-e uses poled ferroelectric crystals, such as PbTiO_3 or PMN-PT, leveraging the enhanced effective electric field $E^* \approx 340$ kV/cm [270, 271, 274–276]. The ^{207}Pb nuclear spins inside the crystal are pre-polarized in a 9 T applied magnetic field; ongoing work explores how to speed up and/or increase this polarization using light-induced paramagnetic centers. The long spin relaxation time $T_1 = 26$ min allows the bias magnetic field B_0 to be swept to lower values without losing polarization. If B_0 is chosen so that the spin Larmor frequency matches the axion Compton frequency ω_a , then the pseudo-magnetic field drives the spins on resonance, the magnetization vector tilts and precesses around the bias field. This precession is detected by an inductively-coupled sensor, such as a SQUID. The search for axion-like dark matter is performed by sweeping the bias field B_0 [271].

Sensitivity and timeline: The first-generation experiments have demonstrated how CASPER-e can search for the defining EDM interaction of the QCD axion [271], Fig. 14(b). In order to achieve QCD axion sensitivity, the experiment will be scaled up in volume, due to the limits imposed by the quantum spin projection noise [277]. An experiment with a 60 cm sample is projected to reach the QCD axion sensitivity in the mass range 10^{-12} eV to 5×10^{-9} eV. In parallel with R&D efforts on a scaled-up experiment, work will proceed on the following activities: (1) integration with quantum electromagnetic sensors that offer superior performance compared to SQUIDS, (2) characterization of optimal material to host the solid-state spin ensemble, (3) application of quantum control tools to optimize spin ensemble coherence time and polarization. An experiment limited only by spin projection noise (standard quantum limit) is projected to reach QCD axion sensitivity up to masses $\approx 5 \times 10^{-8}$ eV. The timeline for CASPER-e aims to demonstrate sensitivity at the QCD axion level on a 5-7 year timescale.

7.2 CASPER-gradient

Physics goals and Status: The CASPER-gradient setups at the Johannes Gutenberg University Mainz, Germany, are dedicated experiments to search for the gradient coupling g_{aNN} of axion-like particle dark matter to liquid hyperpolarized nuclear spin samples. First experimental results were published in 2019 excluding ultralight ALP dark matter in the mass ranges 10^{-22} eV to 1.3×10^{-17} eV with coupling constants $g_{aNN} > 6 \times 10^{-5}$ (95% confidence level) [278] and 1.8×10^{-16} eV to 7.8×10^{-14} eV corresponding to Compton frequencies ranging from 45 mHz to 19 Hz [279] with coupling constants $g_{aNN} > 5 \times 10^{-5}$. The existing CASPER-gradient low field (LF) apparatus will search for ALP masses up to $\approx 1.6 \times 10^{-8}$ eV corresponding to 4 MHz ALP Compton frequency with sensitivities to find ALP dark matter with nucleon couplings at the level of $g_{aNN} > 10^{-14}$. A second apparatus, CASPER gradient high field (HF), currently under construction will be capable of searching for ALPs with masses up to $\approx 2.4 \times 10^{-6}$ eV corresponding to 600 MHz ALP Compton frequency with sample volumes of 1 ml.

Experimental approach: The approach is based on magnetic resonance, in the same way as described in previous section 7.1 for CASPER-electric, Fig. 14(a). CASPER-gradient is only sensitive to the nucleon spin gradient coupling g_{aNN} , which is equivalent to the coupling constant given in eq. (12). CASPER-gradient LF and HF use liquid xenon-129 hyperpolarized via spin-exchange optical pumping with optically polarized rubidium vapor, or protons hyperpolarized by e.g. parahydrogen-induced polarization. The liquid state allows for long coherence time (compared to solid state NMR) matching or exceeding the coherence time of virialized cold dark matter. This allows for a given sample density an optimum search sensitivity. The search for axion-like dark matter is performed by sweeping the bias field B_0 and observing non-trivial transverse magnetization or unexplained modulations of the nuclear magnetic resonance frequency. The detection modality is matched to the maximum Compton frequency in the respective search range: CASPER-gradient LF featuring a superconducting magnet with a maximum field of 100 mT uses superconducting pick-up coils in a gradiometer configuration attached to a superconducting-quantum-interference device (SQUID), CASPER-gradient HF is housed in a superconducting magnet with a maximum field of 14.1 T deploying a tunable inductive pick-up circuit. Ongoing work addresses the production and optimization of hyperpolarized xenon-129 and proton samples as well as characterization of the detection system and optimization of the magnetic field homogeneity.

Projected sensitivity: As for CASPER-E the magnitude of the signal detected by the sensor is proportional to the number of spins in the ensemble, the degree of polarization, the coherence time of the spin ensemble, and the magnitude of the pseudo-magnetic field B_a^* . Electronic noise in the detection circuit, by thermal noise in the circuit that couples to this amplifier, or by fundamental quantum spin projection noise.

Projected timeline: The CASPER Gradient LF experimental measurements are ongoing with a spherical 8 mm-diameter sample of thermally polarized protons. Furthermore upgrades to hyperpolarized liquid xenon-129 are actively pursued. The sensitivity of the apparatus is limited by SQUID detection noise floor at $1 \mu\Phi_0/\sqrt{\text{Hz}}$ and able to search for ALP dark matter well beyond the astrophysical SN1987A constraints. First magnetic field scans are projected to be completed on a 1-year timeline. CASPER Gradient HF is currently being build. The collaboration envisions the experiment to be operational within the next 2 years.

7.3 ARIADNE

Axions can couple to fundamental fermions through a scalar vertex and a pseudoscalar vertex. Depending on the model, the coupling can occur for either electrons or nuclei, with possible allowed interactions being monopole-monopole, monopole-dipole, or dipole-dipole. Monopole-dipole interactions include a scalar coupling, g_s , and a pseudo-scalar coupling, g_p , thereby violating P and T symmetry. In the non-relativistic limit, this interaction is proportional to $g_s g_p \vec{\sigma} \cdot \vec{r}$ where $\vec{\sigma}$ is the spin of one particle, and \vec{r} is the distance between two particles [280]. Although the couplings are extremely small for the interaction between single particles, a macroscopic object with $10^{22} \sim 10^{23}$ components would produce a coherent field which can be detectable with a sensitive laboratory experiment,

with an interaction range set by the Compton wavelength of the axion, which is inversely proportional to its mass [281]. Many of the experimental tests of this interaction have been done with polarized gases [282]. In many cases, combined laboratory measurements taken in parallel with astrophysical data have produced the most stringent constraints on the products of the coupling constants g_s and g_p [283, 284]. Nonetheless, existing constraints are insufficient by several orders of magnitude in order to probe the range of interaction strength expected for the QCD axion.

ARIADNE aims to detect QCD-axion-mediated spin-dependent interactions between an unpolarized source mass and a spin-polarized ^3He low-temperature gas [285, 286]. Unlike other direct axion search experiments which depend on the local dark matter density at the Earth, with the axion being the particle that constitutes dark matter, the signal can be modulated in a controlled way. The experiment probes QCD axion masses in the higher end of the traditionally allowed axion window, up to 6 meV, which are not accessible by any existing experiment including dark matter haloscopes such as ADMX. Thus ARIADNE fills an important gap in the search for the QCD axion in this important region of parameter space. The axion can mediate an interaction between fermions (e.g. nucleons) with a potential given by $U_{sp}(r) = \frac{\hbar^2 g_s^N g_p^N}{8\pi m_f} \left(\frac{1}{r\lambda_a} + \frac{1}{r^2} \right) e^{-\frac{r}{\lambda_a}} (\hat{\sigma} \cdot \hat{r})$, where m_f is their mass, $\hat{\sigma}$ is the Pauli spin matrix, \vec{r} is the vector between them, and $\lambda_a = h/m_A c$ is the axion Compton wavelength. For the QCD axion the scalar and dipole coupling constants g_s^N and g_p^N are correlated to the axion mass. Since it couples to $\hat{\sigma}$ which is proportional to the nuclear magnetic moment, the axion coupling can be treated as a fictitious magnetic field B_{eff} . This fictitious field is used to resonantly drive spin precession in a laser-polarized cold ^3He gas. This is accomplished by spinning an unpolarized tungsten mass sprocket near the ^3He vessel. As the teeth of the sprocket pass by the sample at the nuclear Larmor precession frequency, the magnetization in the longitudinally polarized He gas begins to precess about the axis of an applied field. This precessing transverse magnetization is detected with a superconducting quantum interference device (SQUID). The ^3He sample acts as an amplifier to transduce the small fictitious magnetic field into a larger real magnetic field detectable by the SQUID. Superconducting shielding is needed around the sample to screen it from ordinary magnetic field noise which would otherwise limit the sensitivity of the measurement.

The experiment sources the axion in the lab, and can explore all mass ranges in our sensitivity band simultaneously, unlike experiments which must scan over the allowed axion oscillation frequencies (masses) by tuning a cavity or magnetic field.

Distinct from other magnetometry experiments [287–289], the experiment uses a resonant enhancement technique. Assuming sources of systematic error and noise can be mitigated, the approach is expected to be spin-projection noise limited [285], and in principle allows several orders of magnitude improvement, yielding sufficient sensitivity to detect the QCD axion (Fig. 15).

Projected timeline: Several critical components have been tested for the experiment including the superconducting shielding, magnetic characterization of the source mass, and rotary stage mechanism. Final assembly and commissioning of the experiment is currently underway with first results expected in the next 1-2 years. Assuming systematic uncertainties and background noise can be controlled at the level anticipated, QCD-axion sensitivity

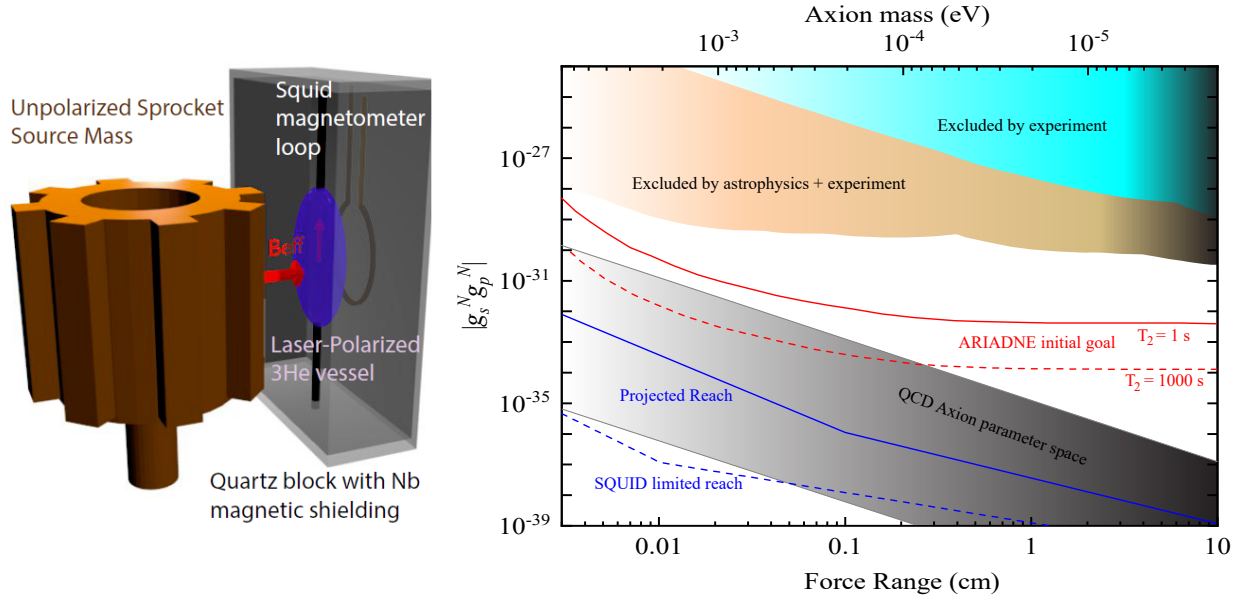


Figure 15: (left) Setup: a sprocket-shaped source mass is rotated so its “teeth” pass near an NMR sample at its resonant frequency. (right) Projected reach for monopole-dipole axion mediated interactions. The band bounded by the red (dark) solid line and dashed line denotes the limit set by transverse magnetization noise, depending on achieved T_2 . Current constraints and expectations for the QCD axion also are shown, adapted from Refs. [284, 285, 287].

is expected within a 3-5 year timescale.

Future prospects for improvements in the search for novel spin dependent interactions could include investigations with a spin polarized source mass, or improved sensitivity with new cryogenic or quantum technologies. Spin squeezing or coherent collective modes in ^3He could offer prospects for improved sensitivity beyond the Standard quantum limit of spin projection noise in experiments such as ARIADNE, potentially allowing sensitivity all the way down to the SQUID-limited sensitivity (dashed-dotted line in Fig. 15). This would allow one to rule out the axion over a wide range of masses, and when combined with other promising techniques [235, 247, 290], and existing experiments [291, 292] already at QCD axion sensitivity, could allow in principle the QCD axion to be searched for over its entire allowed mass range.

7.4 Magnetometer Networks

GNOME: Due to topology or self-interactions, ultralight bosonic fields such as ALPs can form stable, macroscopic field configurations in the form of boson stars [293–296] or topological defects (e.g., domain walls [297–300]). Even in the absence of topological defects or self-interactions, bosonic dark matter fields exhibit stochastic fluctuations [301]. Additionally, it is possible that high-energy astrophysical events could produce intense

bursts of exotic ultralight bosonic fields [302]. In any of these scenarios, instead of being bathed in a uniform flux, terrestrial detectors will witness transient events when ultralight bosonic fields pass through Earth. The Global Network of Optical Magnetometers for Exotic Physics searches (GNOME) is a network of more than a dozen time-synchronized optical atomic magnetometers with stations in North America, Europe, Asia, Australia, and the Middle East. GNOME is designed to search for correlated signals heralding beyond-the-Standard-Model physics [303–305]. There are a limited number of “portals” through which ultralight bosonic fields such as ALPs can couple to Standard Model particles [306], prominent among them spin-dependent interactions to which GNOME is particularly sensitive. GNOME has the potential to search a wide range of unexplored parameter space for such ALP fields [295, 300, 302, 303, 307].

GNOME uses precision optical atomic magnetometers [308, 309] to search for spin torques induced by interaction of axion-like fields with nuclear spins, such as that described by the nonrelativistic Hamiltonian [306]

$$\hat{H}_{aNN} = -2g_{aNN} (\hbar c)^{3/2} \mathbf{S} \cdot \nabla \phi(\mathbf{r}, t), \quad (19)$$

where g_{aNN} is the ALP-nucleon coupling constant, \mathbf{S} is the nuclear spin, and $\phi(\mathbf{r}, t)$ is the ALP field. The form of the Hamiltonian in Eq. (19) is analogous to the Zeeman Hamiltonian, so such effects manifest as pseudo-magnetic fields that can be detected using spin-based magnetometers. GNOME magnetometers are located within multi-layer magnetic shields to reduce the influence of external magnetic noise and perturbations, while still maintaining sensitivity to spin-dependent ALP interactions with nuclei [310]. While a single magnetometer would measure transient and stochastic events associated with ALP fields, in practice it is difficult to confidently distinguish a true ALP signal from false positives induced by changes of magnetometer operational conditions (e.g., magnetic-field spikes, laser mode hops, electronic noise, etc.). Effective vetoing of prosaic noise and transient events (false positives) requires an array of individual, spatially distributed magnetometers to eliminate spurious local effects. Furthermore, a global distribution of sensors is beneficial for event characterization, providing the ability to resolve ALP field properties by observing the relative timing and amplitude of transient events at different sensors [311, 312]. New data analysis efforts and upgrades of GNOME magnetometers to noble gas comagnetometers [313, 314] are underway.

Unshielded magnetometer networks: Recently, it was proposed that the Earth itself could act as a transducer for ultralight dark-matter detection, both for dark (hidden) photons [315, 316] and ALPs [317]. Either via kinetic mixing in the case of hidden photons or via coupling to photons in the case of ALPs, the ultralight dark matter field induces a monochromatic oscillating magnetic field with a particular global vectorial pattern. Such a global magnetic field pattern can be searched for using a network of unshielded magnetometers (as opposed to the shielded magnetometers used in GNOME). Searches for hidden photons and ALPs using a publicly available dataset from the SuperMAG Collaboration [316, 317] established experimental constraints on such scenarios that are competitive with astrophysical limits [318–320] and the CAST experiment [321] in the probed mass ranges (from around 10^{-18} eV to 10^{-16} eV).

7.5 Broadband Axion Dark Matter Searches via Non-Electromagnetic Couplings

Fermion couplings: Non-electromagnetic interactions of an axion or axion-like dark-matter field with standard-model fields can induce time-varying spin-dependent effects. In particular, an axion dark-matter field $a \approx a_0 \cos(m_a t - \mathbf{p}_a \cdot \mathbf{x})$ can couple to the axial-vector currents of fermions via the derivative interaction,

$$\mathcal{L} = -\frac{C_\psi}{2f_a} \partial_\mu a \bar{\psi} \gamma^\mu \gamma^5 \psi, \quad (20)$$

where ψ and $\bar{\psi} = \psi^\dagger \gamma^0$ denote a fermion field and its Dirac adjoint, respectively, f_a is the axion decay constant, and C_ψ are model-dependent dimensionless parameters. In the non-relativistic limit, the spatial components of the derivative interaction (20) give rise to time-varying energy shifts of spin-polarised fermions according to the Hamiltonian [272, 322, 323],

$$H(t) \approx \frac{C_\psi a_0}{2f_a} \sin(m_a t) \boldsymbol{\sigma}_\psi \cdot \mathbf{p}_a, \quad (21)$$

where $\boldsymbol{\sigma}_\psi$ denotes the fermion’s Pauli spin vector and $\mathbf{p}_a \approx m_a \mathbf{v}_a$ denotes the axion momentum relative to the fermion. It has been proposed to search for the “axion wind” spin-precession effect described by Eq. (21) using co-magnetometry [324, 325], spin-polarised torsion pendula [324, 325], Penning traps [326] and storage rings [326, 327].

A co-magnetometry search using mercury atoms and ultracold neutrons constrained the nucleon interaction parameters up to $f_a/C_N \approx 4 \times 10^5$ GeV over the mass range 10^{-22} eV $\lesssim m_a \lesssim 10^{-17}$ eV [328]. A co-magnetometry search using two different transitions of the acetonitrile molecule constrained the nucleon interaction parameters up to $f_a/C_N \approx 2 \times 10^4$ GeV over the mass range 10^{-22} eV $\lesssim m_a \lesssim 10^{-17}$ eV [278]. An ultra-low-field nuclear magnetic resonance search constrained the nucleon interaction parameters up to $f_a/C_N \approx 2 \times 10^4$ GeV over the mass range 10^{-16} eV $\lesssim m_a \lesssim 10^{-13}$ eV [279]. A spin-polarised torsion pendulum search constrained the electron interaction parameter up to $f_a/C_e \approx 2 \times 10^6$ GeV over the mass range 10^{-23} eV $\lesssim m_a \lesssim 10^{-18}$ eV [329]. A Penning trap search with antiprotons constrained the antiproton interaction parameter up to $f_a/C_{\bar{p}} \approx 0.6$ GeV over the mass range 10^{-23} eV $\lesssim m_a \lesssim 10^{-16}$ eV [326]. Existing co-magnetometers using noble-gas species are expected to already be able to probe nucleon interaction parameters up to $f_a/C_N \sim 10^9$ GeV over the mass range 10^{-24} eV $\lesssim m_a \lesssim 10^{-16}$ eV [324], while future co-magnetometers may probe nucleon interaction parameters up to $f_a/C_N \sim 10^{12}$ GeV over the mass range 10^{-24} eV $\lesssim m_a \lesssim 10^{-14}$ eV [325, 330]. Future spin-polarised torsion pendula experiments may probe the electron interaction parameter up to $f_a/C_e \sim 10^{11}$ GeV over the mass range 10^{-22} eV $\lesssim m_a \lesssim 10^{-14}$ eV [325]. Future storage ring experiments using protons may probe the proton interaction parameter up to $f_a/C_p \sim 10^{12}$ GeV over the mass range 10^{-22} eV $\lesssim m_a \lesssim 10^{-18}$ eV, while future storage ring experiments using muons may probe the muon interaction parameter up to $f_a/C_\mu \sim 10^6$ GeV over the mass range 10^{-22} eV $\lesssim m_a \lesssim 10^{-11}$ eV [327].

Gluon coupling: An axion dark-matter field can also couple to the gluons via the non-

derivative interaction,

$$\mathcal{L} = \frac{C_G}{f_a} \frac{g^2}{32\pi^2} a G_{\mu\nu}^b \tilde{G}^{b\mu\nu}, \quad (22)$$

where G and \tilde{G} are the gluonic field tensor and its dual, respectively, $b = 1, 2, \dots, 8$ is the colour index, $g^2/(4\pi)$ is the colour (strong) coupling constant, and C_G is a model-dependent dimensionless parameter. The axion-gluon coupling (22) induces an oscillating electric dipole moment (EDM) of the neutron [331] via a chirally enhanced one-loop process [332, 333]. Additionally, the axion-gluon coupling (22) induces oscillating EDMs of atoms and molecules via the one-loop-level oscillating nucleon EDMs and tree-level oscillating P,T-violating intranuclear forces (which generally give the dominant contribution in diamagnetic species) [323], as well as via two-photon exchange processes between electrons and the nucleus that induce oscillating CP-odd semileptonic interactions (which can give the dominant contribution in paramagnetic species) [334]. A search for an oscillating EDM of the neutron constrained the gluon interaction parameter up to $f_a/C_G \approx 10^{21}$ GeV over the mass range 10^{-24} eV $\lesssim m_a \lesssim 10^{-17}$ eV [328], while a search for an oscillating EDM of the HfF⁺ molecule constrained the gluon interaction parameter up to $f_a/C_G \approx 10^{15}$ GeV over the mass range 10^{-22} eV $\lesssim m_a \lesssim 10^{-15}$ eV [335].

8 Solar Axions

Although this white paper is mainly focused on searches for dark matter axions, experiments that can detect axions independent of its role as dark matter can provide important information on the existence of the axion as well as its properties. One of the most powerful techniques is to look for axions coming from the strongest astrophysical source of axions visible from Earth: the Sun [e.g. 336].

8.1 IAXO and BabyIAXO

Physics goals and status: The International Axion Observatory (IAXO [337–339]) is a next-generation axion helioscope, designed to search for axions from the Sun that are reconverted into X-ray photons via a strong laboratory magnetic field. IAXO will deliver a factor of 20 improvement in sensitivity to the axion-photon coupling $g_{a\gamma}$ over the current leading helioscope, the CERN Axion Solar Telescope (CAST [340]), across a wide mass range extending up to ~ 0.25 eV. BabyIAXO, a preliminary experiment scheduled for 2025, will validate all key technologies and deliver a factor of ~ 5 improvement in sensitivity, already opening novel discovery space for axions and ALPs.

Helioscopes such as BabyIAXO and IAXO are the only experiments sensitive to QCD axions in the $m_a > 10^{-3}$ eV region, which is motivated by several dark matter scenarios [339], as well as to a broad mass range of ALPs that could constitute all of dark matter [80]. The IAXO program is thus a necessary complement to other methods that are sensitive to lower-mass axions, as shown in Fig. 16.

A thorough review of the implications of BabyIAXO and IAXO sensitivity on various physics models has recently been published [339]. Many models permit dark matter ax-

ions up to the meV masses that will be uniquely probed by IAXO and BabyIAXO. These include models in which axion strings and domain-wall decays contribute to QCD axion dark matter [148, 152] or in which there is fine-tuning of the initial axion field value. Models with long-lived domain walls in fact favor QCD axion dark matter in the meV mass range [341]. Generic ALPs have an even larger mass range in which they could constitute all of dark matter, including a large section of the parameter space accessible by IAXO [80]. BabyIAXO and IAXO will resolve if axions are the origin of several long-standing astrophysical anomalies, including the anomalous transparency of the universe to high-energy gamma-rays [342, 343] and the anomalously large cooling rates observed in diverse stellar systems [344–347]. BabyIAXO and IAXO will also investigate non-axion particles at the low-energy frontier of physics, such as hidden photons [348, 349], and possible particle physics solutions to the dark energy problem. These dark energy candidates include new particles, such as chameleons [350], as well as regions of axion parameter space – the so-called “ALP miracle” region at $m_a \approx 0.01\text{--}1\text{ eV}$ and $g_{ay} = 10^{-11}\text{--}10^{-10}\text{ GeV}^{-1}$ – where ALPs would have an adequate potential and coupling to photons to be responsible for both cosmic inflation and dark matter [128, 129]. In the case of axions or ALPs coupled not just with photons but also with electrons or nucleons, IAXO will have the potential to probe the products of couplings $g_{ae} \cdot g_{ay}$ [339] and $g_{ae} \cdot g_{aN}$ [351]. In particular, IAXO will also supersede the astrophysical limits on the g_{ae} coupling, opening investigations of a new set of axion models [346]. Furthermore, if the ALP couplings are large enough to produce a sizeable statistics, the IAXO signal might provide information about the ALP mass [352] and even help distinguish among different axion models [353]. Finally, axions/ALPs could provide the most efficient messenger to probe the magnetic field in the interior of the sun. In fact, due to the coupling to photons, axions can be produced in the solar magnetic field [354, 355] and generate a flux potentially observable with IAXO [356].

Although this generation of solar axion searches will be sensitive to a wide range of dark matter models, the helioscope technique, in contrast to haloscopes, is independent of the assumption that axions are all or part of dark matter. Thus any exclusions are robust to uncertainties in the local dark matter density or specific production mechanisms.

Experimental approach: X-ray photons will convert into axions in the strong fields of ions and electrons in stellar cores, such as our own Sun, via the Primakoff effect. Axion helioscopes are designed to search for axions from the Sun that are reconverted into detectable photons via a strong laboratory magnetic field. The reconverted photons then have energy equal to that of the incident axion, $\sim 1\text{--}10\text{ keV}$ [45, 358, 359]. For low masses, the axion momenta is dominated by this kinematic contribution, and thus the helioscope technique offers sensitivity to a broad mass range. By changing the pressure of a buffer gas in the magnet beam pipes, coherence can be maintained, allowing sensitivity at higher axion masses [360, 361]. If axions exist, such a signal is a robust prediction depending on well-studied solar physics.

Improving on the successful design of CAST, IAXO will consist of a superconducting toroid magnet with eight custom X-ray telescopes that focus the reconverted photons onto ultra-low background detectors (Fig. 16). As a preliminary stage of this program, BabyIAXO will consist of a superconducting magnet with two bores, each instrumented with X-ray optics and detectors with dimensions similar to those foreseen for IAXO.

BabyIAXO will advance technology for all IAXO subsystems at relevant scale while also

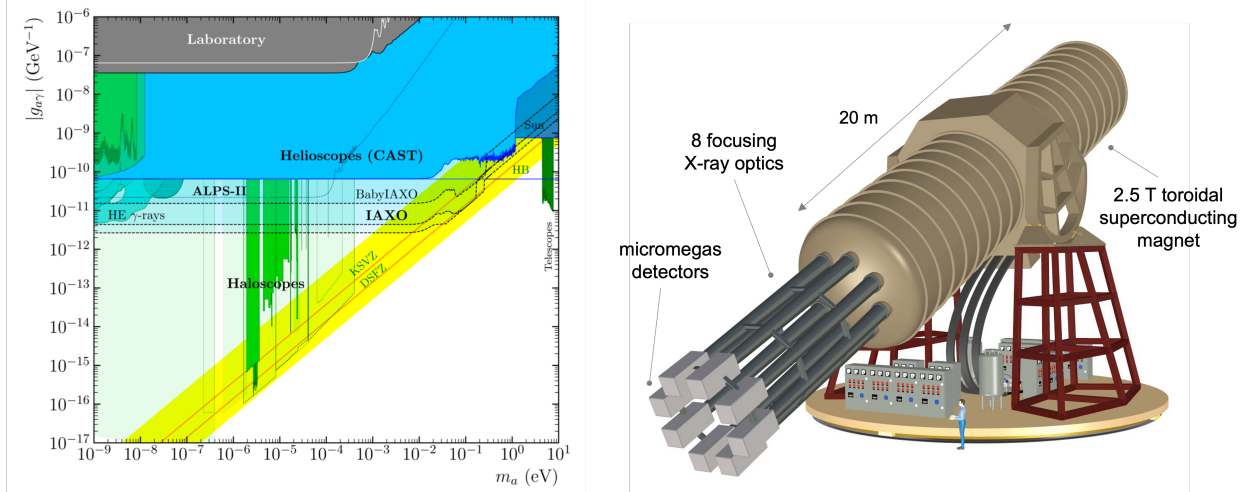


Figure 16: (left:) BabyIAXO and IAXO sensitivity [339], compared with the QCD axion (yellow) band and other current (solid) and future (shaded) experimental limits. BabyIAXO (IAXO) will improve sensitivity to $g_{a\gamma}$ by a factor of 5 (20) for the wide mass range up to 0.25 eV, and are the only experiments with sensitivity to high-mass ($> 10^{-3}$ eV) QCD axions. The lower dotted line refers to an optimized IAXO+ configuration. (right:) Illustration of the IAXO instrument [338, 357]. IAXO will consist of a superconducting toroid magnet with eight custom X-ray telescopes that focus the reconverted photons onto ultra-low background detectors.

offering novel physics reach and discovery potential. Full design details and construction status were recently published in the BabyIAXO CDR [338]. DESY has agreed to provide general infrastructure, with experiment operation scheduled to begin in early 2025. The magnet will feature a common-coil “racetrack” design, with two 10 m-long, 70 cm-diameter bores, demonstrating similar engineering parameters (winding, geometry, etc.) as are necessary for the IAXO toroidal magnet. The detectors are baselined to be small (6 cm wide and 3 cm thick) Time Projection Chambers with pixelated Micromegas read-out, as have been used in CAST [362–364]. Surface tests have already demonstrated the improved shielding and veto necessary to achieve the required background levels of $10^{-7} \text{ keV}^{-1} \text{ cm}^{-2} \text{ s}^{-1}$, and underground tests are underway. The X-ray optics are necessary to focus the X-ray signal, reducing detector size and background. One bore will be instrumented with a custom X-ray optic with the same design and performance requirements of the final IAXO optic. The existing flight-spare telescope from the X-ray Multi-mirror Mission (XMM [365]) is baselined for the second bore, although this may be replaced with another custom optic if funds become available. Support and drive structure will be provided by a modified prototype of the support system for the Cherenkov Telescope Array (CTA) Mid-Size Telescope.

Projected sensitivity and timeline: IAXO will improve helioscope signal-to-noise by a factor of $>10^4$, improving sensitivity to $g_{a\gamma}$ by a factor of ~ 20 . BabyIAXO will already improve the signal-to-noise and $g_{a\gamma}$ sensitivity by factors of $>10^2$ and ~ 5 , respectively.

The current BabyIAXO schedule anticipates data taking beginning in early 2025. The

main physics program will proceed in two phases, each lasting approximately two years. In Run-I, the magnet volume will be in vacuum, providing sensitivity to the wide mass range up to ~ 0.02 eV. In the subsequent Run-II, the magnet volume will be filled with buffer gas, improving sensitivity to QCD axions up to ~ 0.25 eV. Construction of full-scale IAXO could begin as soon as BabyIAXO is commissioned and operational.

The IAXO program builds on the success of the CAST. CAST [321], the most powerful axion helioscope thus far, was the first experiment to surpass the astrophysical limits on $g_{a\gamma}$ for ALPs and placed the leading limits on QCD axions with masses $\sim 0.01 - 1$ eV. In its final phase of operation, CAST hosted a “pathfinder” detection line, including a custom X-ray telescope and a low-background Micromegas detector, both utilizing the same technologies proposed for IAXO.

The IAXO program will also constitute a generic infrastructure, in particular the large magnetic field volume, for axion haloscopes. The BabyIAXO magnet will already surpass the figure of merit (B^2V) of current haloscope magnets, while the IAXO magnet figure of merit one will be an order of magnitude larger. The RADES collaboration is performing R&D on a new RF-cavity haloscope concept, in which sub-cavities coupled by inductive irises are used to instrument large volumes [366]. The RADES proof-of-concept has already been successfully demonstrated at small-scale in CAST [367], as part of a seed program to implement axion haloscopes in BabyIAXO.

Looking toward the future, there is further room for helioscope technology to expand beyond IAXO. Since the conversion probability of axions back into photons increases as B^2 , a stronger magnetic field would substantially increase sensitivity. Though such a strong, large-area magnet is not currently cost-effective, the success of IAXO is a critical step towards allowing helioscopes to take advantage of ongoing advances in magnet technology.

9 Synergies with astrophysical searches

Important constraints on axion/ALPs couplings with the visible sector come from astrophysical probes (see Fig. 17, 18, and 21 for summaries). In many cases astrophysical considerations are still the leading limits thereby setting the benchmark for further exploration in experiments.

Taking the axion-photon coupling as an example, it can be constrained by a large number of astrophysical probes. These include: radio searches for the conversion of axions to photons in neutron star magnetospheres [368–380], the ratio of stars in the horizontal over the RG branch [344, 381–383], the evolution of intermediate mass stars [384, 385], the white dwarf initial-final mass relation [386], the non-observation of γ -rays associated with SN 1987A [318], the diffuse γ -rays from all past supernovae [387, 388], the energy deposit due to ALPs decay in core-collapse supernovae with low explosion energies [389, 390], X-ray searches from super star clusters [391] and from Betelgeuse [392], X-ray spectroscopy from AGN NGC 1275 [393], heating of interstellar medium [320, 394], and HE and VHE gamma-ray searches for spectral irregularities and EBL transparency in AGN sources [395–401].

Astrophysical means offer strategies to probe also the other axion couplings. In particular, RG branch stars and white dwarfs are powerful laboratories to constraint the ax-

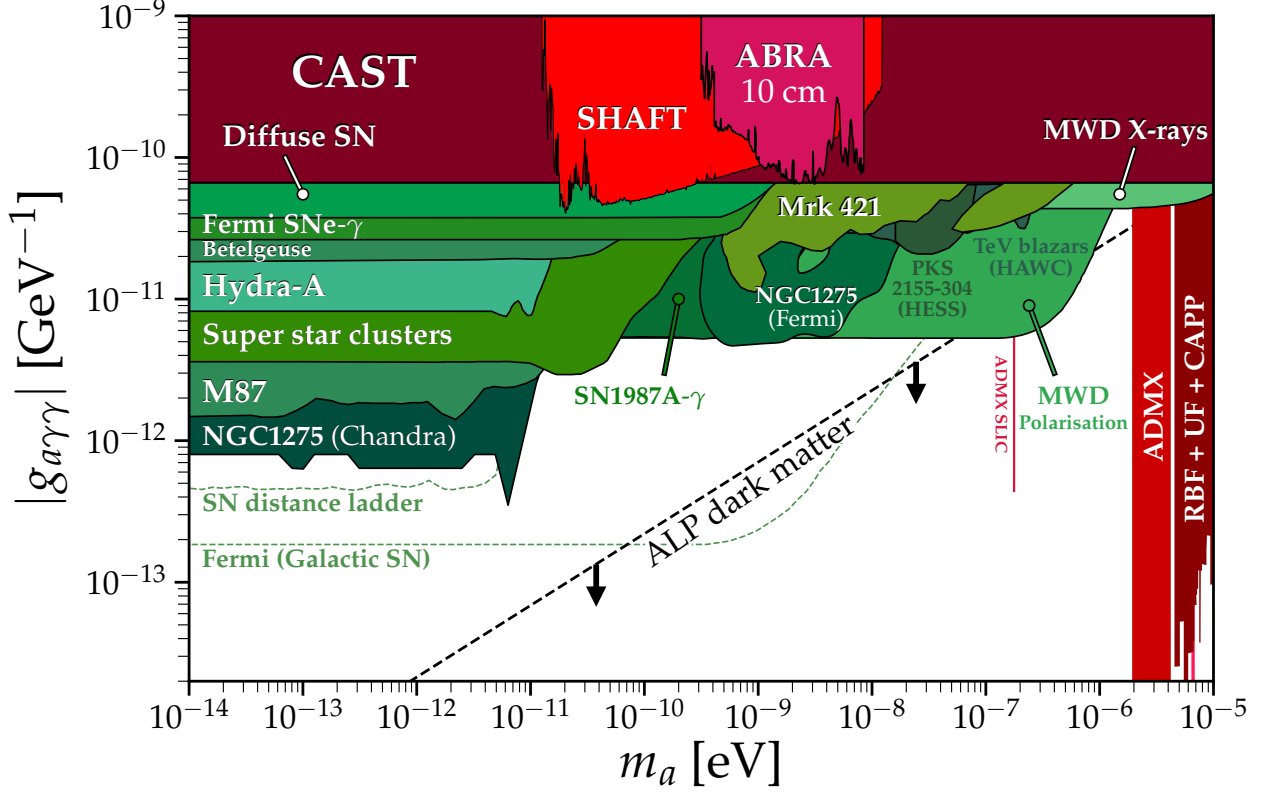


Figure 17: Constraints on low-mass axions, primarily from high-energy astrophysical probes using X-ray and γ -ray data. Astrophysical bounds are shown in shades of green whereas experimental (haloscope/helioscope) bounds are shown in shades of red. We also mark the upper bound on ALP dark matter from Ref. [80] with a dashed black line. The experimental bounds shown in this range are from CAST [321, 359], SHAFT [251], ABRA [233, 234], ADMX [194, 195, 402, 403], ADMX SLIC [404], RBF [405], UF [406], and CAPP [407–409]. The astrophysical bounds shown are from: searches using Fermi-LAT data on extragalactic supernovae γ -rays [410], NGC1275 [411], and for the decay of the diffuse supernova ALP background [387, 388]. NuSTAR observations of super star clusters [391] and Betelgeuse [392]. Chandra observations of M87 [412], NGC1275 [393], and Hydra-A [413]. HESS analysis of PKS 2155-304 [414]. HAWC observations of TeV blazars [415]. Constraints from nearby magnetic white dwarfs observed via X-ray (Chandra) [416] and polarisation signals [417]. Gamma rays from SN1987A [318], and ARGO-YBJ+Fermi observations of the cluster Mrk 421 [418]. Finally we also show projections for constraints (green dashed lines) from the supernova distance ladder [419] and if a $10 M_{\odot}$ SN occurred around the galactic centre and was observed by Fermi [420]. A word of caution should be made about the differing statistical methodologies, and levels of assumption in deriving these bounds—original references should always be consulted when attempting a detailed comparison. Plotting scripts and limit data available at Ref. [421].

ion electron coupling. Currently, the most stringent constraint on this coupling, $g_{ae} \lesssim$

1.5×10^{-13} , was derived in in 2020 in two independent analyses [422, 423] of the RG branch tip in several globular clusters, taking advantage of the newly determined cluster distances from the *Gaia* DR2 data [424]. Leading limits on the axion-muon coupling have also been set using the muons in SN1987A [389, 425, 426].

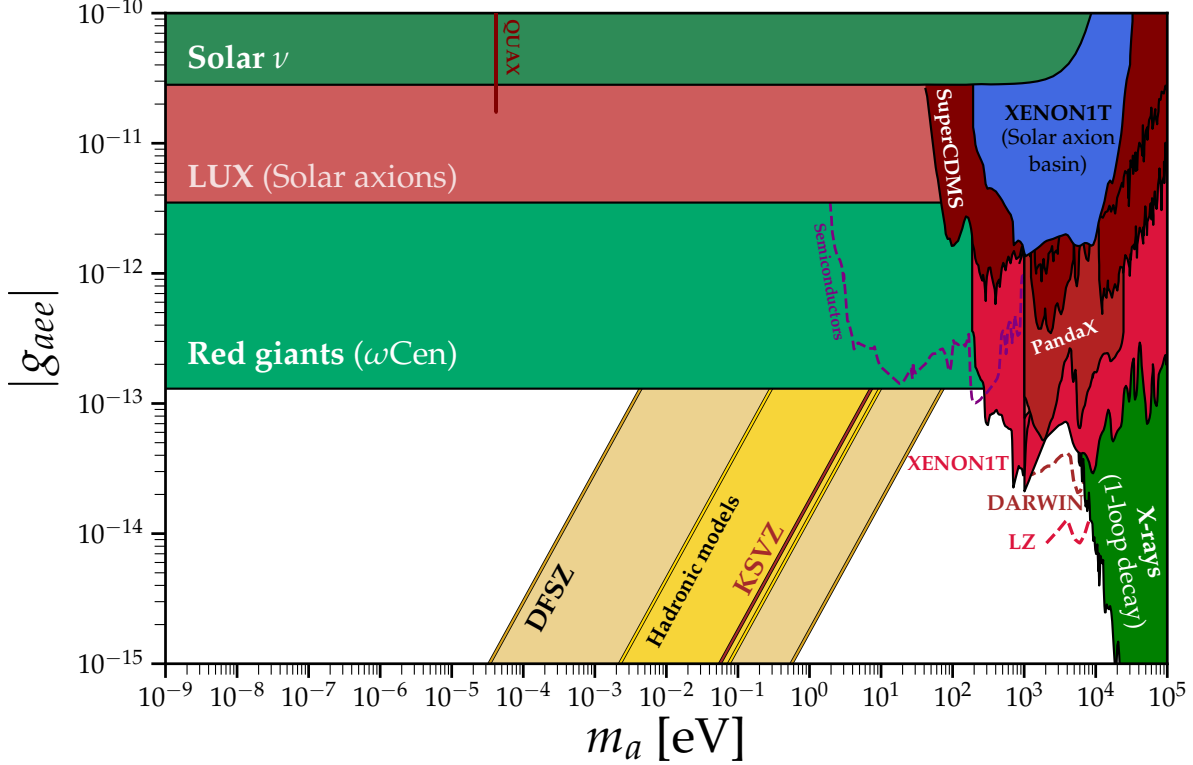


Figure 18: Current and projected constraints on the axion-electron coupling g_{aee} demonstrating the landscape is dominated currently by the stellar cooling bounds across the majority of the mass range, the bound shown here is from the red giants (RG) in the globular cluster ω Centauri [423] (though other derived bounds are comparable). We also show the LUX bound on solar axions [427] and the solar luminosity bound [428]. The only competitive constraints on DM axions exist for $m_a \gtrsim 100$ eV, where underground recoil searches like XENON1T [429–431], PandaX [432], DARWIN [433], LZ [434], and semiconductors [435, 436], can set bounds, before they are superseded by the non-observation of X-rays from the one-electron-loop decay to two photons [437]. Plotting scripts and limit data available at Ref. [421].

The axion-nucleon coupling, on the other hand, can be effectively constrained by observations of neutron stars cooling [438] and by the analysis of the neutrino signal from SN 1987A [439]. Supernovae and neutron stars are difficult objects to model. Nevertheless, the progress in recent years has been substantial. A significant step forward was the recent realization that the pion abundance in supernovae may be considerably larger than expected [440], which led to a substantial revision of the axion production rates [441] and of the expected SN axion spectrum [442]. Finally, the phenomenon of black hole su-

perradiance offers a possibility to probe the axions and ALPs coupled just to gravity [443], allowing to derive very general constraints on the axion mass and its self-coupling strength.

Note that due to the complexity of astrophysical systems, there are discussions regarding alternative scenarios that could potentially loosen up some of the constraints. For example, Ref. [444] proposes a looser bound from SN 1987A cooling due to an alternative modeling of the neutrino emission, while the ICM magnetic field modeling for NGC 1275 bound is questioned in Ref. [445, 446].

Future studies by next-generation very-high energy gamma-ray observatories such as LHAASO and CTA may well contribute further constraints. CTA's improved energy resolution among IACTs will provide greater sensitivity to the spectral irregularities expected in VHE AGN spectra as a result of ALP-photon oscillations in the magnetic fields of sources and the Milky Way [447]. Longitudinal data collected by LHAASO will be able to probe heavier (μeV scale) ALP masses via the transparency of VHE gamma rays to the EBL across cosmological distances [448]. The better understanding of the stellar population, expected in the coming years, will also guarantee a deeper comprehension of the axion/ALPs properties. As discussed above, data from the *Gaia* survey have already allowed to revise the analysis of the impact of ALPs on RG stars and will likely lead to well needed revisions of the white dwarf bound (see discussion in Ref. [346] for further details). Further improvements are likely to follow, in the near future, thanks to the next-generation space-based missions, such as JWST [449], which will enlarge the statistical sample of RG branch members near the cores of GCs, and the Vera Rubin Observatory, expected to detect WDs much fainter than those detected by *Gaia* and to increase the census of WDs to tens of millions [450, 451].

If the programmed experimental effort increases the optimism in a much deeper understanding of the axion properties, on the theoretical side a series of original analyses of novel astrophysical observables is enlarging the region of the axion parameter space accessible to astrophysics and, in several cases, reinforcing the constraints on the ALP couplings with SM fields. Among those are recent studies regarding the ALP DM stimulated decay [452–456] which amplifies the ALPs decay signal through Bose enhancement and can set constraints with SKA and FAST. Observations of the neutron star population around the Galactic Center with SKA, FAST and other radio telescopes can also detect or set strong constraints on axion dark matter which converts to radio photons¹, providing sensitivity even in DM substructure scenarios that render direct detection experiments insensitive [149, 150, 158, 380, 458].

Let us report a few more significant examples. The investigation of exotic contributions to the 511 keV line has recently allowed a new strategy to probe the parameter space of ALPs [459] coupled with multiple SM fields. Another class of observables root from the chiral nature of the Chern-Simons term, which induces photon polarization when photons propagate through ALPs DM or large magnetic fields. This leads to constraints across different bands using AGN [460], protoplanetary disk polarimetry [461], CMB birefringence [462], X-ray polarization [463], polarization measurement of supermassive black holes [464], radio waves from galactic pulsars [465], to polarization of magnetic white

¹Prospects for constraints are described at greater length in CF3 “Dark Matter In Extreme Astrophysical Environments.” [457]

dwarfs [417]. In addition, photon lines from two-body decay of ALPs can be searched for directly [466–470], or they might show up as signals in line intensity mapping [471, 472], or as spectral distortions to the CMB [473]. Lastly, it is shown that with the help of ultralight DM simulations, constraints of energy density fraction can be derived with disk galaxy rotational curves [444, 474, 475].

On cosmological scales, ALPs-induced CMB spectral distortion places strong bounds at $m_a > 10^{-14}$ eV [476, 477]. The coupling between ALPs and photons could lead to an apparent dimming of the photon sources, the effect of which is redshift dependent. This leads to a modification of the inferred distance of the source, which can in turn be constrained using cosmic distance measurement datasets [419, 478–480]. When cosmological history is considered, the suppression of structure formation due to the quantum pressure associated to the light pseudo scalar can be constrained by Lyman- α 1D flux power spectrum [481].

Axions/ALPs contributing to the DM are typically considered as a non-relativistic oscillating field. However, bursts of relativistic axions from transient astrophysical sources allow for unique probes of axion physics and distinct classes of signatures [482]. After formation in the early universe, axions could form gravitationally-bound compact objects such as axion miniclusters and axion stars (see e.g. [293, 483–486]). For the QCD axion, axion bursts from axion star explosions [487, 488] (or other possible transients) can lead to detectable signals [482] over a wide range of axion masses 10^{-15} eV $\lesssim m_a \lesssim 10^{-7}$ eV in experiments such as ABRACADABRA, DMRadio and SHAFT discussed in the previous sections. Since the sensitivity to axion bursts is not strictly suppressed by large decay constant f , such signatures could probe a different parameter space window to conventional searches. Due to axion emission spectrum being intimately related to the fundamental axion potential, axion burst signals can yield new insights into the basic properties of axions that are challenging to probe otherwise [482]. Relativistic axion signals contribute an additional instrument to the multimessenger toolkit for testing physics beyond the Standard Model. Besides, the formation of compact objects also opens up the potential to search for their gravitational and electromagnetic signals [489–494].

10 R&D needs for future axion experiments

As can be easily gleaned from the preceding sections there are a number of common themes in the challenges facing axion dark matter experiments. In particular, we can identify three R&D streams – Quantum sensors, magnets and cavities – that will be important to fully realize the potential of the next generation of experiments. Collaborations on these topics is already underway, both within the axion community and beyond, offering also interesting opportunities for technological spin-offs. Expanding the breadth and scope of these collaborations will be key to fully realizing the existing synergies and to explore the full axion parameter space fast and efficiently.

10.1 Quantum Sensor R&D

Quantum techniques can potentially relax the volume requirements if successfully employed in future haloscopes by suppressing the noise. Quantum-limited amplifiers enabled haloscopes to dig deeper, reaching a few hundred millikelvins of system noise temperature. However, at high frequencies the noise will be dominated by quantum rather than thermal noise. Quantum squeezing and photon-counting are two techniques that can be employed to evade the standard quantum limit, speed up the scan rate, and help in closing the detection volume gap discussed in Section 5. Quantum squeezing was successfully used by the HAYSTAC collaboration to achieve a quantum advantage gain of about 2.5. Single photon counting promises an even larger quantum advantage [205] and a superconducting qubit-based single photon detector was recently used in a dark photon search using a fixed frequency cavity [206]. High Q cavities ($Q > 5 \times 10^5$) are needed for photon counters to allow the quantum sensors employed in the photon counter to do repeatedly enough parity measurements for noise suppression. Recently a magnetic-field-compatible cavity using nested shells of low loss sapphire [204] exhibited $Q = 9 \times 10^6$, thus boosting the signal rate and enabling quantum measurements in axion searches. At higher signal frequencies, superconducting qubits can be used as Cooper-pair breaking sensors rather than as atomic clocks. Although detectors like the Quantum Capacitance Detector [495] have demonstrated the lowest noise equivalent power of any THz photon detection technology, the corresponding dark count rate of 1 Hz is still orders of magnitude too high to be useful in dark matter searches. Ongoing research targets the origins of low energy disturbances that create this dark rate, and results will benefit both dark matter and quantum computing applications.

Quantum technologies have a crucial role in engineering spin ensembles that are used in experiments, such as CASPEr, to search for the EDM and the gradient interactions of ultra-light dark matter [271]. Optical techniques can be used to prepare spin ensembles in low-entropy high-polarization states that have enhanced sensitivity to these interactions. Coherent control and decoupling can extend spin coherence time, also enhancing sensitivity. The goal is to achieve sensitivity to spin ensemble dynamics at the level of quantum spin projection noise. Approaches that make use of spin squeezing and other spin ensemble correlations may ultimately make it possible to extend sensitivity even further. In addition, it is necessary to optimized coupling between a spin ensemble and the electromagnetic sensor used to detects its dynamics, in order to avoid back-action effects [277]. An important part of these activities is to identify and synthesize optimal materials that host spin ensembles with enhanced sensitivity to the EDM and the gradient interactions of ultra-light dark matter [270].

Superconducting-nanowire single-photon detectors are ideally suited for sensing low-count-rate signals due to their high internal efficiency and low dark-count rates. Recent proposals for axion search [218, 496] either require SNSPDs that can operate in the presence of large magnetic fields, or require some means of carrying the light generated by the haloscope from the high-field region to a low-field region where the detectors can operate. The recently established robustness of SNSPDs to operation in high fields [497, 498] and their ability to operate at elevated temperatures (relative to alternative superconducting detector technologies) make them well-suited for photon detection in the mid-infrared

(meV) to visible (eV) energy range. The suitability of SNSPDs to applications requiring low dark-count rates is illustrated by recent progress in the LAMPOST prototype search for dark photon dark-matter using these devices [217].

10.2 Magnet R&D

To maximize axion sensitivity, most axion experiments require optimized magnetic fields. At the same time, these experiments also have to balance the designs against practical engineering considerations such as cooling requirements and quench protection. As cavity based haloscopes [199, 499] push towards higher masses/frequencies the optimal cavity size in order to fully trap the axion energy (proportional to $\approx \lambda/2$) gets smaller. Since the axion signal sensitivity scales as $g_{a\gamma\gamma}^{-1} \propto B_0 V^\alpha$,² this means that in order to maintain the same level of sensitivity down to the DFSZ [499] coupling, a dedicated magnet R&D program for higher strength (up to 45+ Tesla) and optimized magnet designs will be needed for the upcoming experiments. While lumped element based experiments will also require high magnetic fields, they place additional requirements on their overall field profiling necessitating a careful optimization program to meet their sensitivity targets.

For increasing the maximum field strength a sequential two pronged approach is proposed, each targeting a different axion mass region for cavity based axion searches. For the 8–30 μeV range, we seek to design and build a conventional large magnet based on Nb₃Sn and/or NbTi technology with the aim of producing a 15 T field in a 25 cm clear bore and with an overall length of 60 cm. For experiments searching in the 30–50 μeV range, we seek to design a high-temperature superconducting (HTS) insert to allow for a maximum central magnetic field strength of 32 T over a 15 cm diameter. Production and quality of rare-earth barium copper oxide (REBCO) tapes, a vital component of HTS inserts, has risen steadily in recent years due to numerous commercial suppliers worldwide and a strong demand. Over the past six years, the National High Magnetic Field Laboratory (MagLab) has been developing higher field REBCO inserts with current designs reaching a maximum field of 45 T and future designs aiming for even higher field strengths across smaller bore diameters as shown in Figure 19. At the same time as field strengths continue to grow, engineering R&D must be undertaken in order to provide quench management/protection and thermalization management to allow for safe operations of these magnets in cryogenic environments.

Upcoming lumped element axion experiments, looking at axion masses below $\approx 1 \mu\text{eV}$ will have unique field requirements that require precise magnet profiling to minimize signal leakage and detrimental effects on sensitive readout electronics - see Figure 19. These specific axion sensitivity requirements may dictate non-standard toroidal or solenoidal magnet designs in order to optimize the coupled energy between the detector and the axion signal in order to cover multiple mass decades of axion mass parameter space [237, 257, 500]. These upcoming experiments will build on the experience of previous toroidal DM searches [252] as well as the expertise of the LBL, SLAC and the MagLab magnet design groups. In addition to the engineering R&D work discussed above additional work

²The actual value of α depends on the specifics of the axion search and the frequency range, but ranges between $\frac{1}{2}$ and $\frac{5}{6}$.

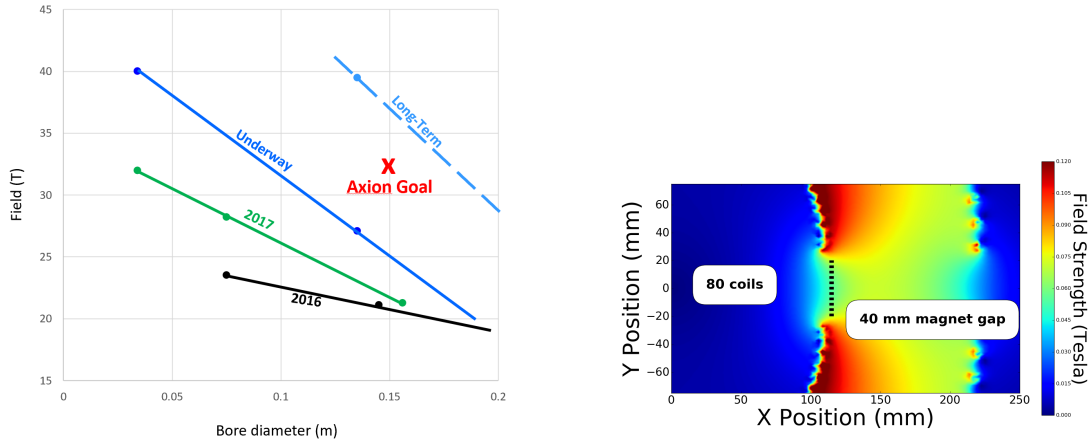


Figure 19: (Left) Evolution of peak fields and bore sizes available from superconducting magnets in recent years. (Right) Magnetic field profile for a 1 Tesla peak spilt toroidal magnet design. The strongest field leakage occurs not only in the gap region, but also in between individual magnet coils. The superconducting elements of this experiment will be placed within 10 mm of the coils/gap region while the field strength falls below 100 mT

aimed at reducing environmental backgrounds such as mechanical vibrations and electromagnetic interference will be vital to ensure the success of these experiments.

All these R&D efforts will allow for the development of cost-effective large-volume high-field magnet designs that will benefit many axion detection experiments. We seek to establish a framework by which experiments can create optimized magnetic field profiles based on the individual experimental needs, minimizing signal losses/leakage while still maximizing the science potential of axion searches in the highest possible magnetic field. We are interested in partnering with experts at national labs and industry in order to design, construct and then successfully implement these next generation of magnets for use in axion experiments.

10.3 Cavity R&D

Cavities with sophisticated geometry and tuning mechanisms are required to allow large volume experiments to be operated at high frequencies [501]. Microwave cavities for axion searches leverage new ideas from both accelerators and quantum information sciences. Moving to higher frequencies cavity volumes run into rapidly degrading volumes and lower quality factors for ordinary metals. There are several methods to recover this:

- Increase volume by coherently adding multiple cavities in phase at the same frequency to take advantage of the axion coherence
- Increase search scan rate but building an array of cavities with complementary frequencies and small tuning range to perform a frequency comb search. Does not take advantage of axion coherence but may be simpler to implement

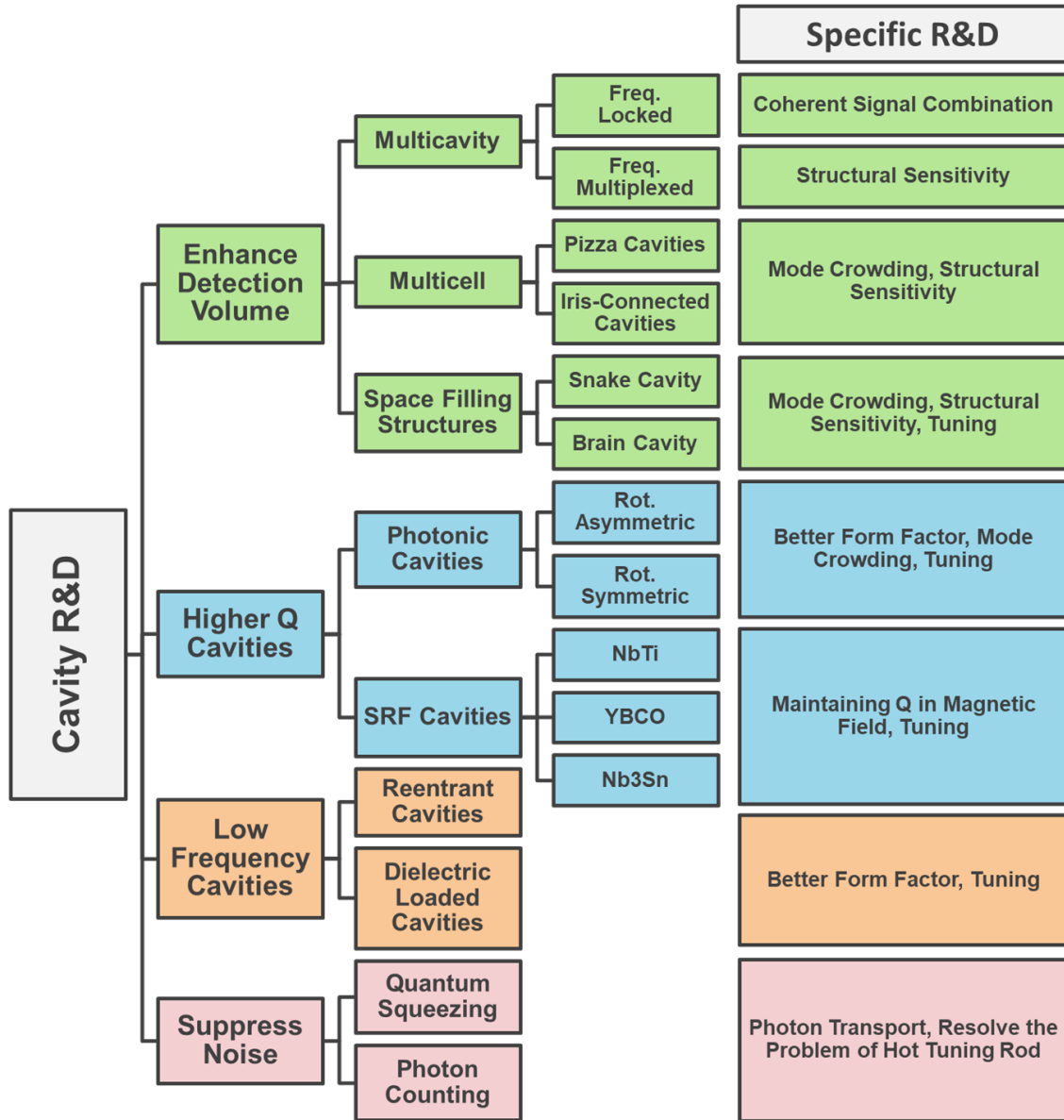


Figure 20: Layout of design challenges and potential R&D avenues to pursue. Enhancing the detection volume can take several general design paths. Multicell cavities can be used in a frequency locked configuration (such as what is being pursued by ADMX-G2 and ADMX-EFR) or in a frequency multiplexed configuration. Multicell cavities consist of geometries in which effective cavities communicate through irises.

- Take advantage of higher order modes in cavities. Clever use of dielectrics in photonic configurations can increase the form-factor and quality factor for such cavities.
- Increase the quality factor of cavities by developing magnetic field tolerant superconducting surfaces that maintain a higher Q than copper in high magnetic fields.

Going in the opposite direction also lower frequency cavities below 500 MHz present

their own unique challenges.

Figure 20 outlines the various design paths to tackle the related issues of scalability to higher and lower masses

11 Conclusion – Towards the Ultimate Axion Facility

Axion physics and in particular the search for axion dark matter is at the dawn of a golden era. In the time since the last Snowmass, the number of experiments but perhaps more importantly the range of axion parameter space they are sensitive to has grown by order(s) of magnitude. This becomes most evident, when looking at Fig. 21, showing the present status (solid) as well as the projections for the future (transparent; many of which are discussed in this Snowmass white paper). From a single experiment sensitive sensitive to axion dark matter in a narrow range of masses (solid “Haloscopes”) we can now see the road to a nearly full coverage of the favored axion dark matter parameter space (various transparent) that spans nine, perhaps more, orders of magnitude in mass.

However, realizing these ambitions is not automatic. The sensitivities indicated in Fig. 21 still require significant developments and even breakthroughs in technology. Achieving this in a timely and efficient will require a concerted effort. Importantly, certain technologies are ubiquitous among axion experiments: superconducting magnets, dilution refrigerators, and the requisite cooling infrastructure. There is therefore strong motivation as well as potential to share resources between and amongst various groups. This could greatly benefit from a shared facility dedicated to axion physics. By investing in several strong, large bore magnets and associated cryogenics that would be able to accommodate multiple experiments, the science reach per experiment could be extended and the search could be conducted more efficiently with shared infrastructure.

References

- [1] R. D. Peccei and H. R. Quinn, *CP Conservation in the Presence of Instantons*, *Phys. Rev. Lett.* **38** (1977) 1440.
- [2] R. D. Peccei and H. R. Quinn, *Constraints Imposed by CP Conservation in the Presence of Instantons*, *Phys. Rev. D* **16** (1977) 1791.
- [3] S. Weinberg, *A New Light Boson?*, *Phys. Rev. Lett.* **40** (1978) 223.
- [4] F. Wilczek, *Problem of Strong P and T Invariance in the Presence of Instantons*, *Phys. Rev. Lett.* **40** (1978) 279.
- [5] J. Billard et al., *Direct Detection of Dark Matter – APPEC Committee Report*, 2104.07634.
- [6] V. C. Rubin and W. K. Ford, Jr., *Rotation of the Andromeda Nebula from a Spectroscopic Survey of Emission Regions*, *Astrophys. J.* **159** (1970) 379.

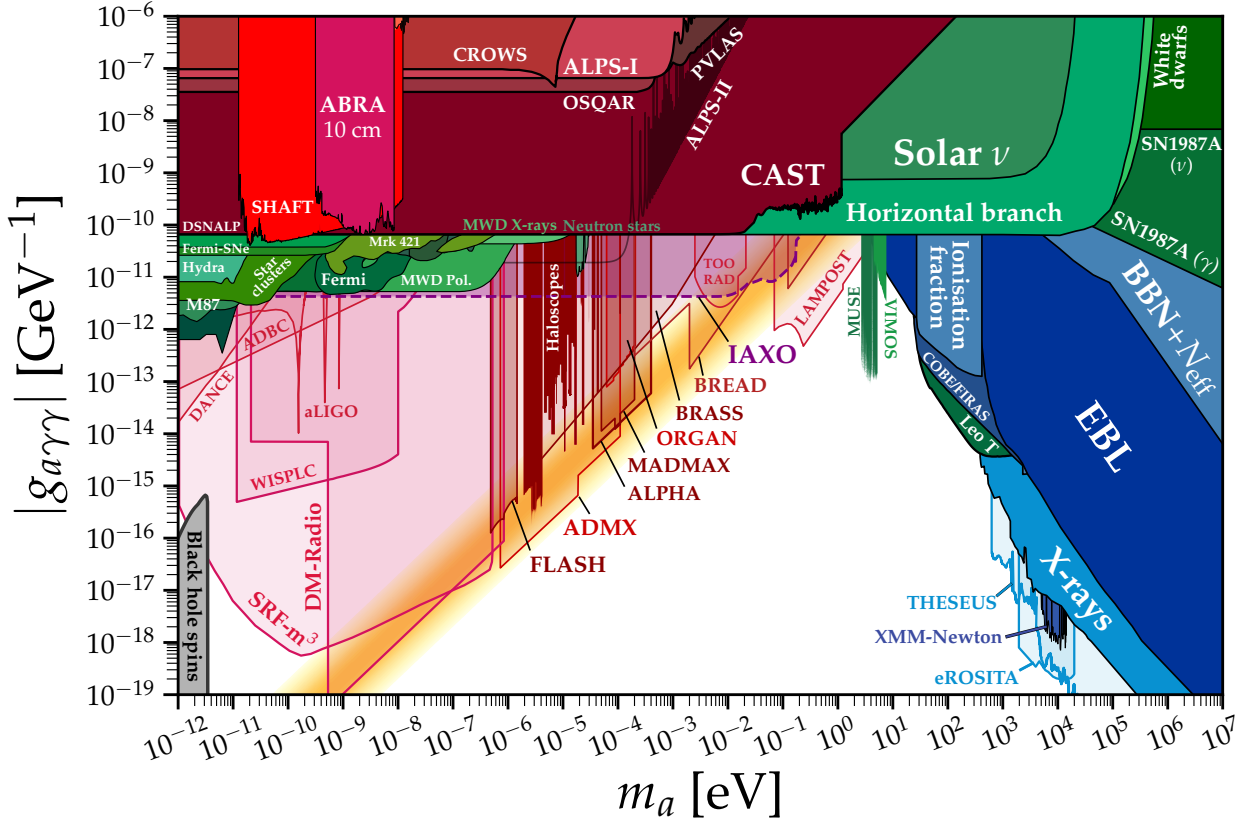


Figure 21: Current (opaque) and projected (transparent) constraints on the axion-photon coupling. All existing constraints are described in the preceding sections. The estimated sensitivities of several proposed and in-construction haloscopes are shown including (from low to high masses, roughly): DANCE [502], ADBC [503], aLIGO [504], SRF cavity [261], WISPLC [505], DM-Radio [235], FLASH [506], ADMX [507], ALPHA [207], MADMAX [508], ORGAN [509], BRASS [510], BREAD [511], TOORAD [512], and LAMPPOST [216]. We also show projections for IAXO [513] and ALPS-II [514]. Finally, we have displayed forecasted sensitivity to heavy dark matter ALP decays to X-rays using eROSITA [515] and THESEUS [516], as well as a projection for a Fermi-LAT observation of a galactic supernova [420]. Plotting scripts and data available at Ref. [421].

[7] J. A. Tyson, G. P. Kochanski and I. P. Dell’Antonio, *Detailed mass map of CL0024+1654 from strong lensing*, *Astrophys. J.* **498** (1998) L107 [[astro-ph/9801193](#)].

[8] SDSS Collaboration, M. Tegmark et al., *Cosmological parameters from SDSS and WMAP*, *Phys. Rev. D* **69** (2004) 103501 [[astro-ph/0310723](#)].

[9] D. Clowe, M. Bradac, A. H. Gonzalez, M. Markevitch, S. W. Randall et al., *A direct empirical proof of the existence of dark matter*, *Astrophys. J.* **648** (2006) L109 [[astro-ph/0608407](#)].

- [10] PLANCK Collaboration, N. Aghanim et al., *Planck 2018 results. I. Overview and the cosmological legacy of Planck*, *Astron. Astrophys.* **641** (2020) A1 [1807.06205].
- [11] G. Bertone, D. Hooper and J. Silk, *Particle dark matter: Evidence, candidates and constraints*, *Phys. Rept.* **405** (2005) 279 [hep-ph/0404175].
- [12] P. G. Harris et al., *New Experimental Limit on the Electric Dipole Moment of the Neutron*, *Phys. Rev. Lett.* **82** (1999) 904.
- [13] C. A. Baker et al., *An Improved experimental limit on the electric dipole moment of the neutron*, *Phys. Rev. Lett.* **97** (2006) 131801 [hep-ex/0602020].
- [14] J. M. Pendlebury et al., *Revised experimental upper limit on the electric dipole moment of the neutron*, *Phys. Rev. D* **92** (2015) 092003 [1509.04411].
- [15] NEDM Collaboration, C. Abel et al., *Measurement of the permanent electric dipole moment of the neutron*, *Phys. Rev. Lett.* **124** (2020) 081803 [2001.11966].
- [16] J. Preskill, M. B. Wise and F. Wilczek, *Cosmology of the invisible axion*, *Physics Letters B* **120** (1983) 127.
- [17] L. F. Abbott and P. Sikivie, *A cosmological bound on the invisible axion*, *Physics Letters B* **120** (1983) 133.
- [18] M. Dine and W. Fischler, *The not-so-harmless axion*, *Physics Letters B* **120** (1983) 137.
- [19] C. Vafa and E. Witten, *Restrictions on Symmetry Breaking in Vector-Like Gauge Theories*, *Nucl. Phys. B* **234** (1984) 173.
- [20] M. Gorghetto and G. Villadoro, *Topological Susceptibility and QCD Axion Mass: QED and NNLO corrections*, *JHEP* **03** (2019) 033 [1812.01008].
- [21] A. Hook, *Solving the Hierarchy Problem Discretely*, *Phys. Rev. Lett.* **120** (2018) 261802 [1802.10093].
- [22] L. Di Luzio, B. Gavela, P. Quilez and A. Ringwald, *An even lighter QCD axion*, *JHEP* **05** (2021) 184 [2102.00012].
- [23] L. Di Luzio, B. Gavela, P. Quilez and A. Ringwald, *Dark matter from an even lighter QCD axion: trapped misalignment*, *JCAP* **10** (2021) 001 [2102.01082].
- [24] V. A. Rubakov, *Grand unification and heavy axion*, *JETP Lett.* **65** (1997) 621 [hep-ph/9703409].
- [25] Z. Berezhiani, L. Gianfagna and M. Giannotti, *Strong CP problem and mirror world: The Weinberg-Wilczek axion revisited*, *Phys. Lett. B* **500** (2001) 286 [hep-ph/0009290].

- [26] L. Gianfagna, M. Giannotti and F. Nesti, *Mirror world, supersymmetric axion and gamma ray bursts*, *JHEP* **10** (2004) 044 [[hep-ph/0409185](#)].
- [27] S. D. H. Hsu and F. Sannino, *New solutions to the strong CP problem*, *Phys. Lett. B* **605** (2005) 369 [[hep-ph/0408319](#)].
- [28] A. Hook, *Anomalous solutions to the strong CP problem*, *Phys. Rev. Lett.* **114** (2015) 141801 [[1411.3325](#)].
- [29] H. Fukuda, K. Harigaya, M. Ibe and T. T. Yanagida, *Model of visible QCD axion*, *Phys. Rev. D* **92** (2015) 015021 [[1504.06084](#)].
- [30] C.-W. Chiang, H. Fukuda, M. Ibe and T. T. Yanagida, *750 GeV diphoton resonance in a visible heavy QCD axion model*, *Phys. Rev. D* **93** (2016) 095016 [[1602.07909](#)].
- [31] S. Dimopoulos, A. Hook, J. Huang and G. Marques-Tavares, *A collider observable QCD axion*, *JHEP* **11** (2016) 052 [[1606.03097](#)].
- [32] T. Gherghetta, N. Nagata and M. Shifman, *A Visible QCD Axion from an Enlarged Color Group*, *Phys. Rev. D* **93** (2016) 115010 [[1604.01127](#)].
- [33] A. Kobakhidze, *Heavy axion in asymptotically safe QCD*, [1607.06552](#).
- [34] P. Agrawal and K. Howe, *Factoring the Strong CP Problem*, *JHEP* **12** (2018) 029 [[1710.04213](#)].
- [35] P. Agrawal and K. Howe, *A Flavorful Factoring of the Strong CP Problem*, *JHEP* **12** (2018) 035 [[1712.05803](#)].
- [36] M. K. Gaillard, M. B. Gavela, R. Houtz, P. Quilez and R. Del Rey, *Color unified dynamical axion*, *Eur. Phys. J. C* **78** (2018) 972 [[1805.06465](#)].
- [37] C. Csáki, M. Ruhdorfer and Y. Shirman, *UV Sensitivity of the Axion Mass from Instantons in Partially Broken Gauge Groups*, *JHEP* **04** (2020) 031 [[1912.02197](#)].
- [38] R. S. Gupta, V. V. Khoze and M. Spannowsky, *Small instantons and the strong CP problem in composite Higgs models*, *Phys. Rev. D* **104** (2021) 075011 [[2012.00017](#)].
- [39] T. Gherghetta and M. D. Nguyen, *A Composite Higgs with a Heavy Composite Axion*, *JHEP* **12** (2020) 094 [[2007.10875](#)].
- [40] A. R. Zhitnitsky, *On Possible Suppression of the Axion Hadron Interactions. (In Russian)*, *Sov. J. Nucl. Phys.* **31** (1980) 260.
- [41] M. Dine, W. Fischler and M. Srednicki, *A Simple Solution to the Strong CP Problem with a Harmless Axion*, *Phys. Lett. B* **104** (1981) 199.
- [42] J. E. Kim, *Weak Interaction Singlet and Strong CP Invariance*, *Phys. Rev. Lett.* **43** (1979) 103.

- [43] M. A. Shifman, A. I. Vainshtein and V. I. Zakharov, *Can Confinement Ensure Natural CP Invariance of Strong Interactions?*, *Nucl. Phys. B* **166** (1980) 493.
- [44] J. E. Kim, *A COMPOSITE INVISIBLE AXION*, *Phys. Rev. D* **31** (1985) 1733.
- [45] P. Sikivie, *Experimental Tests of the Invisible Axion*, *Phys. Rev. Lett.* **51** (1983) 1415. [Erratum: *Phys.Rev.Lett.* 52, 695 (1984)].
- [46] G. Grilli di Cortona, E. Hardy, J. Pardo Vega and G. Villadoro, *The QCD axion, precisely*, *JHEP* **01** (2016) 034 [[1511.02867](#)].
- [47] J. E. Kim, *Constraints on very light axions from cavity experiments*, *Phys. Rev. D* **58** (1998) 055006 [[hep-ph/9802220](#)].
- [48] L. Di Luzio, F. Mescia and E. Nardi, *Redefining the Axion Window*, *Phys. Rev. Lett.* **118** (2017) 031801 [[1610.07593](#)].
- [49] L. Di Luzio, F. Mescia and E. Nardi, *Window for preferred axion models*, *Phys. Rev. D* **96** (2017) 075003 [[1705.05370](#)].
- [50] L. Di Luzio, M. Giannotti, E. Nardi and L. Visinelli, *The landscape of QCD axion models*, *Phys. Rept.* **870** (2020) 1 [[2003.01100](#)].
- [51] V. Plakkot and S. Hoof, *Anomaly ratio distributions of hadronic axion models with multiple heavy quarks*, *Phys. Rev. D* **104** (2021) 075017 [[2107.12378](#)].
- [52] A. V. Sokolov and A. Ringwald, *Photophilic hadronic axion from heavy magnetic monopoles*, *JHEP* **06** (2021) 123 [[2104.02574](#)].
- [53] J. E. Kim, H. P. Nilles and M. Peloso, *Completing natural inflation*, *JCAP* **01** (2005) 005 [[hep-ph/0409138](#)].
- [54] P. Agrawal, J. Fan, M. Reece and L.-T. Wang, *Experimental Targets for Photon Couplings of the QCD Axion*, *JHEP* **02** (2018) 006 [[1709.06085](#)].
- [55] D. E. Kaplan and R. Rattazzi, *Large field excursions and approximate discrete symmetries from a clockwork axion*, *Phys. Rev. D* **93** (2016) 085007 [[1511.01827](#)].
- [56] M. Farina, D. Pappadopulo, F. Rompineve and A. Tesi, *The photo-philic QCD axion*, *JHEP* **01** (2017) 095 [[1611.09855](#)].
- [57] L. Darmé, L. Di Luzio, M. Giannotti and E. Nardi, *Selective enhancement of the QCD axion couplings*, *Phys. Rev. D* **103** (2021) 015034 [[2010.15846](#)].
- [58] Y. Chikashige, R. N. Mohapatra and R. Peccei, *Are There Real Goldstone Bosons Associated with Broken Lepton Number?*, *Phys. Lett. B* **98** (1981) 265.
- [59] C. Froggatt and H. B. Nielsen, *Hierarchy of Quark Masses, Cabibbo Angles and CP Violation*, *Nucl. Phys. B* **147** (1979) 277.

- [60] E. Witten, *Some Properties of $O(32)$ Superstrings*, *Phys. Lett. B* **149** (1984) 351.
- [61] J. P. Conlon, *The QCD axion and moduli stabilisation*, *JHEP* **05** (2006) 078 [[hep-th/0602233](#)].
- [62] P. Svrcek and E. Witten, *Axions In String Theory*, *JHEP* **06** (2006) 051 [[hep-th/0605206](#)].
- [63] K.-S. Choi, H. P. Nilles, S. Ramos-Sanchez and P. K. S. Vaudrevange, *Accions*, *Phys. Lett. B* **675** (2009) 381 [[0902.3070](#)].
- [64] A. Arvanitaki, S. Dimopoulos, S. Dubovsky, N. Kaloper and J. March-Russell, *String Axiverse*, *Phys. Rev. D* **81** (2010) 123530 [[0905.4720](#)].
- [65] B. S. Acharya, K. Bobkov and P. Kumar, *An M Theory Solution to the Strong CP Problem and Constraints on the Axiverse*, *JHEP* **11** (2010) 105 [[1004.5138](#)].
- [66] M. Cicoli, M. Goodsell and A. Ringwald, *The type IIB string axiverse and its low-energy phenomenology*, *JHEP* **10** (2012) 146 [[1206.0819](#)].
- [67] J. Halverson, C. Long and P. Nath, *Ultralight axion in supersymmetry and strings and cosmology at small scales*, *Phys. Rev. D* **96** (2017) 056025 [[1703.07779](#)].
- [68] R. T. Co, L. J. Hall and K. Harigaya, *Predictions for Axion Couplings from ALP Cogenesis*, *JHEP* **01** (2021) 172 [[2006.04809](#)].
- [69] R. T. Co, L. J. Hall and K. Harigaya, *Axion Kinetic Misalignment Mechanism*, *Phys. Rev. Lett.* **124** (2020) 251802 [[1910.14152](#)].
- [70] T. Chiba, F. Takahashi and M. Yamaguchi, *Baryogenesis in a flat direction with neither baryon nor lepton charge*, *Phys. Rev. Lett.* **92** (2004) 011301 [[hep-ph/0304102](#)]. [Erratum: *Phys.Rev.Lett.* 114, 209901 (2015)].
- [71] F. Takahashi and M. Yamaguchi, *Spontaneous baryogenesis in flat directions*, *Phys. Rev. D* **69** (2004) 083506 [[hep-ph/0308173](#)].
- [72] R. T. Co and K. Harigaya, *Axiogenesis*, *Phys. Rev. Lett.* **124** (2020) 111602 [[1910.02080](#)].
- [73] V. M. Mehta, M. Demirtas, C. Long, D. J. E. Marsh, L. Mcallister and M. J. Stott, *Superradiance Exclusions in the Landscape of Type IIB String Theory*, [2011.08693](#).
- [74] W. Hu, R. Barkana and A. Gruzinov, *Cold and fuzzy dark matter*, *Phys. Rev. Lett.* **85** (2000) 1158 [[astro-ph/0003365](#)].
- [75] L. Hui, J. P. Ostriker, S. Tremaine and E. Witten, *Ultralight scalars as cosmological dark matter*, *Phys. Rev. D* **95** (2017) 043541 [[1610.08297](#)].
- [76] J. C. Niemeyer, *Small-scale structure of fuzzy and axion-like dark matter*, [1912.07064](#).

- [77] D. J. E. Marsh, *Axion Cosmology*, *Phys. Rept.* **643** (2016) 1 [[1510.07633](#)].
- [78] M. S. Turner, *Coherent scalar-field oscillations in an expanding universe*, *Physical Review D* **28** (1983) 1243.
- [79] M. S. Turner, *Cosmic and local mass density of “invisible” axions*, *Physical Review D* **33** (1986) 889.
- [80] P. Arias, D. Cadamuro, M. Goodsell, J. Jaeckel, J. Redondo and A. Ringwald, *WISPy Cold Dark Matter*, *JCAP* **06** (2012) 013 [[1201.5902](#)].
- [81] T. W. B. Kibble, *Topology of cosmic domains and strings*, *Journal of Physics A Mathematical General* **9** (1976) 1387.
- [82] T. W. B. Kibble, *Some Implications of a Cosmological Phase Transition*, *Phys. Rept.* **67** (1980) 183.
- [83] R. L. Davis, *Goldstone Bosons in String Models of Galaxy Formation*, *Phys. Rev. D* **32** (1985) 3172.
- [84] R. L. Davis, *Cosmic Axions from Cosmic Strings*, *Phys. Lett. B* **180** (1986) 225.
- [85] D. Harari and P. Sikivie, *On the Evolution of Global Strings in the Early Universe*, *Phys. Lett. B* **195** (1987) 361.
- [86] R. A. Battye and E. P. S. Shellard, *Global string radiation*, *Nucl. Phys. B* **423** (1994) 260 [[astro-ph/9311017](#)].
- [87] P. Di Vecchia and G. Veneziano, *Chiral Dynamics in the Large n Limit*, *Nucl. Phys. B* **171** (1980) 253.
- [88] E. W. Kolb and M. S. Turner, *The Early Universe*, vol. 69. 1990, [10.1201/9780429492860](#).
- [89] S. Weinberg, *Cosmology*. 2008.
- [90] S. Hoof, F. Kahlhoefer, P. Scott, C. Weniger and M. White, *Axion global fits with Peccei-Quinn symmetry breaking before inflation using GAMBIT*, *JHEP* **03** (2019) 191 [[1810.07192](#)]. [Erratum: *JHEP* 11, 099 (2019)].
- [91] D. Karamitros, *MiMeS: Misalignment Mechanism Solver*, [2110.12253](#).
- [92] R. Hlozek, D. Grin, D. J. E. Marsh and P. G. Ferreira, *A search for ultralight axions using precision cosmological data*, *Phys. Rev. D* **91** (2015) 103512 [[1410.2896](#)].
- [93] V. Poulin, T. L. Smith, D. Grin, T. Karwal and M. Kamionkowski, *Cosmological implications of ultralight axionlike fields*, *Phys. Rev. D* **98** (2018) 083525 [[1806.10608](#)].
- [94] D. H. Lyth, *Axions and inflation: Sitting in the vacuum*, *Phys. Rev. D* **45** (1992) 3394.

- [95] K. Strobl and T. J. Weiler, *Anharmonic evolution of the cosmic axion density spectrum*, *Phys. Rev. D* **50** (1994) 7690 [[astro-ph/9405028](#)].
- [96] K. J. Bae, J.-H. Huh and J. E. Kim, *Update of axion CDM energy*, *JCAP* **09** (2008) 005 [[0806.0497](#)].
- [97] L. Visinelli and P. Gondolo, *Dark Matter Axions Revisited*, *Phys. Rev. D* **80** (2009) 035024 [[0903.4377](#)].
- [98] T. Kobayashi, R. Kurematsu and F. Takahashi, *Isocurvature Constraints and Anharmonic Effects on QCD Axion Dark Matter*, *JCAP* **09** (2013) 032 [[1304.0922](#)].
- [99] S. Borsanyi et al., *Calculation of the axion mass based on high-temperature lattice quantum chromodynamics*, *Nature* **539** (2016) 69 [[1606.07494](#)].
- [100] R. T. Co, E. Gonzalez and K. Harigaya, *Axion Misalignment Driven to the Hilltop*, *JHEP* **05** (2019) 163 [[1812.11192](#)].
- [101] F. Takahashi and W. Yin, *QCD axion on hilltop by a phase shift of π* , *JHEP* **10** (2019) 120 [[1908.06071](#)].
- [102] A. Arvanitaki, S. Dimopoulos, M. Galanis, L. Lehner, J. O. Thompson and K. Van Tilburg, *Large-misalignment mechanism for the formation of compact axion structures: Signatures from the QCD axion to fuzzy dark matter*, *Phys. Rev. D* **101** (2020) 083014 [[1909.11665](#)].
- [103] J. Huang, A. Madden, D. Racco and M. Reig, *Maximal axion misalignment from a minimal model*, *JHEP* **10** (2020) 143 [[2006.07379](#)].
- [104] G. R. Dvali, *Removing the cosmological bound on the axion scale*, [hep-ph/9505253](#).
- [105] T. Banks and M. Dine, *The Cosmology of string theoretic axions*, *Nucl. Phys. B* **505** (1997) 445 [[hep-th/9608197](#)].
- [106] K. Choi, H. B. Kim and J. E. Kim, *Axion cosmology with a stronger QCD in the early universe*, *Nucl. Phys. B* **490** (1997) 349 [[hep-ph/9606372](#)].
- [107] R. T. Co, E. Gonzalez and K. Harigaya, *Axion Misalignment Driven to the Bottom*, *JHEP* **05** (2019) 162 [[1812.11186](#)].
- [108] C.-F. Chang and Y. Cui, *New Perspectives on Axion Misalignment Mechanism*, *Phys. Rev. D* **102** (2020) 015003 [[1911.11885](#)].
- [109] V. Domcke, Y. Ema, K. Mukaida and M. Yamada, *Spontaneous Baryogenesis from Axions with Generic Couplings*, *JHEP* **08** (2020) 096 [[2006.03148](#)].
- [110] R. T. Co, N. Fernandez, A. Ghalsasi, L. J. Hall and K. Harigaya, *Lepto-Axiogenesis*, *JHEP* **21** (2020) 017 [[2006.05687](#)].
- [111] K. Harigaya and R. Wang, *Axiogenesis from $SU(2)_R$ phase transition*, [2107.09679](#).

- [112] S. Chakraborty, T. H. Jung and T. Okui, *Composite neutrinos and the QCD axion: baryogenesis, dark matter, small Dirac neutrino masses, and vanishing neutron EDM*, [2108.04293](#).
- [113] J. Kawamura and S. Raby, *Lepto-axiogenesis in minimal SUSY KSVZ model*, [2109.08605](#).
- [114] R. T. Co, K. Harigaya, Z. Johnson and A. Pierce, *R-parity violation axiogenesis*, *JHEP* **11** (2021) 210 [[2110.05487](#)].
- [115] R. T. Co, L. J. Hall and K. Harigaya, *QCD Axion Dark Matter with a Small Decay Constant*, *Phys. Rev. Lett.* **120** (2018) 211602 [[1711.10486](#)].
- [116] K. Harigaya and J. M. Leedom, *QCD Axion Dark Matter from a Late Time Phase Transition*, *JHEP* **06** (2020) 034 [[1910.04163](#)].
- [117] R. T. Co, L. J. Hall, K. Harigaya, K. A. Olive and S. Verner, *Axion Kinetic Misalignment and Parametric Resonance from Inflation*, *JCAP* **08** (2020) 036 [[2004.00629](#)].
- [118] L. Visinelli and P. Gondolo, *Axion cold dark matter in non-standard cosmologies*, *Phys. Rev. D* **81** (2010) 063508 [[0912.0015](#)].
- [119] P. Arias, N. Bernal, D. Karamitros, C. Maldonado, L. Roszkowski and M. Venegas, *New opportunities for axion dark matter searches in nonstandard cosmological models*, *JCAP* **11** (2021) 003 [[2107.13588](#)].
- [120] P. J. Steinhardt and M. S. Turner, *Saving the Invisible Axion*, *Phys. Lett. B* **129** (1983) 51.
- [121] S. Dimopoulos and L. J. Hall, *Inflation and Invisible Axions*, *Phys. Rev. Lett.* **60** (1988) 1899.
- [122] H. Davoudiasl, D. Hooper and S. D. McDermott, *Inflatable Dark Matter*, *Phys. Rev. Lett.* **116** (2016) 031303 [[1507.08660](#)].
- [123] S. Hoof and J. Jaeckel, *QCD axions and axionlike particles in a two-inflation scenario*, *Phys. Rev. D* **96** (2017) 115016 [[1709.01090](#)].
- [124] P. W. Graham and A. Scherlis, *Stochastic axion scenario*, *Phys. Rev. D* **98** (2018) 035017 [[1805.07362](#)].
- [125] F. Takahashi, W. Yin and A. H. Guth, *QCD axion window and low-scale inflation*, *Phys. Rev. D* **98** (2018) 015042 [[1805.08763](#)].
- [126] N. Kitajima, Y. Tada and F. Takahashi, *Stochastic inflation with an extremely large number of e-folds*, *Phys. Lett. B* **800** (2020) 135097 [[1908.08694](#)].
- [127] P. W. Graham, D. E. Kaplan and S. Rajendran, *Cosmological Relaxation of the Electroweak Scale*, *Phys. Rev. Lett.* **115** (2015) 221801 [[1504.07551](#)].

- [128] R. Daido, F. Takahashi and W. Yin, *The ALP miracle: unified inflaton and dark matter*, *JCAP* **05** (2017) 044 [[1702.03284](#)].
- [129] R. Daido, F. Takahashi and W. Yin, *The ALP miracle revisited*, *JHEP* **02** (2018) 104 [[1710.11107](#)].
- [130] N. Fonseca, E. Morgante, R. Sato and G. Servant, *Axion fragmentation*, *JHEP* **04** (2020) 010 [[1911.08472](#)].
- [131] E. Morgante, W. Ratzinger, R. Sato and B. A. Stefanek, *Axion fragmentation on the lattice*, *JHEP* **12** (2021) 037 [[2109.13823](#)].
- [132] D. Cyncynates, T. Giurgica-Tiron, O. Simon and J. O. Thompson, *Friendship in the Axiverse: Late-time direct and astrophysical signatures of early-time nonlinear axion dynamics*, [2109.09755](#).
- [133] K. Freese, J. A. Frieman and A. V. Olinto, *Natural inflation with pseudo - Nambu-Goldstone bosons*, *Phys. Rev. Lett.* **65** (1990) 3233.
- [134] S. Dimopoulos, S. Kachru, J. McGreevy and J. G. Wacker, *N-flation*, *JCAP* **08** (2008) 003 [[hep-th/0507205](#)].
- [135] E. Silverstein and A. Westphal, *Monodromy in the CMB: Gravity Waves and String Inflation*, *Phys. Rev. D* **78** (2008) 106003 [[0803.3085](#)].
- [136] L. McAllister, E. Silverstein and A. Westphal, *Gravity Waves and Linear Inflation from Axion Monodromy*, *Phys. Rev. D* **82** (2010) 046003 [[0808.0706](#)].
- [137] G. W. Gibbons and S. W. Hawking, *Cosmological Event Horizons, Thermodynamics, and Particle Creation*, *Phys. Rev. D* **15** (1977) 2738.
- [138] M. Axenides, R. H. Brandenberger and M. S. Turner, *Development of Axion Perturbations in an Axion Dominated Universe*, *Phys. Lett. B* **126** (1983) 178.
- [139] M. S. Turner, F. Wilczek and A. Zee, *Formation of Structure in an Axion Dominated Universe*, *Phys. Lett. B* **125** (1983) 35. [Erratum: *Phys.Lett.B* 125, 519 (1983)].
- [140] M. P. Hertzberg, M. Tegmark and F. Wilczek, *Axion Cosmology and the Energy Scale of Inflation*, *Phys. Rev. D* **78** (2008) 083507 [[0807.1726](#)].
- [141] M. Tegmark, A. Aguirre, M. Rees and F. Wilczek, *Dimensionless constants, cosmology and other dark matters*, *Phys. Rev. D* **73** (2006) 023505 [[astro-ph/0511774](#)].
- [142] K. J. Mack, *Axions, Inflation and the Anthropic Principle*, *JCAP* **07** (2011) 021 [[0911.0421](#)].
- [143] R. A. Battye and E. P. S. Shellard, *Axion string constraints*, *Phys. Rev. Lett.* **73** (1994) 2954 [[astro-ph/9403018](#)]. [Erratum: *Phys.Rev.Lett.* 76, 2203–2204 (1996)].

- [144] C. Hagmann, S. Chang and P. Sikivie, *Axions from string decay*, *Nucl. Phys. B Proc. Suppl.* **72** (1999) 81 [[hep-ph/9807428](#)].
- [145] T. Hiramatsu, M. Kawasaki, T. Sekiguchi, M. Yamaguchi and J. Yokoyama, *Improved estimation of radiated axions from cosmological axionic strings*, *Phys. Rev. D* **83** (2011) 123531 [[1012.5502](#)].
- [146] V. B. Klaer and G. D. Moore, *How to simulate global cosmic strings with large string tension*, *JCAP* **10** (2017) 043 [[1707.05566](#)].
- [147] V. B. Klaer and G. D. Moore, *The dark-matter axion mass*, *JCAP* **1711** (2017) 049 [[1708.07521](#)].
- [148] M. Gorghetto, E. Hardy and G. Villadoro, *Axions from Strings: the Attractive Solution*, *JHEP* **07** (2018) 151 [[1806.04677](#)].
- [149] A. Vaquero, J. Redondo and J. Stadler, *Early seeds of axion miniclusters*, *JCAP* **04** (2019) 012 [[1809.09241](#)].
- [150] M. Buschmann, J. W. Foster and B. R. Safdi, *Early-Universe Simulations of the Cosmological Axion*, *Phys. Rev. Lett.* **124** (2020) 161103 [[1906.00967](#)].
- [151] M. Hindmarsh, J. Lizarraga, A. Lopez-Eiguren and J. Urrestilla, *Scaling Density of Axion Strings*, *Phys. Rev. Lett.* **124** (2020) 021301 [[1908.03522](#)].
- [152] M. Gorghetto, E. Hardy and G. Villadoro, *More axions from strings*, *SciPost Phys.* **10** (2021) 050 [[2007.04990](#)].
- [153] M. Dine, N. Fernandez, A. Ghalsasi and H. H. Patel, *Comments on axions, domain walls, and cosmic strings*, *JCAP* **11** (2021) 041 [[2012.13065](#)].
- [154] M. Buschmann, J. W. Foster, A. Hook, A. Peterson, D. E. Willcox, W. Zhang and B. R. Safdi, *Dark Matter from Axion Strings with Adaptive Mesh Refinement*, [2108.05368](#).
- [155] M. Hindmarsh, J. Lizarraga, A. Lopez-Eiguren and J. Urrestilla, *Comment on "More Axions from Strings"*, [2109.09679](#).
- [156] G. B. Gelmini, A. Simpson and E. Vitagliano, *Gravitational waves from axionlike particle cosmic string-wall networks*, *Phys. Rev. D* **104** (2021) 061301 [[2103.07625](#)].
- [157] C. A. J. O'Hare, G. Pierobon, J. Redondo and Y. Y. Y. Wong, *Simulations of axion-like particles in the post-inflationary scenario*, [2112.05117](#).
- [158] B. Eggemeier, J. Redondo, K. Dolag, J. C. Niemeyer and A. Vaquero, *First Simulations of Axion Minicluster Halos*, *Phys. Rev. Lett.* **125** (2020) 041301 [[1911.09417](#)].

- [159] W. Giarè, E. Di Valentino, A. Melchiorri and O. Mena, *New cosmological bounds on hot relics: axions and neutrinos*, *Mon. Not. Roy. Astron. Soc.* **505** (2021) 2703 [2011.14704].
- [160] D. Cadamuro and J. Redondo, *Cosmological bounds on pseudo Nambu-Goldstone bosons*, *JCAP* **02** (2012) 032 [1110.2895].
- [161] D. Cadamuro, S. Hannestad, G. Raffelt and J. Redondo, *Cosmological bounds on sub-MeV mass axions*, *JCAP* **02** (2011) 003 [1011.3694].
- [162] M. Millea, L. Knox and B. Fields, *New Bounds for Axions and Axion-Like Particles with keV-GeV Masses*, *Phys. Rev. D* **92** (2015) 023010 [1501.04097].
- [163] D. Green, Y. Guo and B. Wallisch, *Cosmological implications of axion-matter couplings*, *JCAP* **02** (2022) 019 [2109.12088].
- [164] CMB-S4 Collaboration Science Council, *CMB-S4: Probes of the Dark Universe*, Letter of Interest for the the Particle Physics Community Planning Exercise (Snowmass) 2021.
- [165] S. Bird, S. Birrer, D. Croon, A. Drlica-Wagner, J. A. Dror, D. Grin, P. M. David J. E. Marsh, E. Nadler, C. Prescod-Weinstein, K. K. Rogers, K. Schutz, N. Sehgal, Y.-D. Tsai, T.-T. Yu and Y. Zhong, *Cosmic probes of ultra-light axion dark matter*, Letter of Interest for the the Particle Physics Community Planning Exercise (Snowmass) 2021.
- [166] K. A. *et al.*, *Insights for Fundamental Physics and Cosmology with Light Relics*, Letter of Interest for the the Particle Physics Community Planning Exercise (Snowmass) 2021.
- [167] J. B. M. noz, C. Dvorkin, N. DePorzio, D. Green, J. Meyers, B. Wallisch and W. L. Xu, *Light but Massive Relics in Cosmology*, Letter of Interest for the the Particle Physics Community Planning Exercise (Snowmass) 2021.
- [168] J. C. *et al.*, *CMB Spectral Distortions: A new window to fundamental physics*, Letter of Interest for the the Particle Physics Community Planning Exercise (Snowmass) 2021.
- [169] L. Di Luzio, G. Martinelli and G. Piazza, *Breakdown of chiral perturbation theory for the axion hot dark matter bound*, *Phys. Rev. Lett.* **126** (2021) 241801 [2101.10330].
- [170] K. Abazajian *et al.*, *CMB-S4 Science Case, Reference Design, and Project Plan*, 1907.04473.
- [171] W. Giarè, F. Renzi, A. Melchiorri, O. Mena and E. Di Valentino, *Cosmological forecasts on thermal axions, relic neutrinos and light elements*, 2110.00340.
- [172] F. D’Eramo, F. Hajkarim and S. Yun, *Thermal axion production at low temperatures: a smooth treatment of the QCD phase transition*, 2108.04259.

- [173] F. D’Eramo, F. Hajkarim and S. Yun, *Thermal QCD Axions across Thresholds*, *JHEP* **10** (2021) 224 [2108.05371].
- [174] V. Springel et al., *First results from the IllustrisTNG simulations: matter and galaxy clustering*, *Mon. Not. Roy. Astron. Soc.* **475** (2018) 676 [1707.03397].
- [175] N.-C. H. (SSC/Caltech), *The milky way galaxy*, 2008.
- [176] MADMAX Collaboration, P. Brun et al., *A new experimental approach to probe QCD axion dark matter in the mass range above 40 μeV* , *Eur. Phys. J.* **C79** (2019) 186 [1901.07401].
- [177] A. Díaz-Morcillo, J. M. García Barceló, A. J. Lozano Guerrero, P. Navarro, B. Gimeno, S. Arguedas Cuendis, A. Álvarez Melcón, C. Cogollos, S. Calatroni, B. Döbrich, J. D. Gallego-Puyol, J. Golm, I. G. Irastorza, C. Malbrunot, J. Miralda-Escudé, C. Peña Garay, J. Redondo and W. Wuensch, *Design of new resonant haloscopes in the search for the dark matter axion: A review of the first steps in the rades collaboration*, *Universe* **8** (2022) .
- [178] M. S. Turner, *Periodic signatures for the detection of cosmic axions*, *Phys. Rev. D* **42** (1990) 3572.
- [179] P. Sikivie, *Caustic rings of dark matter*, *Physics Letters B* **432** (1998) 139–144.
- [180] M. A. A. et al., *Ultralight Bosonic Dark Matter Theory*, Letter of Interest for the the Particle Physics Community Planning Exercise (Snowmass) 2021.
- [181] H.-Y. Schive, T. Chiueh and T. Broadhurst, *Cosmic structure as the quantum interference of a coherent dark wave*, *Nature Physics* **10** (2014) 496 [1406.6586].
- [182] Z. Li, J. Shen and H.-Y. Schive, *Testing the Prediction of Fuzzy Dark Matter Theory in the Milky Way Center*, *ApJ* **889** (2020) 88 [2001.00318].
- [183] J. Veltmaat, B. Schwabe and J. C. Niemeyer, *Baryon-driven growth of solitonic cores in fuzzy dark matter halos*, *PhysRevD* **101** (2020) 083518 [1911.09614].
- [184] B. Schwabe and J. C. Niemeyer, *Deep zoom-in simulation of a fuzzy dark matter galactic halo*, *arXiv e-prints* (2021) arXiv:2110.09145 [2110.09145].
- [185] E. W. Lentz, T. R. Quinn, L. J. Rosenberg and M. J. Tremmel, *A new signal model for axion cavity searches from N-body simulations*, *The Astrophysical Journal* **845** (2017) 121.
- [186] E. W. Lentz, T. R. Quinn and L. J. Rosenberg, *Axion structure formation – I: the co-motion picture*, *Monthly Notices of the Royal Astronomical Society* **485** (2019) 1809 [https://academic.oup.com/mnras/article-pdf/485/2/1809/28013054/stz488.pdf].

- [187] E. W. Lentz, T. R. Quinn and L. J. Rosenberg, *Axion structure formation – II. The wrath of collapse*, *Monthly Notices of the Royal Astronomical Society* **493** (2020) 5944 [<https://academic.oup.com/mnras/article-pdf/493/4/5944/32980097/staa557.pdf>].
- [188] E. W. Lentz, T. R. Quinn, L. J. Rosenberg and ADMX collaboration, *Many-Body Effects in Axion Dark Matter Structure*, Letter of Interest for the the Particle Physics Community Planning Exercise (Snowmass) 2021.
- [189] P. Tinyakov, I. Tkachev and K. Zioutas, *Tidal streams from axion miniclusters and direct axion searches*, *Journal of Cosmology and Astroparticle Physics* **2016** (2015) .
- [190] V. I. Dokuchaev, Y. N. Eroshenko and I. I. Tkachev, *Destruction of axion miniclusters in the Galaxy*, *Soviet Journal of Experimental and Theoretical Physics* **125** (2017) 434 [1710.09586].
- [191] B. J. Kavanagh, T. D. P. Edwards, L. Visinelli and C. Weniger, *Stellar disruption of axion miniclusters in the milky way*, *Phys. Rev. D* **104** (2021) 063038.
- [192] C. A. J. O’Hare and A. M. Green, *Axion astronomy with microwave cavity experiments*, *Phys. Rev. D* **95** (2017) 063017 [1701.03118].
- [193] ADMX Collaboration, T. Braine et al., *Extended Search for the Invisible Axion with the Axion Dark Matter Experiment*, *Phys. Rev. Lett.* **124** (2020) 101303 [1910.08638].
- [194] ADMX Collaboration, N. Du et al., *A Search for Invisible Axion Dark Matter with the Axion Dark Matter Experiment*, *Phys. Rev. Lett.* **120** (2018) 151301 [1804.05750].
- [195] ADMX Collaboration, C. Bartram et al., *Search for “Invisible” Axion Dark Matter in the 3.3–4.2 μeV Mass Range*, 2110.06096.
- [196] V. B. Klaer and G. D. Moore, *“The Dark-Matter Axion Mass”*, *Journal of Cosmology and Astroparticle Physics* **2017** (2017) 049.
- [197] B. M. Brubaker et al., *“First Results from a Microwave Cavity Axion Search at 24 μeV ”*, *Phys. Rev. Lett.* **118** (2017) 061302.
- [198] L. Zhong et al., *“Results from Phase 1 of the HAYSTAC Microwave Cavity Axion Experiment”*, *Phys. Rev. D* **97** (2018) 092001.
- [199] K. M. Backes, D. A. Palken, S. A. Kenany, B. M. Brubaker, S. B. Cahn, A. Droster, G. C. Hilton, S. Ghosh, H. Jackson, S. K. Lamoreaux, A. F. Leder, K. W. Lehnert, S. M. Lewis, M. Malnou, R. H. Maruyama, N. M. Rapidis, M. Simanovskaia, S. Singh, D. H. Speller, I. Urdinaran, L. R. Vale, E. C. van Assendelft, K. van Bibber and H. Wang, *A quantum enhanced search for dark matter axions*, *Nature* **590** (2021) 238 [2008.01853].
- [200] D. A. Palken et al., *“Improved analysis framework for axion dark matter searches”*, *Phys. Rev. D* **101** (2020) 123011.

- [201] J. Choi, S. Ahn, B. R. Ko, S. Lee and Y. K. Semertzidis, "CAPP-8TB: Axion Dark Matter Search Experiment around $6.7 \mu\text{eV}$ ", *arXiv preprint arXiv:2007.07468* (2020) [[2007.07468](#)].
- [202] M. Simanovskaia, A. Droster, H. Jackson, I. Urdinaran and K. van Bibber, "A Symmetric Multi-rod Tunable Microwave Cavity for the HAYSTAC Dark Matter Axion Search", *arXiv preprint arXiv:2006.01248* (2020) [[2006.01248](#)].
- [203] K. Wurtz, B. Brubaker, Y. Jiang, E. Ruddy, D. Palken and K. Lehnert, *Cavity Entanglement and State Swapping to Accelerate the Search for Axion Dark Matter*, *PRX Quantum* **2** (2021) 1 [[2107.04147](#)].
- [204] R. Di Vora et al., *A high-Q microwave dielectric resonator for axion dark matter haloscopes*, [2201.04223](#).
- [205] S. K. Lamoreaux, K. A. van Bibber, K. W. Lehnert and G. Carosi, *Analysis of single-photon and linear amplifier detectors for microwave cavity dark matter axion searches*, *Phys. Rev. D* **88** (2013) 035020 [[1306.3591](#)].
- [206] A. V. Dixit, S. Chakram, K. He, A. Agrawal, R. K. Naik, D. I. Schuster and A. Chou, *Searching for Dark Matter with a Superconducting Qubit*, *Phys. Rev. Lett.* **126** (2021) 141302 [[2008.12231](#)].
- [207] M. Lawson, A. J. Millar, M. Pancaldi, E. Vitagliano and F. Wilczek, *Tunable axion plasma haloscopes*, [1904.11872](#).
- [208] J. B. Pendry, A. J. Holden, D. J. Robbins and W. J. Stewart, *Low frequency plasmons in thin-wire structures*, *J. Phys. Condens. Matter* **10** (1998) 4785.
- [209] G. B. Gelmini, A. J. Millar, V. Takhistov and E. Vitagliano, *Probing dark photons with plasma haloscopes*, *Phys. Rev. D* **102** (2020) 043003 [[2006.06836](#)].
- [210] R. Balafendiev, C. Simovski, A. J. Millar and P. Belov, *Wire metamaterial filled metallic resonators*, [2203.10083](#).
- [211] M. Wooten, A. Droster, A. Kenany, D. Sun, S. M. Lewis and K. van Bibber, "Exploration of Wire Array Metamaterials for the Plasma Axion Haloscope", *arXiv preprint arXiv:2203.13945* (2022) [[2203.13945](#)].
- [212] MADMAX WORKING GROUP Collaboration, A. Caldwell, G. Dvali, B. Majorovits, A. Millar, G. Raffelt, J. Redondo, O. Reimann, F. Simon and F. Steffen, *Dielectric Haloscopes: A New Way to Detect Axion Dark Matter*, *Phys. Rev. Lett.* **118** (2017) 091801 [[1611.05865](#)].
- [213] ADMX collaboration, *Axion Dark Matter eXperiment (ADMX) 2-4 GHz*, Letter of Interest for the the Particle Physics Community Planning Exercise (Snowmass) 2021.

- [214] J. Jaeckel and J. Redondo, *Resonant to broadband searches for cold dark matter consisting of weakly interacting slim particles*, *Phys. Rev.* **D88** (2013) 115002 [1308.1103].
- [215] A. J. Millar, G. G. Raffelt, J. Redondo and F. D. Steffen, *Dielectric Haloscopes to Search for Axion Dark Matter: Theoretical Foundations*, *JCAP* **1701** (2017) 061 [1612.07057].
- [216] M. Baryakhtar, J. Huang and R. Lasenby, *Axion and hidden photon dark matter detection with multilayer optical haloscopes*, *Phys. Rev. D* **98** (2018) 035006 [1803.11455].
- [217] J. Chiles et al., *First Constraints on Dark Photon Dark Matter with Superconducting Nanowire Detectors in an Optical Haloscope*, 2110.01582.
- [218] BREAD Collaboration, J. Liu et al., *Broadband solenoidal haloscope for terahertz axion detection*, *Accepted Phys. Rev. Lett.* (2022) [2111.12103].
- [219] D. Horns, J. Jaeckel, A. Lindner, A. Lobanov, J. Redondo and A. Ringwald, *Searching for WISPy Cold Dark Matter with a Dish Antenna*, *JCAP* **1304** (2013) 016 [1212.2970].
- [220] O. Kwon, D. Lee, W. Chung, D. Ahn, H. Byun, F. Caspers, H. Choi, J. Choi, Y. Chong, H. Jeong, J. Jeong, J. E. Kim, J. Kim, i. m. c. b. u. Kutlu, J. Lee, M. Lee, S. Lee, A. Matlashov, S. Oh, S. Park, S. Uchaikin, S. Youn and Y. K. Semertzidis, *First results from an axion haloscope at capp around 10.7 μ eV*, *Phys. Rev. Lett.* **126** (2021) 191802.
- [221] B. T. McAllister, G. Flower, E. N. Ivanov, M. Goryachev, J. Bourhill and M. E. Tobar, *The organ experiment: An axion haloscope above 15 ghz*, *Physics of the Dark Universe* **18** (2017) 67.
- [222] A. P. Quiskamp, B. T. McAllister, P. Altin, E. N. Ivanov, M. Goryachev and M. E. Tobar, *Direct search for dark matter axions excluding alpogenesis in the 63-67 micro-ev range, with the organ experiment*, 2203.12152.
- [223] A. P. Quiskamp, B. T. McAllister, G. Rybka and M. E. Tobar, *Dielectric-boosted sensitivity to cylindrical azimuthally varying transverse-magnetic resonant modes in an axion haloscope*, *Phys. Rev. Applied* **14** (2020) 044051.
- [224] B. T. McAllister, G. Flower, L. E. Tobar and M. E. Tobar, *Tunable supermode dielectric resonators for axion dark-matter haloscopes*, *Phys. Rev. Applied* **9** (2018) 014028.
- [225] M. Diaz Ortiz, J. Gleason, H. Grote, A. Hallal, M. Hartman, H. Hollis, K.-S. Isleif, A. James, K. Karan, T. Kozlowski, A. Lindner, G. Messineo, G. Mueller, J. Pöld, R. Smith, A. Spector, D. Tanner, L.-W. Wei and B. Willke, *Design of the alps ii optical system*, *Physics of the Dark Universe* **35** (2022) 100968.

- [226] A. Hallal, G. Messineo, M. D. Ortiz, J. Gleason, H. Hollis, D. Tanner, G. Mueller and A. Spector, *The heterodyne sensing system for the alps ii search for sub-ev weakly interacting particles*, *Physics of the Dark Universe* **35** (2022) 100914.
- [227] M. Meyer, D. Horns and M. Raue, *First lower limits on the photon-axion-like particle coupling from very high energy gamma-ray observations*, *Phys. Rev. D* **87** (2013) 035027.
- [228] M. Giannotti, I. Irastorza, J. Redondo and A. Ringwald, *Cool WISPs for stellar cooling excesses*, *Journal of cosmology and astroparticle physics* **2016** (2016) 057 [1512.08108].
- [229] K. Ehret, M. Frede, S. Ghazaryan, M. Hildebrandt, E.-A. Knabbe, D. Kracht, A. Lindner, J. List, T. Meier, N. Meyer, D. Notz, J. Redondo, A. Ringwald, G. Wiedemann and B. Willke, *New alps results on hidden-sector lightweights*, *Physics Letters B* **689** (2010) 149.
- [230] A. Ejlli, F. Della Valle, U. Gastaldi, G. Messineo, R. Pengo, G. Ruoso and G. Zavattini, *The pvlas experiment: A 25 year effort to measure vacuum magnetic birefringence*, *Physics Reports* **871** (2020) 1. The PVLAS experiment: A 25 year effort to measure vacuum magnetic birefringence.
- [231] A. Ejlli, F. Della Valle, U. Gastaldi, G. Messineo, R. Pengo, G. Ruoso and G. Zavattini, *Upper limits on the amplitude of ultra-high-frequency gravitational waves from graviton to photon conversion*, *The European Physical Journal C* **79**(12) (2019) 1032.
- [232] L. Visinelli and P. Gondolo, *Axion cold dark matter revisited*, *J. Phys. Conf. Ser.* **203** (2010) 012035 [0910.3941].
- [233] J. L. Ouellet et al., *First Results from ABRACADABRA-10 cm: A Search for Sub- μ eV Axion Dark Matter*, *Phys. Rev. Lett.* **122** (2019) 121802 [1810.12257].
- [234] C. P. Salemi et al., *Search for Low-Mass Axion Dark Matter with ABRACADABRA-10 cm*, *Phys. Rev. Lett.* **127** (2021) 081801 [2102.06722].
- [235] M. Silva-Feaver, S. Chaudhuri, H. Cho, C. Dawson, P. Graham, K. Irwin, S. Kuenstner, D. Li, J. Mardon, H. Moseley, R. Mule, A. Phipps, S. Rajendran, Z. Steffen and B. Young, *Design overview of dm radio pathfinder experiment*, *IEEE Transactions on Applied Superconductivity* **27** (2017) 1.
- [236] Y. Kahn, B. R. Safdi and J. Thaler, *Broadband and Resonant Approaches to Axion Dark Matter Detection*, *Physical Review Letters* **117** (2016) 141801.
- [237] S. Chaudhuri and Others, *”Radio for Hidden-Photon Dark Matter Detection”*, *Physical Review D* **92** (2015) .
- [238] P. Sikivie, N. Sullivan and D. B. Tanner, *Proposal for axion dark matter detection using an LC circuit.*, *Physical Review Letters* **112** (2014) 131301.

- [239] A. Romanenko, A. Grassellino, A. C. Crawford, D. A. Sergatskov and O. Melnychuk, *Ultra-high quality factors in superconducting niobium cavities in ambient magnetic fields up to 190 mG*, *Appl. Phys. Lett.* **105** (2014) 234103 [[1410.7877](#)].
- [240] D. Ahn, O. Kwon, W. Chung, W. Jang, D. Lee, J. Lee, S. W. Youn, D. Youm and Y. K. Semertzidis, *Superconducting cavity in a high magnetic field*, [2002.08769](#).
- [241] C. Alduino et al., *The cuore cryostat: An infrastructure for rare event searches at millikelvin temperatures*, *Cryogenics* **102** (2019) 9.
- [242] DMRadio Collaboration, *to appear*, .
- [243] S. Chaudhuri, K. Irwin, P. W. Graham and J. Mardon, "Fundamental Limits of Electromagnetic Axion and Hidden-Photon Dark Matter Searches: Part I - The Quantum Limit", *arXiv preprint arXiv:1803.01627* (2018) [[1803.01627](#)].
- [244] J. L. Ouellet et al., *Design and implementation of the abracadabra-10 cm axion dark matter search*, *Phys. Rev. D* **99** (2019) 052012.
- [245] C. P. Salemi, J. W. Foster, J. L. Ouellet, A. Gavin, K. M. Pappas, S. Cheng, K. A. Richardson, R. Henning, Y. Kahn, R. Nguyen, N. L. Rodd, B. R. Safdi and L. Winslow, *Search for Low-Mass Axion Dark Matter with ABRACADABRA-10 cm*, *Physical Review Letters* **127** (2021) 081801.
- [246] J. W. Foster, N. L. Rodd and B. R. Safdi, *Revealing the dark matter halo with axion direct detection*, *Phys. Rev. D* **97** (2018) 123006.
- [247] J. L. Ouellet, C. P. Salemi, J. W. Foster, R. Henning, Z. Bogorad, J. M. Conrad, J. A. Formaggio, Y. Kahn, J. Minervini, A. Radovinsky, N. L. Rodd, B. R. Safdi, J. Thaler, D. Winklehner and L. Winslow, *First results from abracadabra-10 cm: A search for sub- μ eV axion dark matter*, *Phys. Rev. Lett.* **122** (2019) 121802.
- [248] S. Matsuura, T. Arai, J. J. Bock, A. Cooray, P. M. Korngut, M. G. Kim, H. M. Lee, D. H. Lee, L. R. Levenson, T. Matsumoto, Y. Onishi, M. Shirahata, K. Tsumura, T. Wada and M. Zemcov, *New Spectral Evidence of an Unaccounted Component of the Near-infrared Extragalactic Background Light from the CIBER*, *The Astrophysical Journal* **839** (2017) 7.
- [249] K. Kohri and H. Kodama, *Axion-like particles and recent observations of the cosmic infrared background radiation*, *Physical Review D* **96** (2017) 051701.
- [250] M. Tanabashi et al. (Particle Data Group), *2019 Review of Particle Physics*, *Phys. Rev. D* **98** (2018) 030001.
- [251] A. V. Gramolin, D. Aybas, D. Johnson, J. Adam and A. O. Sushkov, *Search for axion-like dark matter with ferromagnets*, *Nature Physics* **17** (2021) 79.
- [252] J. L. Ouellet and Others, "First Results from ABRACADABRA-10 cm: A Search for Sub- μ eV Axion Dark Matter", *Phys. Rev. Lett.* **122** (2019) 121802.

- [253] L. Brouwer et al., *Introducing DMRadio-GUT, a search for GUT-scale QCD axions*, [2203.11246](#).
- [254] L. Bottura, G. De Rijk, L. Rossi and E. Todesco, *Advanced accelerator magnets for upgrading the lhc*, *IEEE Transactions on Applied Superconductivity* **22** (2012) 4002008.
- [255] E. Todesco, M. Annarella, G. Ambrosio, G. Apollinari, A. Ballarino, H. Bajas, M. Bajko, B. Bordini, R. Bossert, L. Bottura et al., *Progress on hl-lhc nb 3 sn magnets*, *IEEE Transactions on Applied Superconductivity* **28** (2018) 1.
- [256] A. J. Creely et al., *Overview of the sparcs tokamak*, *Journal of Plasma Physics* **86** (2020) .
- [257] S. Chaudhuri, K. D. Irwin, P. W. Graham and J. Mardon, “*Optimal Electromagnetic Searches for Axion and Hidden-Photon Dark Matter*”, *arXiv preprint arXiv:1904.0580* (2019) [[1904.05806](#)].
- [258] S. Kuenstner et al., *Quantum metrology of low frequency electromagnetic modes with frequency upconverters, in preparation*, 2022.
- [259] S. Kuenstner et al., *Optimizing frequency upconverters for quantum metrology of low frequency electromagnetic modes, in preparation*, 2022.
- [260] A. Berlin, R. T. D’Agnolo, S. A. R. Ellis, C. Nantista, J. Neilson, P. Schuster, S. Tantawi, N. Toro and K. Zhou, *Axion Dark Matter Detection by Superconducting Resonant Frequency Conversion*, *JHEP* **07** (2020) 088 [[1912.11048](#)].
- [261] A. Berlin, R. T. D’Agnolo, S. A. R. Ellis and K. Zhou, *Heterodyne broadband detection of axion dark matter*, *Phys. Rev. D* **104** (2021) L111701 [[2007.15656](#)].
- [262] R. Lasenby, *Microwave cavity searches for low-frequency axion dark matter*, *Phys. Rev. D* **102** (2020) 015008 [[1912.11056](#)].
- [263] R. Ballantini et al., *Microwave apparatus for gravitational waves observation*, [gr-qc/0502054](#).
- [264] A. Grassellino, *SRF-based dark matter search: Experiment*, 2020, <https://indico.physics.lbl.gov/event/939/contributions/4371/attachments/2162/2915/DarkSRFAspen-2.pdf>.
- [265] A. Berlin, S. Belomestnykh, D. Blas et al., *Searches for New Particles, Dark Matter, and Gravitational Waves with SRF Cavities*, *Snowmass 2021 White Paper*, 2022.
- [266] M. Goryachev, B. T. McAllister and M. E. Tobar, *Axion detection with precision frequency metrology*, *Physics of the Dark Universe* **26** (2019) 100345.
- [267] C. Thomson, M. Goryachev, B. T. McAllister and M. E. Tobar, *Corrigendum to “axion detection with precision frequency metrology” [phys. dark universe 26 (2019) 100345]*, *Physics of the Dark Universe* **32** (2021) 100787.

- [268] C. A. Thomson, B. T. McAllister, M. Goryachev, E. N. Ivanov and M. E. Tobar, *Upconversion loop oscillator axion detection experiment: A precision frequency interferometric axion dark matter search with a cylindrical microwave cavity*, *Phys. Rev. Lett.* **126** (2021) 081803.
- [269] C. A. Thomson, B. T. McAllister, M. Goryachev, E. N. Ivanov and M. E. Tobar, *Erratum: Upconversion loop oscillator axion detection experiment: A precision frequency interferometric axion dark matter search with a cylindrical microwave cavity* [*phys. rev. lett.* 126, 081803 (2021)], *Phys. Rev. Lett.* **127** (2021) 019901.
- [270] D. Budker, P. W. Graham, M. Ledbetter, S. Rajendran and A. O. Sushkov, *Proposal for a Cosmic Axion Spin Precession Experiment (CASPER)*, *Physical Review X* **4** (2014) 021030.
- [271] *Search for Axionlike Dark Matter Using Solid-State Nuclear Magnetic Resonance*, *Physical Review Letters* **126** (2021) 141802.
- [272] P. W. Graham and S. Rajendran, *New observables for direct detection of axion dark matter*, *Phys. Rev. D* **88** (2013) 035023.
- [273] J. H. Chang, R. Essig and S. D. McDermott, *Supernova 1987A constraints on sub-GeV dark sectors, millicharged particles, the QCD axion, and an axion-like particle*, *Journal of High Energy Physics* **2018:09** (2018) 051.
- [274] T. N. Mukhamedjanov and O. P. Sushkov, *Suggested search for Pb207 nuclear Schiff moment in PbTiO3 ferroelectric*, *Physical Review A* **72** (2005) 34501.
- [275] J. A. Ludlow and O. P. Sushkov, *Investigating the nuclear Schiff moment of 207 Pb in ferroelectric PbTiO 3*, *Journal of Physics B: Atomic, Molecular and Optical Physics* **46** (2013) 085001.
- [276] L. V. Skripnikov and A. V. Titov, *LCAO-based theoretical study of PbTiO3 crystal to search for parity and time reversal violating interaction in solids*, *Journal of Chemical Physics* **145** (2016) 054115.
- [277] D. Aybas, H. Bekker, J. Blanchard, D. Budker, G. Centers, N. Figueroa, A. Gramolin, D. F. Kimball, A. Wickenbrock and A. Sushkov, *Quantum sensitivity limits of nuclear magnetic resonance experiments searching for new fundamental physics*, *Quantum Science and Technology* **6** (2021) 034007.
- [278] T. Wu, J. W. Blanchard, G. P. Centers, N. L. Figueroa, A. Garcon, P. W. Graham, D. F. J. Kimball, S. Rajendran, Y. V. Stadnik, A. O. Sushkov, A. Wickenbrock and D. Budker, *Search for axionlike dark matter with a liquid-state nuclear spin comagnetometer*, *Phys. Rev. Lett.* **122** (2019) 191302.
- [279] A. Garcon, J. W. Blanchard, G. P. Centers, N. L. Figueroa, P. W. Graham, D. F. J. Kimball, S. Rajendran, A. O. Sushkov, Y. V. Stadnik, A. Wickenbrock, T. Wu and D. Budker, *Constraints on bosonic dark matter from ultralow-field nuclear magnetic*

- resonance, *Science Advances* **5** (2019) eaax4539
[<https://www.science.org/doi/pdf/10.1126/sciadv.aax4539>].
- [280] P. Fadeev, Y. V. Stadnik, F. Ficek, M. G. Kozlov, V. V. Flambaum and D. Budker, *Revisiting spin-dependent forces mediated by new bosons: Potentials in the coordinate-space representation for macroscopic- and atomic-scale experiments*, *Phys. Rev. A* **99** (2019) 022113 [[1810.10364](https://arxiv.org/abs/1810.10364)].
- [281] J. E. Moody and F. Wilczek, *New macroscopic forces?*, *Physical Review D* **30** (1984) 130.
- [282] A. N. Youdin, J. Krause, D., K. Jagannathan, L. R. Hunter and S. K. Lamoreaux, *Limits on Spin-Mass Couplings within the Axion Window*, *Physical Review Letters* **77** (1996) 2170.
- [283] G. Raffelt, *Limits on a cp-violating scalar axion-nucleon interaction*, *Phys. Rev. D* **86** (2012) 015001.
- [284] C. A. J. O'Hare and E. Vitagliano, *Cornering the axion with CP-violating interactions*, *Phys. Rev. D* **102** (2020) 115026 [[2010.03889](https://arxiv.org/abs/2010.03889)].
- [285] A. Arvanitaki and A. A. Geraci, *Resonantly detecting axion-mediated forces with nuclear magnetic resonance*, *Physical review letters* **113** (2014) 161801.
- [286] H. Fosbinder-Elkins, C. Lohmeyer, J. Dargert, M. Cunningham, M. Harkness, E. Levenson-Falk, S. Mumford, A. Kapitulnik, A. Arvanitaki, I. Lee, E. Smith, E. Wiesman, J. Shortino, J. C. Long, W. M. Snow, C.-Y. Liu, Y. Shin, Y. Semertzidis and Y.-H. Lee, *Progress on the ariadne axion experiment*, in *Microwave Cavities and Detectors for Axion Research* (G. Carosi, G. Rybka and K. van Bibber, eds.), (Cham), pp. 151–161, Springer International Publishing, 2018.
- [287] J. Lee, A. Almasi and M. Romalis, *Improved limits on spin-mass interactions*, *Phys. Rev. Lett.* **120** (2018) 161801.
- [288] P.-H. Chu, A. Dennis, C. B. Fu, H. Gao, R. Khatiwada, G. Laskaris, K. Li, E. Smith, W. M. Snow, H. Yan and W. Zheng, *Laboratory search for spin-dependent short-range force from axionlike particles using optically polarized ^3He gas*, *Phys. Rev. D* **87** (2013) 011105.
- [289] M. Bulatowicz, R. Griffith, M. Larsen, J. Mirijanian, C. B. Fu, E. Smith, W. M. Snow, H. Yan and T. G. Walker, *Laboratory search for a long-range t-odd, p-odd interaction from axionlike particles using dual-species nuclear magnetic resonance with polarized ^{129}Xe and ^{131}Xe gas*, *Phys. Rev. Lett.* **111** (2013) 102001.
- [290] D. Budker, P. W. Graham, M. Ledbetter, S. Rajendran and A. O. Sushkov, *Proposal for a cosmic axion spin precession experiment (casper)*, *Phys. Rev. X* **4** (2014) 021030.

- [291] ADMX Collaboration, N. Du, N. Force, R. Khatriwada, E. Lentz, R. Ottens, L. J. Rosenberg, G. Rybka, G. Carosi, N. Woollett, D. Bowring, A. S. Chou, A. Sonnenschein, W. Wester, C. Boutan, N. S. Oblath, R. Bradley, E. J. Daw, A. V. Dixit, J. Clarke, S. R. O’Kelley, N. Crisosto, J. R. Gleason, S. Jois, P. Sikivie, I. Stern, N. S. Sullivan, D. B. Tanner and G. C. Hilton, *Search for invisible axion dark matter with the axion dark matter experiment*, *Phys. Rev. Lett.* **120** (2018) 151301.
- [292] L. Zhong, S. Al Kenany, K. M. Backes, B. M. Brubaker, S. B. Cahn, G. Carosi, Y. V. Gurevich, W. F. Kindel, S. K. Lamoreaux, K. W. Lehnert, S. M. Lewis, M. Malnou, R. H. Maruyama, D. A. Palken, N. M. Rapidis, J. R. Root, M. Simanovskaia, T. M. Shokair, D. H. Speller, I. Urdinaran and K. A. van Bibber, *Results from phase 1 of the haystac microwave cavity axion experiment*, *Phys. Rev. D* **97** (2018) 092001.
- [293] E. W. Kolb and I. I. Tkachev, *Axion miniclusters and Bose stars*, *Phys. Rev. Lett.* **71** (1993) 3051 [[hep-ph/9303313](#)].
- [294] E. Braaten, A. Mohapatra and H. Zhang, *Dense axion stars*, *Phys. Rev. Lett.* **117** (2016) 121801.
- [295] D. F. Jackson Kimball, D. Budker, J. Eby, M. Pospelov, S. Pustelny, T. Scholtes, Y. V. Stadnik, A. Weis and A. Wickenbrock, *Searching for axion stars and Q-balls with a terrestrial magnetometer network*, *Phys. Rev. D* **97** (2018) 043002.
- [296] J. Eby, M. Leembruggen, L. Street, P. Suranyi and L. Wijewardhana, *Global view of QCD axion stars*, *Phys. Rev. D* **100** (2019) 063002.
- [297] P. Sikivie, *Axions, domain walls, and the early universe*, *Phys. Rev. Lett.* **48** (1982) 1156.
- [298] A. Vilenkin, *Cosmic strings and domain walls*, *Phys. Rep.* **121** (1985) 263.
- [299] M. Kawasaki, K. Saikawa and T. Sekiguchi, *Axion dark matter from topological defects*, *Phys. Rev. D* **91** (2015) 065014.
- [300] M. Pospelov, S. Pustelny, M. P. Ledbetter, D. F. Jackson Kimball, W. Gawlik and D. Budker, *Detecting Domain Walls of Axionlike Models Using Terrestrial Experiments*, *Phys. Rev. Lett.* **110** (2013) 021803.
- [301] G. P. Centers, J. W. Blanchard, J. Conrad, N. L. Figueroa, A. Garcon, A. V. Gramolin, D. F. J. Kimball, M. Lawson, B. Pelssers, J. A. Smiga et al., *Stochastic fluctuations of bosonic dark matter*, *Nature Communications* **12** (2021) 7321.
- [302] C. Dailey, C. Bradley, D. F. Jackson Kimball, I. A. Sulai, S. Pustelny, A. Wickenbrock and A. Derevianko, *Quantum sensor networks as exotic field telescopes for multi-messenger astronomy*, *Nature Astronomy* **5** (2021) 150.
- [303] S. Pustelny, D. F. Jackson Kimball, C. Pankow, M. P. Ledbetter, P. Wlodarczyk, P. Wcislo, M. Pospelov, J. R. Smith, J. Read, W. Gawlik and D. Budker, *The Global Network of Optical Magnetometers for Exotic physics (GNOME): A novel scheme to search for physics beyond the Standard Model*, *Annalen der Physik* **525** (2013) 659.

- [304] S. Afach, D. Budker, G. DeCamp, V. Dumont, Z. D. Grujić, H. Guo, D. F. Jackson Kimball, T. W. Kornack, V. Lebedev, W. Li et al., *Characterization of the Global Network of Optical Magnetometers to Search for Exotic Physics (GNOME), Physics of the Dark Universe* **22** (2018) 162.
- [305] S. Afach, B. C. Buchler, D. Budker, C. Dailey, A. Derevianko, V. Dumont, N. L. Figueroa, I. Gerhardt, Z. D. Grujić, H. Guo et al., *Search for topological defect dark matter with a global network of optical magnetometers, Nature Physics* **17** (2021) 1396.
- [306] M. S. Safronova, D. Budker, D. DeMille, D. F. Jackson Kimball, A. Derevianko and C. W. Clark, *Search for new physics with atoms and molecules, Rev. Mod. Phys.* **90** (2018) 025008.
- [307] H. Masia-Roig, N. L. Figueroa, A. Bordon, J. A. Smiga, D. Budker, G. P. Centers, A. V. Gramolin, P. S. Hamilton, S. Khamis, C. A. Palm, S. Pustelny, A. O. Sushkov, A. Wickenbrock and D. F. Jackson Kimball, *Intensity interferometry for ultralight bosonic dark matter detection, arXiv:2202.02645* (2022) .
- [308] D. Budker and M. Romalis, *Optical magnetometry, Nature physics* **3** (2007) 227.
- [309] D. Budker and D. F. Jackson Kimball, *Optical Magnetometry*. Cambridge University Press, 2013.
- [310] D. F. Jackson Kimball, J. Dudley, Y. Li, S. Thulasi, S. Pustelny, D. Budker and M. Zolotarev, *Magnetic shielding and exotic spin-dependent interactions, Phys. Rev. D* **94** (2016) 082005.
- [311] H. Masia-Roig, J. A. Smiga, D. Budker, V. Dumont, Z. Grujic, D. Kim, D. F. Jackson Kimball, V. Lebedev, M. Monroy, S. Pustelny et al., *Analysis method for detecting topological defect dark matter with a global magnetometer network, Physics of the Dark Universe* **28** (2020) 100494.
- [312] D. Kim, D. F. J. Kimball, H. Masia-Roig, J. A. Smiga, A. Wickenbrock, D. Budker, Y. Kim, Y. C. Shin and Y. K. Semertzidis, *A machine learning algorithm for direct detection of axion-like particle domain walls, arXiv:2110.00139* (2021) .
- [313] T. Kornack and M. Romalis, *Dynamics of Two Overlapping Spin Ensembles Interacting by Spin Exchange, Phys. Rev. Lett.* **89** (2002) 253002.
- [314] T. Kornack, R. Ghosh and M. Romalis, *Nuclear Spin Gyroscope Based on an Atomic Comagnetometer, Phys. Rev. Lett.* **95** (2005) 230801.
- [315] M. A. Fedderke, P. W. Graham, D. F. J. Kimball and S. Kalia, *Earth as a transducer for dark-photon dark-matter detection, Phys. Rev. D* **104** (2021) 075023 [2106.00022].

- [316] M. A. Fedderke, P. W. Graham, D. F. Jackson Kimball and S. Kalia, *Search for dark-photon dark matter in the SuperMAG geomagnetic field dataset*, *Phys. Rev. D* **104** (2021) 095032 [2108.08852].
- [317] A. Arza, M. A. Fedderke, P. W. Graham, D. F. Jackson Kimball and S. Kalia, *Earth as a transducer for axion dark-matter detection*, 2112.09620.
- [318] A. Payez, C. Evoli, T. Fischer, M. Giannotti, A. Mirizzi and A. Ringwald, *Revisiting the SN1987A gamma-ray limit on ultralight axion-like particles*, *JCAP* **02** (2015) 006 [1410.3747].
- [319] S. D. McDermott and S. J. Witte, *Cosmological Evolution of Light Dark Photon Dark Matter*, *Phys. Rev. D* **101** (2020) 063030 [1911.05086].
- [320] D. Wadekar and Z. Wang, *Strong constraints on decay and annihilation of dark matter from heating of gas-rich dwarf galaxies*, *arXiv e-prints* (2021) arXiv:2111.08025 [2111.08025].
- [321] CAST Collaboration, V. Anastassopoulos et al., *New CAST Limit on the Axion-Photon Interaction*, *Nature Phys.* **13** (2017) 584 [1705.02290].
- [322] V. V. Flambaum, *Axioelectric effect and other manifestations of dark matter and dark energy in laboratory experiments*, Proceedings of the 9th Patras Workshop on Axions, WIMPs and WISPs, Mainz, Germany, 2013, https://axion-wimp2013.desy.de/e201031/index_eng.html.
- [323] Y. V. Stadnik and V. V. Flambaum, *Axion-induced effects in atoms, molecules, and nuclei: Parity nonconservation, anapole moments, electric dipole moments, and spin-gravity and spin-axion momentum couplings*, *Phys. Rev. D* **89** (2014) 043522.
- [324] Y. V. Stadnik, *Manifestations of dark matter and variations of the fundamental constants of nature in atoms and astrophysical phenomena*, PhD Thesis, Springer, Cham, Switzerland, 2017.
- [325] P. W. Graham, D. E. Kaplan, J. Mardon, S. Rajendran, W. A. Terrano, L. Trahms and T. Wilkason, *Spin precession experiments for light axionic dark matter*, *Phys. Rev. D* **97** (2018) 055006.
- [326] C. Smorra, Y. Stadnik, P. Blessing, M. Bohman, M. Borchert, J. Devlin, S. Erlewein, J. Harrington, T. Higuchi, A. Mooser et al., *Direct limits on the interaction of antiprotons with axion-like dark matter*, *Nature* **575** (2019) 310.
- [327] P. W. Graham, S. Hacıömeroğlu, D. E. Kaplan, Z. Omarov, S. Rajendran and Y. K. Semertzidis, *Storage ring probes of dark matter and dark energy*, *Phys. Rev. D* **103** (2021) 055010.
- [328] C. Abel et al., *Search for Axionlike Dark Matter through Nuclear Spin Precession in Electric and Magnetic Fields*, *Phys. Rev. X* **7** (2017) 041034 [1708.06367].

- [329] W. A. Terrano, E. G. Adelberger, C. A. Hagedorn and B. R. Heckel, *Constraints on axionlike dark matter with masses down to 10^{-23} eV/ c^2* , *Phys. Rev. Lett.* **122** (2019) 231301.
- [330] I. M. Bloch, Y. Hochberg, E. Kuflik and T. Volansky, *Axion-like relics: new constraints from old comagnetometer data*, *Journal of High Energy Physics* **2020** (2020) 1.
- [331] P. W. Graham and S. Rajendran, *Axion dark matter detection with cold molecules*, *Phys. Rev. D* **84** (2011) 055013.
- [332] R. Crewther, P. Di Vecchia, G. Veneziano and E. Witten, *Chiral estimate of the electric dipole moment of the neutron in quantum chromodynamics*, *Physics Letters B* **88** (1979) 123.
- [333] M. Pospelov and A. Ritz, *Theta-induced electric dipole moment of the neutron via qcd sum rules*, *Phys. Rev. Lett.* **83** (1999) 2526.
- [334] V. V. Flambaum, M. Pospelov, A. Ritz and Y. V. Stadnik, *Sensitivity of edm experiments in paramagnetic atoms and molecules to hadronic cp violation*, *Phys. Rev. D* **102** (2020) 035001.
- [335] T. S. Roussy, D. A. Palken, W. B. Cairncross, B. M. Brubaker, D. N. Gresh, M. Grau, K. C. Cossel, K. B. Ng, Y. Shagam, Y. Zhou, V. V. Flambaum, K. W. Lehnert, J. Ye and E. A. Cornell, *Experimental constraint on axionlike particles over seven orders of magnitude in mass*, *Phys. Rev. Lett.* **126** (2021) 171301.
- [336] G. G. Raffelt, *Stars as laboratories for fundamental physics: The astrophysics of neutrinos, axions, and other weakly interacting particles*. 5, 1996.
- [337] IAXO Collaboration, I. Irastorza et al., *Towards a new generation axion helioscope*, *JCAP* **1106** (2011) 013 [1103.5334].
- [338] IAXO Collaboration, A. Abeln et al., *Conceptual design of BabyIAXO, the intermediate stage towards the International Axion Observatory*, *JHEP* **05** (2021) 137 [2010.12076].
- [339] IAXO Collaboration, E. Armengaud et al., *Physics potential of the International Axion Observatory (IAXO)*, *JCAP* **06** (2019) 047 [1904.09155].
- [340] CAST Collaboration, M. Arik et al., *New solar axion search using the CERN Axion Solar Telescope with ^4He filling*, *Phys. Rev.* **D92** (2015) 021101 [1503.00610].
- [341] A. Ringwald and K. Saikawa, *Axion dark matter in the post-inflationary Peccei-Quinn symmetry breaking scenario*, *Phys. Rev.* **D93** (2016) 085031 [1512.06436]. [Addendum: *Phys. Rev.*D94,no.4,049908(2016)].
- [342] M. Meyer, D. Horns and M. Raue, *First lower limits on the photon-axion-like particle coupling from very high energy gamma-ray observations*, *Phys. Rev. D* **87** (2013) 035027 [1302.1208].

- [343] K. Kohri and H. Kodama, *Axion-Like Particles and Recent Observations of the Cosmic Infrared Background Radiation*, *Phys. Rev. D* **96** (2017) 051701 [1704.05189].
- [344] A. Ayala, I. Domínguez, M. Giannotti, A. Mirizzi and O. Straniero, *Revisiting the bound on axion-photon coupling from Globular Clusters*, *Phys. Rev. Lett.* **113** (2014) 191302 [1406.6053].
- [345] O. Straniero, *Axion-Photon Coupling: Astrophysical Constraints*, *PoS* (2015) 77.
- [346] L. Di Luzio, M. Fedele, M. Giannotti, F. Mescia and E. Nardi, *Stellar Evolution confronts Axion Models*, 2109.10368.
- [347] M. Giannotti, I. G. Irastorza, J. Redondo, A. Ringwald and K. Saikawa, *Stellar Recipes for Axion Hunters*, *JCAP* **10** (2017) 010 [1708.02111].
- [348] M. Schwarz, A. Lindner, J. Redondo, A. Ringwald and G. Wiedemann, *Solar Hidden Photon Search*, in *Axions, WIMPs and WISPs. Proceedings, 7th Patras Workshop, PATRAS 2011, Mykonos, Greece, June 27-July 1, 2011*, pp. 129–132, 2011, 1111.5797, <http://inspirehep.net/record/955162/files/arXiv:1111.5797.pdf>.
- [349] J. Redondo and G. Raffelt, *Solar constraints on hidden photons re-visited*, *JCAP* **1308** (2013) 034 [1305.2920].
- [350] P. Brax and K. Zioutas, *Solar Chameleons*, *Phys. Rev.* **D82** (2010) 043007 [1004.1846].
- [351] L. Di Luzio et al., *Probing the axion–nucleon coupling with the next generation of axion helioscopes*, *Eur. Phys. J. C* **82** (2022) 120 [2111.06407].
- [352] T. Dafni, C. A. J. O’Hare, B. Lakić, J. Galán, F. J. Iguaz, I. G. Irastorza, K. Jakovčić, G. Luzón, J. Redondo and E. Ruiz Chóliz, *Weighing the solar axion*, *Phys. Rev. D* **99** (2019) 035037 [1811.09290].
- [353] J. Jaeckel and L. J. Thormaehlen, *Distinguishing Axion Models with IAXO*, *JCAP* **03** (2019) 039 [1811.09278].
- [354] A. Caputo, A. J. Millar and E. Vitagliano, *Revisiting longitudinal plasmon-axion conversion in external magnetic fields*, *Phys. Rev. D* **101** (2020) 123004 [2005.00078].
- [355] E. Guarini, P. Carena, J. Galan, M. Giannotti and A. Mirizzi, *Production of axionlike particles from photon conversions in large-scale solar magnetic fields*, *Phys. Rev. D* **102** (2020) 123024 [2010.06601].
- [356] C. A. J. O’Hare, A. Caputo, A. J. Millar and E. Vitagliano, *Axion helioscopes as solar magnetometers*, *Phys. Rev. D* **102** (2020) 043019 [2006.10415].
- [357] I. G. Irastorza, *The international axion observatory iaxo. letter of intent to the cern sps committee*, Tech. Rep. CERN-SPSC-2013-022. SPSC-I-242, CERN, Geneva, Aug, 2013.

- [358] CAST Collaboration, K. Zioutas and the CAST Collaboration, *First results from the CERN Axion Solar Telescope (CAST)*, *Phys. Rev. Lett.* **94** (2005) 121301 [[hep-ex/0411033](#)].
- [359] CAST Collaboration, S. Andriamonje and the CAST Collaboration, *An Improved limit on the axion-photon coupling from the CAST experiment*, *JCAP* **0704** (2007) 010 [[hep-ex/0702006](#)].
- [360] K. van Bibber, P. M. McIntyre, D. E. Morris and G. G. Raffelt, *A Practical Laboratory Detector for Solar Axions*, *Phys. Rev.* **D39** (1989) 2089.
- [361] CAST Collaboration, E. Arik and the CAST Collaboration, *Probing eV-scale axions with CAST*, *JCAP* **0902** (2009) 008 [[0810.4482](#)].
- [362] I. G. Irastorza et al., *Status of R&D on Micromegas for Rare Event Searches : The T-REX project*, *EAS Publ. Ser.* **53** (2012) 147 [[1109.4021](#)].
- [363] T. Dafni et al., *Rare event searches based on micromegas detectors: The T-REX project*, *J. Phys. Conf. Ser.* **375** (2012) 022003.
- [364] T. Dafni et al., *The T-REX project: Micromegas for rare event searches*, *J. Phys. Conf. Ser.* **347** (2012) 012030.
- [365] D. H. Lumb, F. A. Jansen and N. ScharTEL, *X-ray Multi-mirror Mission (XMM-Newton) observatory*, *Optical Engineering* **51** (2012) 1 .
- [366] A. A. Melcon et al., *Axion Searches with Microwave Filters: the RADES project*, *JCAP* **1805** (2018) 040 [[1803.01243](#)].
- [367] CAST Collaboration, A. A. Melcón et al., *First results of the CAST-RADES haloscope search for axions at 34.67 μeV* , *JHEP* **21** (2020) 075 [[2104.13798](#)].
- [368] M. S. Pshirkov and S. B. Popov, *Conversion of Dark matter axions to photons in magnetospheres of neutron stars*, *J. Exp. Theor. Phys.* **108** (2009) 384 [[0711.1264](#)].
- [369] F. P. Huang, K. Kadota, T. Sekiguchi and H. Tashiro, *Radio telescope search for the resonant conversion of cold dark matter axions from the magnetized astrophysical sources*, *Phys. Rev. D* **97** (2018) 123001 [[1803.08230](#)].
- [370] A. Hook, Y. Kahn, B. R. Safdi and Z. Sun, *Radio Signals from Axion Dark Matter Conversion in Neutron Star Magnetospheres*, *Phys. Rev. Lett.* **121** (2018) 241102 [[1804.03145](#)].
- [371] B. R. Safdi, Z. Sun and A. Y. Chen, *Detecting Axion Dark Matter with Radio Lines from Neutron Star Populations*, *Phys. Rev. D* **99** (2019) 123021 [[1811.01020](#)].
- [372] M. Leroy, M. Chianese, T. D. P. Edwards and C. Weniger, *Radio Signal of Axion-Photon Conversion in Neutron Stars: A Ray Tracing Analysis*, *Phys. Rev. D* **101** (2020) 123003 [[1912.08815](#)].

- [373] J. W. Foster, Y. Kahn, O. Macias, Z. Sun, R. P. Eatough, V. I. Kondratiev, W. M. Peters, C. Weniger and B. R. Safdi, *Green Bank and Effelsberg Radio Telescope Searches for Axion Dark Matter Conversion in Neutron Star Magnetospheres*, *Phys. Rev. Lett.* **125** (2020) 171301 [2004.00011].
- [374] J. Darling, *Search for Axionic Dark Matter Using the Magnetar PSR J1745-2900*, *Phys. Rev. Lett.* **125** (2020) 121103 [2008.01877].
- [375] J. Darling, *New Limits on Axionic Dark Matter from the Magnetar PSR J1745-2900*, *Astrophys. J. Lett.* **900** (2020) L28 [2008.11188].
- [376] S. J. Witte, D. Noordhuis, T. D. P. Edwards and C. Weniger, *Axion-photon conversion in neutron star magnetospheres: The role of the plasma in the Goldreich-Julian model*, *Phys. Rev. D* **104** (2021) 103030 [2104.07670].
- [377] R. A. Battye, B. Garbrecht, J. I. McDonald and S. Srinivasan, *Radio line properties of axion dark matter conversion in neutron stars*, *JHEP* **09** (2021) 105 [2104.08290].
- [378] A. J. Millar, S. Baum, M. Lawson and M. C. D. Marsh, *Axion-photon conversion in strongly magnetised plasmas*, *JCAP* **11** (2021) 013 [2107.07399].
- [379] R. A. Battye, J. Darling, J. McDonald and S. Srinivasan, *Towards Robust Constraints on Axion Dark Matter using PSR J1745-2900*, 2107.01225.
- [380] J. W. Foster, S. J. Witte, M. Lawson, T. Linden, V. Gajjar, C. Weniger and B. R. Safdi, *Extraterrestrial Axion Search with the Breakthrough Listen Galactic Center Survey*, 2202.08274.
- [381] O. Straniero, A. Ayala, M. Giannotti, A. Mirizzi and I. Dominguez, *Axion-Photon Coupling: Astrophysical Constraints*, in *11th Patras Workshop on Axions, WIMPs and WISPs*, pp. 77–81, 2015, DOI.
- [382] P. Carena, O. Straniero, B. Döbrich, M. Giannotti, G. Lucente and A. Mirizzi, *Constraints on the coupling with photons of heavy axion-like-particles from Globular Clusters*, *Phys. Lett. B* **809** (2020) 135709 [2004.08399].
- [383] G. Lucente, O. Straniero, P. Carena, M. Giannotti and A. Mirizzi, *Constraining heavy axion-like particles by energy deposition in Globular Cluster stars*, 2203.01336.
- [384] A. Friedland, M. Giannotti and M. Wise, *Constraining the Axion-Photon Coupling with Massive Stars*, *Phys. Rev. Lett.* **110** (2013) 061101 [1210.1271].
- [385] G. Carosi, A. Friedland, M. Giannotti, M. Pivovarov, J. Ruz and J. Vogel, *Probing the axion-photon coupling: phenomenological and experimental perspectives. A snowmass white paper*, in *Community Summer Study 2013: Snowmass on the Mississippi*, 9, 2013, 1309.7035.
- [386] M. J. Dolan, F. J. Hiskens and R. R. Volkas, *Constraining axion-like particles using the white dwarf initial-final mass relation*, *JCAP* **09** (2021) 010 [2102.00379].

- [387] F. Calore, P. Carenza, M. Giannotti, J. Jaeckel and A. Mirizzi, *Bounds on axionlike particles from the diffuse supernova flux*, *Phys. Rev. D* **102** (2020) 123005 [2008.11741].
- [388] F. Calore, P. Carenza, C. Eckner, T. Fischer, M. Giannotti, J. Jaeckel, K. Kotake, T. Kuroda, A. Mirizzi and F. Sivo, *3D template-based Fermi-LAT constraints on axion-like particles*, 2110.03679.
- [389] A. Caputo, G. Raffelt and E. Vitagliano, *Muonic boson limits: Supernova redux*, *Phys. Rev. D* **105** (2022) 035022 [2109.03244].
- [390] A. Caputo, H.-T. Janka, G. Raffelt and E. Vitagliano, *Low-Energy Supernovae Severely Constrain Radiative Particle Decays*, 2201.09890.
- [391] C. Dessert, J. W. Foster and B. R. Safdi, *X-ray Searches for Axions from Super Star Clusters*, *Phys. Rev. Lett.* **125** (2020) 261102 [2008.03305].
- [392] M. Xiao, K. M. Perez, M. Giannotti, O. Straniero, A. Mirizzi, B. W. Grefenstette, B. M. Roach and M. Nynka, *Constraints on Axionlike Particles from a Hard X-Ray Observation of Betelgeuse*, *Phys. Rev. Lett.* **126** (2021) 031101 [2009.09059].
- [393] C. S. Reynolds, M. D. Marsh, H. R. Russell, A. C. Fabian, R. Smith, F. Tombesi and S. Veilleux, *Astrophysical limits on very light axion-like particles from Chandra grating spectroscopy of NGC 1275*, 1907.05475.
- [394] D. Wadekar and Z. Wang, *Constraining compact and axion dark matter from interstellar medium heating, in preparation* (2022) .
- [395] FERMI-LAT Collaboration, M. Ajello et al., *Search for Spectral Irregularities due to Photon-Axionlike-Particle Oscillations with the Fermi Large Area Telescope*, *Phys. Rev. Lett.* **116** (2016) 161101 [1603.06978].
- [396] H.E.S.S. Collaboration, A. Abramowski et al., *Constraints on axionlike particles with H.E.S.S. from the irregularity of the PKS 2155-304 energy spectrum*, *Phys. Rev. D* **88** (2013) 102003 [1311.3148].
- [397] R. Buehler, G. Gallardo, G. Maier, A. Domínguez, M. López and M. Meyer, *Search for the imprint of axion-like particles in the highest-energy photons of hard γ -ray blazars*, *JCAP* **2020** (2020) 027 [2004.09396].
- [398] J.-G. Cheng, Y.-J. He, Y.-F. Liang, R.-J. Lu and E.-W. Liang, *Revisiting the analysis of axion-like particles with the Fermi-LAT gamma-ray observation of NGC1275*, *Phys. Lett. B* **821** (2021) 136611 [2010.12396].
- [399] J.-G. Guo, H.-J. Li, X.-J. Bi, S.-J. Lin and P.-F. Yin, *Implications of axion-like particles from the Fermi-LAT and H.E.S.S. observations of PG 1553+113 and PKS 2155-304*, *Chinese Physics C* **45** (2021) 025105.

- [400] D. Horns, L. Maccione, M. Meyer, A. Mirizzi, D. Montanino and M. Roncadelli, *Hardening of TeV gamma spectrum of active galactic nuclei in galaxy clusters by conversions of photons into axionlike particles*, *Phys. Rev. D* **86** (2012) 075024 [1207.0776].
- [401] C. Zhang, Y.-F. Liang, S. Li, N.-H. Liao, L. Feng, Q. Yuan, Y.-Z. Fan and Z.-Z. Ren, *New bounds on axionlike particles from the Fermi Large Area Telescope observation of PKS 2155 -304*, *Phys. Rev. D* **97** (2018) 063009 [1802.08420].
- [402] S. J. Asztalos, G. Carosi, C. Hagmann, D. Kinion, K. van Bibber, M. Hotz, L. J. Rosenberg, G. Rybka, J. Hoskins, J. Hwang, P. Sikivie, D. B. Tanner, R. Bradley, J. Clarke and ADMX Collaboration, *SQUID-Based Microwave Cavity Search for Dark-Matter Axions*, *Phys. Rev. Lett.* **104** (2010) 041301 [0910.5914].
- [403] ADMX Collaboration, T. Braine et al., *Extended Search for the Invisible Axion with the Axion Dark Matter Experiment*, *Phys. Rev. Lett.* **124** (2020) 101303 [1910.08638].
- [404] N. Crisosto, P. Sikivie, N. S. Sullivan, D. B. Tanner, J. Yang and G. Rybka, *ADMX SLIC: Results from a Superconducting LC Circuit Investigating Cold Axions*, *Phys. Rev. Lett.* **124** (2020) 241101 [1911.05772].
- [405] S. DePanfilis, A. C. Melissinos, B. E. Moskowitz, J. T. Rogers, Y. K. Semertzidis, W. U. Wuensch, H. J. Halama, A. G. Prodell, W. B. Fowler and F. A. Nezrick, *Limits on the abundance and coupling of cosmic axions at $4.5 < m_a < 5.0 \mu\text{eV}$* , *Phys. Rev. Lett.* **59** (1987) 839.
- [406] C. Hagmann, P. Sikivie, N. S. Sullivan and D. B. Tanner, *Results from a search for cosmic axions*, *Phys. Rev. D* **42** (1990) 1297.
- [407] S. Lee, S. Ahn, J. Choi, B. R. Ko and Y. K. Semertzidis, *Axion Dark Matter Search around $6.7 \mu\text{eV}$* , *Phys. Rev. Lett.* **124** (2020) 101802 [2001.05102].
- [408] J. Jeong, S. Youn, S. Bae, J. Kim, T. Seong, J. E. Kim and Y. K. Semertzidis, *Search for Invisible Axion Dark Matter with a Multiple-Cell Haloscope*, *Phys. Rev. Lett.* **125** (2020) 221302 [2008.10141].
- [409] CAPP Collaboration, O. Kwon et al., *First Results from an Axion Haloscope at CAPP around $10.7 \mu\text{eV}$* , *Phys. Rev. Lett.* **126** (2021) 191802 [2012.10764].
- [410] M. Meyer and T. Petrushevska, *Search for Axionlike-Particle-Induced Prompt γ -Ray Emission from Extragalactic Core-Collapse Supernovae with the Fermi Large Area Telescope*, *Phys. Rev. Lett.* **124** (2020) 231101 [2006.06722]. [Erratum: *Phys.Rev.Lett.* 125, 119901 (2020)].
- [411] FERMI-LAT Collaboration, M. Ajello et al., *Search for Spectral Irregularities due to Photon–Axionlike-Particle Oscillations with the Fermi Large Area Telescope*, *Phys. Rev. Lett.* **116** (2016) 161101 [1603.06978].

- [412] M. C. D. Marsh, H. R. Russell, A. C. Fabian, B. P. McNamara, P. Nulsen and C. S. Reynolds, *A New Bound on Axion-Like Particles*, *JCAP* **12** (2017) 036 [1703.07354].
- [413] D. Wouters and P. Brun, *Constraints on Axion-like Particles from X-Ray Observations of the Hydra Galaxy Cluster*, *Astrophys. J.* **772** (2013) 44 [1304.0989].
- [414] H.E.S.S. Collaboration, A. Abramowski et al., *Constraints on axionlike particles with H.E.S.S. from the irregularity of the PKS 2155-304 energy spectrum*, *Phys. Rev. D* **88** (2013) 102003 [1311.3148].
- [415] S. Jacobsen, T. Linden and K. Freese, *Constraining Axion-Like Particles with HAWC Observations of TeV Blazars*, 2203.04332.
- [416] C. Dessert, A. J. Long and B. R. Safdi, *No Evidence for Axions from Chandra Observation of the Magnetic White Dwarf RE J0317-853*, *Phys. Rev. Lett.* **128** (2022) 071102 [2104.12772].
- [417] C. Dessert, D. Dunsky and B. R. Safdi, *Upper limit on the axion-photon coupling from magnetic white dwarf polarization*, 2203.04319.
- [418] H.-J. Li, J.-G. Guo, X.-J. Bi, S.-J. Lin and P.-F. Yin, *Limits on axionlike particles from Mrk 421 with 4.5-year period observations by ARGO-YBJ and Fermi-LAT*, *Phys. Rev. D* **103** (2021) 083003 [2008.09464].
- [419] M. A. Buen-Abad, J. Fan and C. Sun, *Constraints on axions from cosmic distance measurements*, *JHEP* **02** (2022) 103 [2011.05993].
- [420] M. Meyer, M. Giannotti, A. Mirizzi, J. Conrad and M. A. Sánchez-Conde, *Fermi Large Area Telescope as a Galactic Supernovae Axionscope*, *Phys. Rev. Lett.* **118** (2017) 011103 [1609.02350].
- [421] C. O'Hare, *cajohare/axionlimits: Axionlimits*, <https://cajohare.github.io/AxionLimits/>, July, 2020. 10.5281/zenodo.3932430.
- [422] O. Straniero, C. Pallanca, E. Dalessandro, I. Dominguez, F. R. Ferraro, M. Giannotti, A. Mirizzi and L. Piersanti, *The RGB tip of galactic globular clusters and the revision of the axion-electron coupling bound*, *Astron. Astrophys.* **644** (2020) A166 [2010.03833].
- [423] F. Capozzi and G. Raffelt, *Axion and neutrino bounds improved with new calibrations of the tip of the red-giant branch using geometric distance determinations*, *Phys. Rev. D* **102** (2020) 083007 [2007.03694].
- [424] S. Chen, H. Richer, I. Caiazzo and J. Heyl, *Distances to the Globular Clusters 47 Tucanae and NGC 362 Using Gaia DR2 Parallaxes*, *Astrophys. J.* **867** (2018) 132 [1807.07089].

- [425] R. Bollig, W. DeRocco, P. W. Graham and H.-T. Janka, *Muons in Supernovae: Implications for the Axion-Muon Coupling*, *Phys. Rev. Lett.* **125** (2020) 051104 [2005.07141]. [Erratum: Phys.Rev.Lett. 126, 189901 (2021)].
- [426] D. Croon, G. Elor, R. K. Leane and S. D. McDermott, *Supernova Muons: New Constraints on Z' Bosons, Axions and ALPs*, *JHEP* **01** (2021) 107 [2006.13942].
- [427] LUX Collaboration, D. S. Akerib et al., *First Searches for Axions and Axionlike Particles with the LUX Experiment*, *Phys. Rev. Lett.* **118** (2017) 261301 [1704.02297].
- [428] P. Gondolo and G. G. Raffelt, *Solar neutrino limit on axions and keV-mass bosons*, *Phys. Rev. D* **79** (2009) 107301 [0807.2926].
- [429] XENON Collaboration, E. Aprile et al., *Light Dark Matter Search with Ionization Signals in XENON1T*, *Phys. Rev. Lett.* **123** (2019) 251801 [1907.11485].
- [430] XENON Collaboration, E. Aprile et al., *Excess electronic recoil events in XENON1T*, *Phys. Rev. D* **102** (2020) 072004 [2006.09721].
- [431] K. Van Tilburg, *Stellar basins of gravitationally bound particles*, *Phys. Rev. D* **104** (2021) 023019 [2006.12431].
- [432] PANDAX Collaboration, C. Fu et al., *Limits on Axion Couplings from the First 80 Days of Data of the PandaX-II Experiment*, *Phys. Rev. Lett.* **119** (2017) 181806 [1707.07921].
- [433] DARWIN Collaboration, J. Aalbers et al., *DARWIN: towards the ultimate dark matter detector*, *JCAP* **11** (2016) 017 [1606.07001].
- [434] LZ Collaboration, D. S. Akerib et al., *Projected sensitivities of the LUX-ZEPLIN (LZ) experiment to new physics via low-energy electron recoils*, 2102.11740.
- [435] EDELWEISS Collaboration, E. Armengaud et al., *Searches for electron interactions induced by new physics in the EDELWEISS-III Germanium bolometers*, *Phys. Rev. D* **98** (2018) 082004 [1808.02340].
- [436] I. M. Bloch, R. Essig, K. Tobioka, T. Volansky and T.-T. Yu, *Searching for Dark Absorption with Direct Detection Experiments*, *JHEP* **06** (2017) 087 [1608.02123].
- [437] R. Z. Ferreira, M. C. D. Marsh and E. Müller, *Do direct detection experiments constrain axionlike particles coupled to electrons?*, 2202.08858.
- [438] M. Buschmann, C. Dessert, J. W. Foster, A. J. Long and B. R. Safdi, *Upper Limit on the QCD Axion Mass from Isolated Neutron Star Cooling*, *Phys. Rev. Lett.* **128** (2022) 091102 [2111.09892].
- [439] P. Carena, T. Fischer, M. Giannotti, G. Guo, G. Martínez-Pinedo and A. Mirizzi, *Improved axion emissivity from a supernova via nucleon-nucleon bremsstrahlung*, *JCAP* **10** (2019) 016 [1906.11844]. [Erratum: JCAP 05, E01 (2020)].

- [440] B. Fore and S. Reddy, *Pions in hot dense matter and their astrophysical implications*, *Phys. Rev. C* **101** (2020) 035809 [1911.02632].
- [441] P. Carena, B. Fore, M. Giannotti, A. Mirizzi and S. Reddy, *Enhanced Supernova Axion Emission and its Implications*, *Phys. Rev. Lett.* **126** (2021) 071102 [2010.02943].
- [442] T. Fischer, P. Carena, B. Fore, M. Giannotti, A. Mirizzi and S. Reddy, *Observable signatures of enhanced axion emission from protoneutron stars*, *Phys. Rev. D* **104** (2021) 103012 [2108.13726].
- [443] A. Arvanitaki, M. Baryakhtar and X. Huang, *Discovering the QCD Axion with Black Holes and Gravitational Waves*, *Phys. Rev. D* **91** (2015) 084011 [1411.2263].
- [444] N. Bar, K. Blum and G. D’Amico, *Is there a supernova bound on axions?*, *Phys. Rev. D* **101** (2020) 123025 [1907.05020].
- [445] M. Libanov and S. Troitsky, *On the impact of magnetic-field models in galaxy clusters on constraints on axion-like particles from the lack of irregularities in high-energy spectra of astrophysical sources*, *Phys. Lett. B* **802** (2020) 135252 [1908.03084].
- [446] J. H. Matthews, C. S. Reynolds, M. C. D. Marsh, J. Sisk-Reynés and P. E. Rodman, *How do Magnetic Field Models Affect Astrophysical Limits on Light Axion-like Particles? An X-ray Case Study with NGC 1275*, 2202.08875.
- [447] CTA Collaboration, H. Abdalla et al., *Sensitivity of the Cherenkov Telescope Array for probing cosmology and fundamental physics with gamma-ray propagation*, *JCAP* **02** (2021) 048 [2010.01349].
- [448] G. Long, S. Chen, S. Xu and H.-H. Zhang, *Probing μeV ALPs with future LHAASO observations of AGN γ -ray spectra*, *Phys. Rev. D* **104** (2021) 083014 [2101.10270].
- [449] J. P. Gardner et al., *The James Webb Space Telescope*, *Space Sci. Rev.* **123** (2006) 485 [astro-ph/0606175].
- [450] LSST DARK MATTER GROUP Collaboration, A. Drlica-Wagner et al., *Probing the Fundamental Nature of Dark Matter with the Large Synoptic Survey Telescope*, 1902.01055.
- [451] Y.-Y. Mao et al., *Snowmass2021: Vera C. Rubin Observatory as a Flagship Dark Matter Experiment*, 3, 2022, 2203.07252.
- [452] A. Caputo, M. Regis, M. Taoso and S. J. Witte, *Detecting the Stimulated Decay of Axions at RadioFrequencies*, *JCAP* **03** (2019) 027 [1811.08436].
- [453] A. Arza and P. Sikivie, *Production and detection of an axion dark matter echo*, *Phys. Rev. Lett.* **123** (2019) 131804 [1902.00114].
- [454] O. Ghosh, J. Salvado and J. Miralda-Escudé, *Axion Gegendeschein: Probing Back-scattering of Astrophysical Radio Sources Induced by Dark Matter*, 2008.02729.

- [455] M. A. Buen-Abad, J. Fan and C. Sun, *Axion Echos from the Supernova Graveyard*, [2110.13916](#).
- [456] Y. Sun, K. Schutz, A. Nambrath, C. Leung and K. Masui, *An axion dark matter-induced echo of supernova remnants*, [2110.13920](#).
- [457] M. Baryakhtar et al., *Dark Matter In Extreme Astrophysical Environments*, in *2022 Snowmass Summer Study*, 3, 2022, [2203.07984](#).
- [458] B. J. Kavanagh, T. D. P. Edwards, L. Visinelli and C. Weniger, *Stellar disruption of axion miniclusters in the Milky Way*, *Phys. Rev. D* **104** (2021) 063038 [[2011.05377](#)].
- [459] F. Calore, P. Carenza, M. Giannotti, J. Jaeckel, G. Lucente and A. Mirizzi, *Supernova bounds on axionlike particles coupled with nucleons and electrons*, *Phys. Rev. D* **104** (2021) 043016 [[2107.02186](#)].
- [460] M. Ivanov, Y. Kovalev, M. Lister, A. Panin, A. Pushkarev, T. Savolainen and S. Troitsky, *Constraining the photon coupling of ultra-light dark-matter axion-like particles by polarization variations of parsec-scale jets in active galaxies*, *JCAP* **02** (2019) 059 [[1811.10997](#)].
- [461] T. Fujita, R. Tazaki and K. Toma, *Hunting Axion Dark Matter with Protoplanetary Disk Polarimetry*, *Phys. Rev. Lett.* **122** (2019) 191101 [[1811.03525](#)].
- [462] M. A. Fedderke, P. W. Graham and S. Rajendran, *Axion Dark Matter Detection with CMB Polarization*, *Phys. Rev. D* **100** (2019) 015040 [[1903.02666](#)].
- [463] F. Day and S. Krippendorf, *Searching for Axion-Like Particles with X-ray Polarimeters*, *Galaxies* **6** (2018) 45 [[1801.10557](#)].
- [464] Y. Chen, J. Shu, X. Xue, Q. Yuan and Y. Zhao, *Probing Axions with Event Horizon Telescope Polarimetric Measurements*, *Phys. Rev. Lett.* **124** (2020) 061102 [[1905.02213](#)].
- [465] A. Castillo, J. Martin-Camalich, J. Terol-Calvo, D. Blas, A. Caputo, R. T. G. Santos, L. Sberna, M. Peel and J. A. Rubiño Martín, *Searching for dark-matter waves with PPTA and QUIJOTE pulsar polarimetry*, [2201.03422](#).
- [466] B. D. Blout, E. J. Daw, M. P. Decowski, P. T. P. Ho, L. J. Rosenberg and D. B. Yu, *A Radio telescope search for axions*, *Astrophys. J.* **546** (2001) 825 [[astro-ph/0006310](#)].
- [467] D. Grin, G. Covone, J.-P. Kneib, M. Kamionkowski, A. Blain and E. Jullo, *A Telescope Search for Decaying Relic Axions*, *Phys. Rev. D* **75** (2007) 105018 [[astro-ph/0611502](#)].
- [468] M. Regis, M. Taoso, D. Vaz, J. Brinchmann, S. L. Zoutendijk, N. F. Bouché and M. Steinmetz, *Searching for light in the darkness: Bounds on ALP dark matter with the optical MUSE-faint survey*, *Phys. Lett. B* **814** (2021) 136075 [[2009.01310](#)].

- [469] A. Keller, S. O'Brien, A. Kamdar, N. Rapidis, A. Leder and K. van Bibber, *A Model-Independent Radio Telescope Dark Matter Search*, [2112.03439](#).
- [470] J. W. Foster, M. Kongsore, C. Dessert, Y. Park, N. L. Rodd, K. Cranmer and B. R. Safdi, *Deep Search for Decaying Dark Matter with XMM-Newton Blank-Sky Observations*, *Phys. Rev. Lett.* **127** (2021) 051101 [[2102.02207](#)].
- [471] J. B. Bauer, D. J. E. Marsh, R. Hložek, H. Padmanabhan and A. Laguë, *Intensity Mapping as a Probe of Axion Dark Matter*, *Mon. Not. Roy. Astron. Soc.* **500** (2020) 3162 [[2003.09655](#)].
- [472] J. L. Bernal, A. Caputo and M. Kamionkowski, *Strategies to Detect Dark-Matter Decays with Line-Intensity Mapping*, *Phys. Rev. D* **103** (2021) 063523 [[2012.00771](#)].
- [473] B. Bolliet, J. Chluba and R. Battye, *Spectral distortion constraints on photon injection from low-mass decaying particles*, *Mon. Not. Roy. Astron. Soc.* **507** (2021) 3148 [[2012.07292](#)].
- [474] N. Bar, K. Blum and C. Sun, *Galactic rotation curves vs. ultralight dark matter II*, [2111.03070](#).
- [475] N. Bar, D. Blas, K. Blum and S. Sibiryakov, *Galactic rotation curves versus ultralight dark matter: Implications of the soliton-host halo relation*, *Phys. Rev. D* **98** (2018) 083027 [[1805.00122](#)].
- [476] A. Mirizzi, G. G. Raffelt and P. D. Serpico, *Photon-axion conversion as a mechanism for supernova dimming: Limits from CMB spectral distortion*, *Phys. Rev. D* **72** (2005) 023501 [[astro-ph/0506078](#)].
- [477] A. Mirizzi, J. Redondo and G. Sigl, *Constraining resonant photon-axion conversions in the Early Universe*, *JCAP* **0908** (2009) 001 [[0905.4865](#)].
- [478] A. Avgoustidis, C. Burrage, J. Redondo, L. Verde and R. Jimenez, *Constraints on cosmic opacity and beyond the standard model physics from cosmological distance measurements*, *JCAP* **10** (2010) 024 [[1004.2053](#)].
- [479] K. Liao, A. Avgoustidis and Z. Li, *Is the Universe Transparent?*, *Phys. Rev. D* **92** (2015) 123539 [[1512.01861](#)].
- [480] P. Tiwari, *Constraining axionlike particles using the distance-duality relation*, *Phys. Rev. D* **95** (2017) 023005 [[1610.06583](#)].
- [481] T. Kobayashi, R. Murgia, A. De Simone, V. Iršič and M. Viel, *Lyman- α constraints on ultralight scalar dark matter: Implications for the early and late universe*, *Phys. Rev. D* **96** (2017) 123514 [[1708.00015](#)].
- [482] J. Eby, S. Shirai, Y. V. Stadnik and V. Takhistov, *Probing relativistic axions from transient astrophysical sources*, *Phys. Lett. B* **825** (2022) 136858 [[2106.14893](#)].

- [483] M. Colpi, S. L. Shapiro and I. Wasserman, *Boson Stars: Gravitational Equilibria of Selfinteracting Scalar Fields*, *Phys. Rev. Lett.* **57** (1986) 2485.
- [484] E. Seidel and W.-M. Suen, *Formation of solitonic stars through gravitational cooling*, *Phys. Rev. Lett.* **72** (1994) 2516 [gr-qc/9309015].
- [485] B. Eggemeier and J. C. Niemeyer, *Formation and mass growth of axion stars in axion miniclusters*, *Phys. Rev. D* **100** (2019) 063528 [1906.01348].
- [486] H. Xiao, I. Williams and M. McQuinn, *Simulations of axion minihalos*, *Phys. Rev. D* **104** (2021) 023515 [2101.04177].
- [487] D. G. Levkov, A. G. Panin and I. I. Tkachev, *Relativistic axions from collapsing Bose stars*, *Phys. Rev. Lett.* **118** (2017) 011301 [1609.03611].
- [488] J. Eby, M. Leembruggen, P. Suranyi and L. C. R. Wijewardhana, *Collapse of Axion Stars*, *JHEP* **12** (2016) 066 [1608.06911].
- [489] J. A. Dror, H. Ramani, T. Trickle and K. M. Zurek, *Pulsar Timing Probes of Primordial Black Holes and Subhalos*, *Phys. Rev. D* **100** (2019) 023003 [1901.04490].
- [490] L. Dai and J. Miralda-Escudé, *Gravitational Lensing Signatures of Axion Dark Matter Minihalos in Highly Magnified Stars*, *Astron. J.* **159** (2020) 49 [1908.01773].
- [491] M. Fairbairn, D. J. E. Marsh, J. Quevillon and S. Rozier, *Structure formation and microlensing with axion miniclusters*, *Phys. Rev. D* **97** (2018) 083502 [1707.03310].
- [492] D. Croon, D. McKeen, N. Raj and Z. Wang, *Subaru-HSC through a different lens: Microlensing by extended dark matter structures*, *Phys. Rev. D* **102** (2020) 083021 [2007.12697].
- [493] M. P. Hertzberg, Y. Li and E. D. Schiappacasse, *Merger of Dark Matter Axion Clumps and Resonant Photon Emission*, *JCAP* **07** (2020) 067 [2005.02405].
- [494] M. A. Amin and Z.-G. Mou, *Electromagnetic Bursts from Mergers of Oscillons in Axion-like Fields*, *JCAP* **02** (2021) 024 [2009.11337].
- [495] P. Echternach et al., *Single photon detection of 1.5 thz radiation with the quantum capacitance detector*, *Nat. Astron.* **2** (2018) 90.
- [496] M. Baryakhtar, J. Huang and R. Lasenby, *Axion and hidden photon dark matter detection with multilayer optical haloscopes*, *Phys. Rev. D* **98** (2018) 035006.
- [497] B. J. Lawrie, C. E. Marvinney, Y.-Y. Pai, M. A. Feldman, J. Zhang, A. J. Miller, C. Hua, E. Dumitrescu and G. B. Halász, *Multifunctional Superconducting Nanowire Quantum Sensors*, *Phys. Rev. Applied* **16** (2021) 064059 [2103.09896].

- [498] T. Polakovic, W. R. Armstrong, V. Yefremenko, J. E. Pearson, K. Hafidi, G. Karapetrov, Z. E. Meziani and V. Novosad, *Superconducting nanowires as high-rate photon detectors in strong magnetic fields*, *Nucl. Instrum. Meth. A* **959** (2020) 163543 [1907.13059].
- [499] T. Braine et al., *Extended Search for the Invisible Axion with the Axion Dark Matter Experiment*, *Physical Review Letters* **124** (2020) 101303 [1910.08638].
- [500] S. Chaudhuri, K. D. Irwin, P. W. Graham and J. Mardon, "Optimal Electromagnetic Searches for Axion and Hidden-Photon Dark Matter", *arXiv preprint arXiv:1904.05806* (2019) .
- [501] C.-L. Kuo, *Symmetrically tuned large-volume conic shell-cavities for axion searches*, *Journal of Cosmology and Astroparticle Physics* **2021** (2021) 018.
- [502] Y. Michimura, Y. Oshima, T. Watanabe, T. Kawasaki, H. Takeda, M. Ando, K. Nagano, I. Obata and T. Fujita, *DANCE: Dark matter Axion search with riNg Cavity Experiment*, *J. Phys. Conf. Ser.* **1468** (2020) 012032 [1911.05196].
- [503] H. Liu, B. D. Elwood, M. Evans and J. Thaler, *Searching for Axion Dark Matter with Birefringent Cavities*, *Phys. Rev. D* **100** (2019) 023548 [1809.01656].
- [504] K. Nagano, T. Fujita, Y. Michimura and I. Obata, *Axion Dark Matter Search with Interferometric Gravitational Wave Detectors*, *Phys. Rev. Lett.* **123** (2019) 111301 [1903.02017].
- [505] Z. Zhang, O. Ghosh and D. Horns, *WISPLC: Search for Dark Matter with LC Circuit*, 2111.04541.
- [506] D. Alesini, D. Babusci, D. Di Gioacchino, C. Gatti, G. Lamanna and C. Ligi, *The KLASH Proposal*, 1707.06010.
- [507] I. Stern, *ADMX Status*, *PoS ICHEP2016* (2016) 198 [1612.08296].
- [508] S. Beurthey et al., *MADMAX Status Report*, 2003.10894.
- [509] B. T. McAllister, G. Flower, E. N. Ivanov, M. Goryachev, J. Bourhill and M. E. Tobar, *The ORGAN Experiment: An axion haloscope above 15 GHz*, *Phys. Dark Univ.* **18** (2017) 67 [1706.00209].
- [510] Brass, <https://www1.physik.uni-hamburg.de/iexp/gruppe-horns/forschung/brass.html>.
- [511] J. Liu et al., *Broadband solenoidal haloscope for terahertz axion detection*, 2111.12103.
- [512] J. Schütte-Engel, D. J. E. Marsh, A. J. Millar, A. Sekine, F. Chadha-Day, S. Hoof, M. N. Ali, K.-C. Fong, E. Hardy and L. Šmejkal, *Axion quasiparticles for axion dark matter detection*, *JCAP* **08** (2021) 066 [2102.05366].

- [513] I. Shilon, A. Dudarev, H. Silva, U. Wagner and H. H. J. ten Kate, *The Superconducting Toroid for the New International AXion Observatory (IAXO)*, *IEEE Trans. Appl. Supercond.* **24** (2014) 4500104 [1309.2117].
- [514] M. D. Ortiz et al., *Design of the ALPS II Optical System*, 2009.14294.
- [515] A. Dekker, E. Peerbooms, F. Zimmer, K. C. Y. Ng and S. Ando, *Searches for sterile neutrinos and axionlike particles from the Galactic halo with eROSITA*, *Phys. Rev. D* **104** (2021) 023021 [2103.13241].
- [516] C. Thorpe-Morgan, D. Malyshev, A. Santangelo, J. Jochum, B. Jäger, M. Sasaki and S. Saeedi, *THESEUS insights into axionlike particles, dark photon, and sterile neutrino dark matter*, *Phys. Rev. D* **102** (2020) 123003 [2008.08306].

Note

Some of the text may be based on the respective LOIs on https://snowmass21.org/cosmic/dm_wave.